

**University for Development Studies West African Centre for Water, Irrigation
and Sustainable Agriculture (UDS/WACWISA)**

**APPLICATION OF HYDRAULIC FLOODING MODELING FOR PLANT
SELECTION AND LAND MANAGEMENT IN THE OUÉMÉ DELTA (BENIN):
CASE OF ADJOHOUN DISTRICT**

BY

AMOUSSOU Toundé Félix

**(BSc. Science and Technology/Quantitative Hydrology, Mphil. Irrigation and Drainage
Engineering)**

(UDS/MID/0028/21)

August 2023



DECLARATION

Student

I affirm that this dissertation/thesis represents the outcome of my own original effort, and no portion of it has been submitted for another degree within this University or any other institution.

Candidate's

Signature:

Date:

Name: AMOUSSOU TOUNDE FÉLIX

Supervisors'

I affirm that the process of preparing and presenting the dissertation/thesis adhered to the guidelines for supervision of dissertation/thesis set forth by the University for Development Studies.

Main Supervisor's

Signature:

Date:

Name: Prof ABDUL HALIM ABUBAKARI

Co- Supervisor's

Signature:

Date:

Name: Dr. Elias Salifu

Head of Department Signature:

Date:

Name: Dr ELIASU SALIFU

WACWISA Director Signature:

Date:

Name: Prof. FELIX KOFI ABAGALE



ABSTRACT

This study assessed the causes of human and agricultural losses and damages and presents a unique solution for optimal plant selection and land-use planning. In terms of agricultural potential, the Lower Ouémé Valley is the second richest after the Nile in the world, but due to flooding this potential is being lost or destroyed. The district of Adjohoun is located in this valley and is crossed by the Ouémé River. This research aims to (i) characterize hydroclimatic events and the occurrence of exceptional hydro-rainfall phenomena for return periods of 2 and 5 years, (ii) delimit flood-prone areas to characterize the maximum height of water submersion, (iii) evaluate the best model for statistical forecasting of seasonal flood discharges and (iv) develop a web-based tool for optimal plant selection and assistance with thoughtful territorial planning. Results showed that: (i) the Adjohoun valley is influenced by two sources of flooding capable of destroying crops and other properties; often the rains in July and the increase in the discharge of the Ouémé river during the month of September. Values of rainfall 115 mm/day and 780 m³/s are expected each year with a 50% probability of occurrence, compared with 153 mm/day and 1150m³/s for a 5-year return period under Gumbel's distribution; (ii) at the advent of these observations, under a rainfall of 115mm/day about 17.05% (53.92 km²) of the surface area will be affected, compared to 50.87% (160.61 km²) of area for a rainfall of 153 mm/day. Despite a maximum submersion height of around 396.24 cm (60 m²), only 1.81% (3.72 km²) of the valley is unsuitable for the production of plants that do not tolerate a maximum water level below 0.9 m (*Solanum lycopersicum*, *Oryza sativa*, *Capsicum*). The contrary observation is found during river flooding (month of September) when the majority of floods inundate crops on the right bank of the Ouémé River for a proportion of 28.32% (89.81km²) of area with predominant submersion height classes of 30.48 cm (~30 km²); 60.96 cm (~29 km²), 91.44 cm (~15 km²) and 121.92cm (~5 km²). (iii) To alert the valley's population and farmers on a seasonal forecast that describes the extent of flooding, the best statistical prediction model following the current discharge regime is the Holt Winter Exponential Smooth (HWES) model [RMSE=104.97, MAE=60.13, MAPE=27.70]; and (iv) Finally, a web-based assistance tool has been developed for the broadcasting of seasonal forecast information and for 3D visualization of flood-prone areas, giving information on maximum water submersion height of each area, optimal crop type, etc., by using a smartphone/computer and Google Earth. However, we recommend farmers to opt for flood-resistant plants and local authorities to envisage the installation of hydraulic structures to prevent annual flooding.



ACKNOWLEDGE

I am grateful to my heavenly Father for his divine love and mercy.

I would like to acknowledge the **West African Centre for Water, Irrigation and Sustainable Agriculture (WACWISA), University for Development Studies, Ghana**, for the working environment. I am thankful for the funding support provided by the Government of Ghana and the World Bank through the African Centres of Excellence for Development Impact (ACE Impact).

I would like to show my gratitude to my supervisors Prof Abdul Halim Abubakari and Dr Eliasu Salifu for their support in the writing process, their orientation and their relevant contributions during this thesis. I wish you good health, a successful professional career and may Allah bless you.

To my colleagues at the Center of Excellence, thank you for the unique moments of sharing and scientific exchange.



DEDICATION

I dedicate this work, to SBJ Oshoffa and my adoptive father,

Ernest AMOUSSOU.

Thanks



Table of contents

DECLARATION.....	2
ABSTRACT	3
ACKNOWLEDGE	4
DEDICATION	5
List of figures	9
List of Table	10
Abbreviation and acronym	11
CHAPTER ONE:.....	13
INTRODUCTION	13
1.1. Background	13
1.2. Problem Statement and Justification	14
1.3. Study Objectives	17
1.3.1. General objective	17
1.3.2. Specifics objectives	17
CHAPTER TWO:.....	19
LITERATURE REVIEW	19
2.1. Definitions	19
2.2. Agricultural Activity and Flooding	20
2.3. Tests statistics	21
<i>Tests of homogeneity (Wilcoxon)</i>	22
<i>Tests of independence (Kolmogorov-Smirnov)</i>	22
2.3.1. Stationarity test (Dickey-Fuller & KPSS)	22
<i>Dickey-Fuller test</i>	23
<i>KPSS stationarity test</i>	24
<i>Holt winters smoothing exponential forecasting model</i>	26
<i>ARIMA & SARIMA forecasting model</i>	27
2.4. Plant Selection and Land Management	28
CHAPTER THREE:	30
3.1. Study Area	30
3.2. Data Used and Methods	34
3.2.1. Data collection	35
3.2.2. Data corrections	35



3.5. Data Processing Methods.....	36
3.5.1 Characterize the hydroclimate (rain & streamflow) events of the study environment and the occurrence of exceptional phenomena (2-year and 5-year)	36
<i>Calculation of empirical frequencies and characterization of return periods</i>	<i>37</i>
<i>Law of adjustment: GEV, Gumbel, Weibull</i>	<i>39</i>
<i>Validation of the statistical model: AIC, BIC and graph</i>	<i>40</i>
3.5.2 Delimit the cultivation and flooding areas according to the occurrence of extreme floods events (2-year and 5-year).....	40
<i>Trend of spatial repartition of land use in the study</i>	<i>40</i>
<i>Hydraulic modelling</i>	<i>41</i>
3.5.3. Identifying the best fitting flood forecasting models for the study region.....	44
<i>The evaluation criteria: MAE, RMSE, MAPE, graphic</i>	<i>44</i>
3.6 Develop a dynamic early warning decision-making tool for crop selection and land management	45
CHAPTER FOUR:	48
RESULTS AND DISCUSSION.....	48
4-1. Hydroclimate (Rain & Discharge) Events of the Study Environment	48
4-2-Characteristics of extreme events.....	56
4-1-1. Precipitation adjustment	56
4-1-2. Discharge adjustment	61
4-2- Delimit the Cultivation and Flooding Areas According to the Occurrence of Extreme Floods Events (2-Year And 5-Year)	65
4-2-1 Trend of spatial repartition of land use in the study	65
4-2-2 Hydraulic modeling	69
<i>Rainfall flood events</i>	<i>71</i>
<i>River flood events.....</i>	<i>76</i>
4-3. Identify the Best Fitting Flood Forecasting Models for The Study Region	81
4-3-1. Seasonal forecasting of river floods.....	81
<i>Tests on seasonality, stationarity and autocorrelation</i>	<i>82</i>
<i>Evaluation of forecasting models.....</i>	<i>83</i>
4-4. Early Warning Decision-Making Tool for Crop Selection and Land Management	87
CHAPTER FIVE:.....	93



CONCLUSION AND RECOMMENDATIONS	93
5.1. Conclusion	93
5.2. Recommendations for management policy	94
5.3. Further research	95
References	96
APENDICES	124



List of figures

Figure 3-1: Study area map	30
Figure 3- 2: Land cover of study area, (source: European Spatial Agency, Sentinel 2A).....	31
Figure 3- 3: Geology map study area	32
Figure 3- 4: Contour line map study area	32
Figure 3- 5: Ouémé region population size 1979 – 2030 (source : INSAE, 2013)	34
Figure 3- 6:Adjohoun district population size (source: INSAE, 2013)	34
Figure 3- 7:Adjohoun sub-district population size (source: INSAE, 2013)	34
Figure 4- 1: Monthly average of precipitation and discharge at Adjohoun district.....	48
Figure 4- 2: Precipitation daily/monthly/annually Cotonou time series plots	49
Figure 4- 3: Monthly precipitation matrix at Cotonou from 1989 to 2017	49
Figure 4- 4: Seasonal flow variation at Bonou station	50
Figure 4- 5:Seasonal water level variation at Bonou station	50
Figure 4- 6:(A)-Standardized Precipitation Index (SPI) from 1922 to 2017, (B)-Standardized Discharge Index (SDI) from 1949 to 2017, (C)- SPI & SDI for Adjohoun region from 1949 to 2017.....	54
Figure 4- 7:correlation matrix between daily variable (flow, water level, precipitation).....	55
Figure 4- 8: Distribution of the maximum annual daily rainfall on the Hazen probability paper	57
Figure 4- 9: Graphical comparison of the fitting laws.....	60
Figure 4- 10: Distribution of Qjmax on Hazen probability paper	61
Figure 4- 11:Graphical comparison of the fitting laws.....	64
Figure 4- 12: Land use diagram.....	66
Figure 4- 13: Cover data extraction. (A)-LULC of Adjohoun district year 2020, (B) Built up areas of Adjohoun district, (C)-Cropland of Adjohoun district, (D)- Grassland of Adjohoun district	68
Figure 4- 14: Rain flood hyetograph input	70
Figure 4- 15: Cumulative River flood input	70
Figure 4- 16: Map of flood zones under a 2-year and 5-year return period rainfall.....	75
Figure 4- 17: Map of flood zones under different discharge	76
Figure 4- 18:- summary plots water vs Area (km ²) for each discharge	77
Figure 4- 19: Land cover & flood (rain, river) events	79
Figure 4- 20: Time series used for seasonal forecasting.....	81
Figure 4- 21: Break in stationarity on the chronology of raw observations	82
Figure 4- 22: Flow prediction for the year 1959 under a stable regime with a strong seasonal amplitude	84
Figure 4- 23: Flow prediction for 1978 under a declining regime & low amplitude seasonality	85
Figure 4- 24: Flow prediction for 2004 under an increasing regime & high amplitude seasonality	85
Figure 4- 25: Display of the page on a smartphone.....	89
Figure 4- 26: Opening of the *.kmz file and rendering on Google Earth.....	91
Figure 1: Ras mapper, application of manning coefficient for simulation	127
Figure 2: Hyetograph curve for 115mm/24h under HEC RAS	128
Figure 3: Water level profil during 115mm & 153mm at (Xcoord=440474.21, Ycoord=736906.10)	128



List of Table

Table 3- 1: Land cover class statistic year 2016 (source: European Spatial Agency, Sentinel 2A).....	33
Table 4- 1: Extreme statistical summary	52
Table 4- 2: Results of test hypothesis.....	57
Table 4- 3: Data fitting to GEV, Gumbel and Weibull laws	59
Table 4- 4: Assessment of the laws of adjustment to the AIC and BIC criteria.....	60
Table 4- 5: Estimation of the maximum daily rainfall of return period 2 years and 5 years (Gumbel)	60
Table 4- 6: Results of test hypothesis.....	62
Table 4- 7: Test fit of annual maximum daily streamflow data to GEV, Gumbel and Weibull laws ...	63
Table 4- 8: Assessment of the laws of adjustment to the AIC and BIC criteria.....	64
Table 4- 9: Results of the estimation of the maximum daily rainfall of return period 2 years and 5 years (Gumbel)	64
Table 4- 10:summary on crops and soil characterization	70
Table 4- 11: statistics summary on rainfall events for 2yrs and 5yrs return periods	72
Table 4- 12: statistics on the distribution of water level classes for 115mm and 153mm scenarios	73
Table 4- 13: statistics summary on river flood	77
Table 4- 14: summary on ADF, PP and KPSS tests and ACF &PACF	83
Table 4- 15: Performance evaluation of forecasting models under RMSE, MAE and MAPE criteria .	86
Table 1: Land Use and Land Cover classification summary (source: ESA, 2016)	125
Table 2: Manning coefficient	127



Abbreviation and acronym

ADF:	Augmented Dickey Fuller
ACF:	AutoCorelation Function
AIC:	Akaike Information Criterion
ARIMA:	Auto Regressive Integrated Moving Average
BIC:	Bayesian Information Criterion
CENATEL:	National Center for Remote Sensing and Ecological Monitoring
DEM:	Digital Elevation Model
DG-Eau:	Directorate General for Water
ESA:	European Spatial Agency
HEC RAS:	Hydrologic Engineering Center's River Analysis System
HyFRAN:	Hydrology FRequency ANalysis
HWES:	Holt Winter Exponential Smooth
GEV:	Generalized Extreme Value
IGN:	National Geographic Institute
INSEA:	National Institute of Statistics and Economic Analysis
IPCC:	Intergovernmental Panel on Climate Change
KPSS:	Kwiatkowski, Phillips, Schmidt and Shin
MAE:	Mean Absolute Error
MAPE:	Mean Absolute Percentage Error
PP:	Philip Perron
PCM:	Projet Commune du Millénaire
PACF:	Partial AutoCorelation Function
Qref:	reference discharge (m^3/s)
Qpred:	predict discharge (m^3/s)



RGPH4:	General Census of Population and Housing 4
RMSE:	Root Mean Square Error
SARIMA:	Seasonal Auto Regressive Integrated Moving Average
SNU :	Système des Nations Unies
SPI:	Standardized Precipitation Index
SDI:	Standardized Discharge Index
USGS:	U.S. Geological Survey



CHAPTER ONE:

INTRODUCTION

1.1. Background

Climate change and population increase are the most prominent features of the twenty-first century. Climate change, with its rising temperatures, extreme precipitation sequences and other meteorological phenomena, is having an impact on human life and the ecosystem in which we live (Moreno & Møller, 2011). Societal observations are often only linked to perceptions of a rising ambient temperature (Capstick *et al.*, 2014). This state of heat perception is not unique to temperature, but also to other components of the hydrometeorological cycle (Shelton, 2009; Hunter *et al.*, 2015). In the wake of global warming, the science of extreme hydroclimatic events has been born. This science analyzes, studies, alerts and proposes sustainable management solutions (McMichael, 2011; Intergovernmental Panel on Climate Change [IPCC], 2022). Scientific research and results show that the effects and consequences of climate change are heterogeneously distributed across the planet (Arnell *et al.*, 2016; IPCC, 2022). Depending on their geographical location of occurrence, certain regions of the globe are either under the influence of intense heat waves, drought sequences or violent precipitation (cyclones or typhoons), or rising sea levels, etc. (Kundzewicz *et al.*, 2007; Peter, 2010; Aghakouchak *et al.*, 2020). In the Mediterranean and parts of India and Asia, for example, this involves the occurrence of intense heat waves, pockets of drought and forest fires (Robinne, 2021).

In Africa, specifically in West Africa, these phenomena are not uncommon, but are potentially animated by pockets of local or seasonal drought, and much more by floods (Ekwezuo & Ezech, 2020; Dibi *et al.*, 2023). This concerns the majority of West African countries, such as Benin, Togo, Nigeria, Ghana, Mali, Niger, etc. and other countries in the sub-region (Hounkpè, 2015). In these cases of recurrent flooding, it is relatively complicated to meet the Sustainable Development Goals (IPCC, 2022). Pertinently, beyond the public services affected, households



and primary infrastructures (roads, health centers, schools, markets, etc.) that are impacted, the agricultural sector is not spared (Mashael, 2009). In Africa, agriculture is not only a source of food, but also a key sector for socio-economic and political stability. Indeed, a stable and sustainable agricultural model mitigates the risks of potential food insecurity (Kizito, 2014).

In Benin, agriculture is considered to be a high-value-added sector, with more farmers than any other, and the main source of income for the majority of the population (Cissé, 2015; Tiina et al., 2004; Allen & Heinrigs, 2016). However, flooding is regularly observed in the southern basins of the country, causing heavy losses and plunging the population into crisis (Ernest *et al.*, 2022). These events mainly occur in the base agricultural valleys with high community impact ('*Projet Commune du Millénaire*' [PCM], 2015), including Adjohoun. The Adjohoun agricultural valley is part of the great Ouémé valley, considered to be the second richest valley in the world after the Nile (Barnabé, 2015; Basile *et al.*, 2017; Fêmi *et al.*, 2020). According to studies, it is capable of feeding the entire population of Benin (Basile *et al.*, 2017). In view of its vital importance for food security, like authors such as Koumassi *et al.* (2014); Adjakpa *et al.* (2016); Kpoha *et al.*, (2023) who tackle the subject globally on the axes of mapping, remote sensing, frequency analysis and vulnerability to flooding. Up to now, the Adjohoun valley has not been the focus of any studies, focusing on seasonal prediction, hydraulic flood modelling and the development of a dynamic early warning and decision-making tool. Beyond these aspects, our vision is to include the property of selecting and choosing seasonal crop plantations that are resilient to future flooding.

1.2. Problem Statement and Justification

The 2019 floods after torrential rains during affected 600,000 people with several damage in sixteen West African countries (Baldassarre *et al.*, 2010; Ansah *et al.*, 2020, Atiah *et al.*, 2023). In 2012, Nigeria experienced one of the most devastating flooding events ever recorded (Amangabara *et al.*, 2015). This flooding incident led to the deaths and displacement of 363 and



2.3 million people, respectively, and the destruction of 59,000 houses and also affected large tracts of farmland and livestock. In 2015, the southern Ghana experienced heavy thunderstorms and rain. This flooding incident and an explosion of a fuel filling station at Kwame Nkrumah Circle, a suburb of Accra, claimed over 150 lives and destroyed lots of properties while displacing hundreds of people (Ansah *et al.*, 2020).

The Republic of Benin is not exempted from drastic floods. The most recent catastrophic event dates back to the year 2010 (Ahouangan *et al.*, 2014). Now, the country is recording after these very rare phenomena, secondary flood events that affect most of the valley areas of the country, such as the Adjohoun region, like 1999, 2007, 2009, 2010, 2012, 2013 (Amoussou *et al.*, 2011; Kodja, 2018; Akpadja *et al.*, 2016). According to the World Bank (2008), although Sub-Saharan Africa is not a disaster-prone region, its greatest vulnerability is related to physical, socio-economic and environmental factors that negatively affect people's ability to secure and protect their income-generating activities. In Benin, floods are increasing due to the frequency of exceptional rains and anarchic land use (Ogouwalé *et al.*, 2003; Houndakinou, 2005; Houndenou, 2011).

The damage caused by the 2010 floods in Benin was so enormous that the country was declared a disaster (Adjakpa *et al.*, 2016). The costs of damages and losses resulting from the floods are estimated at nearly 120 billion CFA francs with an incidence of 0.8% decline in the Gross Domestic Product (“*Système des Nations Unies*” [SNU], 2011). Adjakpa (2016) noted that the flood waters cross the gallery forests along the banks and invade the fields of crops bordering the river, with a massive destruction of crops and granaries for 66.28% of the population surveyed after the flood of 2013. According to the results of Ahouangan *et al.* (2014) of surveys on 2010 flood, the victims described the disaster as being exceptional by the surprise effect, the height of water and the level of damage caused. Moreover, on the socio-demographic level, the floods caused temporary migrations for the majority of the population and permanent





displacements which affected approximately 50% of the young population (Chauhan *et al.*, 2023). These facts testify to the severity of the effects of flooding on the population. In a broader sense, the impact can extend to human health and the degradation of agricultural resources (Faye *et al.*, 2023). Such a consideration will make it possible to kill two birds with one stone by dynamically resolving the damage to the human species and to their primary living resources. Most studies conducted on the environment have focused on the negative and destructive effects of flooding in the valley on environmental goods and services (Ahouangan *et al.*, 2014; Adjakpa 2016; Adjakpa *et al.*, 2016). In most cases, scientific research deals with environmental monitoring using hydrological models (Bacharou *et al.*, 2015; Tania, 2016; Kodja, 2018; Degan *et al.*, 2019) or estimating extreme quantiles for different return periods (Bacharou *et al.*, 2013; Hounkpè *et al.*, 2015; Biao *et al.*, 2016) without assessing the associated levels of vulnerability. On the other hand, studies of maps of flood-prone areas (Neisingh, 2018; Akpla *et al.*, 2022) have been assessed with a lack of information on rainfall or hydrological quantiles and agricultural activities. In most cases, these research projects do not combine flood zone mapping with agricultural activities and hydrological quantiles, and are often confined to scientific or political circles. These scientific results, whether in hydrometeorology, hydraulics or environmental sciences, are in most cases limited to scientific publications or workshops. Of course, scientific articles/publications and communication workshops are a convincing way of disseminating research results, but they can have their limits in the informative science of seasonal forecasting. In Benin, flood warnings are broadcast very vaguely, giving just the state of the river Ouémé at four levels (red-orange-yellow-green warning) (Kedowide & Satoguina, 2016). This information is often relayed by national television and radio stations over a very wide area, without any specific spatial details of the areas of land that will be affected, the expected height of the flood water and the likely damage to human and agricultural resources. Today's technological revolution is pushing the limits of scientific research to a new level of

efficiency in the service of societal problems (Betz *et al.*, 2023). It is therefore possible to put the population concerned at the source of the information by using the current open-source web of Google. This is an aspect that has been lacking in most of the work carried out to date in the study environment.

To fill this gap, and given that it is impossible to avoid the occurrence of seasonal floods through torrential rains and overflowing of rivers, we ask ourselves the question of how do we reduce the impact of the occurrence of hydroclimatic events on the population and agriculture? Therefore, the following research topic was formulated: “application of hydraulic flooding modeling for plant selection and land management in the Ouémé Delta (Benin): case of Adjohoun district”. This study is based on the principles of fluid dynamics to evaluate certain quantile of rain or discharge, the range of a flood according to the height of submersion and the space occupied by the water. Basically, the present research aims to make a hydraulic modeling to circumscribe the flood zones for plant selection and land management according to the occurrence of hydroclimatic events adjusted with the forecasting models. In other words, it is a question to forecast the future quantile of rainfall and discharge, which compared to the value of 2-5 years return period (water height & areas of submersion) to enable decision making on the cultivation areas and the type of cultivation to be adapted in the zone according to the probability of the occurrence of floods.

1.3. Study Objectives

1.3.1. General objective

The main objective of this research is to determine the flood zones for plant selection and land management according to the occurrence of hydroclimatic events adjusted with numerical predictions.

1.3.2. Specifics objectives

The specific objectives of this research are:



1. to evaluate the hydroclimate (rain & streamflow) events of the study environment and the occurrence of exceptional phenomena (2-year and 5-year)
2. to delimit the cultivation and flooding areas according to the occurrence of extreme floods events (2-year and 5-year)
3. to determine the best fitting flood forecasting models for the study region
4. to develop a dynamic early warning decision-making tool for crop selection and land management.



CHAPTER TWO:

LITERATURE REVIEW

2.1. Definitions

Rainfall flooding: "Rainfall flooding is caused by an intense rainfall event that generates a volume of water greater than the absorption capacity of soils and infrastructure" (Sjöberg *et al.*, 2014).

Fluvial flooding: "Fluvial flooding is caused by an increase in the discharge of a river that exceeds its capacity to hold rainwater, resulting in overflow" (Li *et al.*, 2015). They often occur when the amount of precipitation that falls on a watershed exceeds the river's capacity to carry that water away.

Hydraulic Modeling: "Hydraulic modeling is the simulation of the behavior of water discharges in complex systems using mathematical models" (Wu *et al.*, 2016). Hydraulic modeling is the use of mathematical models to simulate water discharge in river or urban drainage systems. Models are used to understand how runoff moves through a watershed and how it can be stored, absorbed, or discharged through drainage systems.

Intelligent plant selection for flood-prone areas: "Intelligent plant breeding for flood-prone areas involves selecting plant species that can tolerate flooding" (Klimkowska *et al.*, 2016). Intelligent plant breeding for flood-prone areas is an approach that involves selecting plants that are adapted to the specific environmental conditions of flood-prone areas. Selected plants must be able to withstand frequent flooding, waterlogged soils, and other harsh conditions. This may involve selecting water-resistant varieties or creating new varieties through hybridization and selective breeding.



Land management: "Land use planning can be referred to the planning and management of land use for sustainable social, economic, and environmental purposes" (Zhang *et al.*, 2019). Spatial planning is an approach to land use planning and management that aims to create sustainable and functional areas and environments for human communities and local wildlife. This can include the design of transportation systems, industrial areas, parks and open spaces, and residential areas that are functional, sustainable, and aesthetically pleasing.

2.2.Agricultural Activity and Flooding

For ages, human society has always been confronted with the problem of floods. Floods represent a major natural hazard in Africa, causing over 27 000 fatalities during the period 1950–2019 (Tramblay *et al.*, 2020). Extreme floods are unavoidable, but the lessons learned from experience can be used to reduce the damage they inflict and address “the probability of harmful consequences, or expected losses (deaths, injuries, property, livelihoods, economic activity disrupted or environment damaged) resulting from interactions between (natural, human-induced or man-made) hazards and vulnerable conditions” (Westen, 2010). The current challenge in flood damage research consists in developing a better understanding of the interrelations and social dynamics of flood risk perception, preparedness, vulnerability, flood damage, and management, and taking this into account in a modern design of flood damage analysis and flood risk management (Messner and Meyer, 2006).

The productivity of crops grown for human consumption is at risk due to the incidence of pests, especially weeds, pathogens, and animal pests (Oerke, 2006). For him, minor crop losses are economically acceptable; however, an increase in crop productivity without adequate crop protection does not make sense, because an increase in attainable yields is often associated with an increased vulnerability to damage inflicted. However, extreme rainfall causes flooding has increased in agricultural regions of the world over the past 50 years (Aderonmu, 2015; Bailey-



Serres *et al.*, 2012). In our case, the “crop flooding” term is used when all or part of a plant is underwater (Bailey-Serres *et al.*, 2012), and can be divided into either submergence or waterlogging (Sullivan *et al.*, 2001). Globally, flooding affects over 17 million km² of land surface annually, causing severe damage to plants and causes crop production losses (Voesenek & Sasidharan, 2013). Arable farmers incurred direct losses in the form of crop loss or yield reduction due to flooding and associated waterlogging of fields (Posthumus *et al.*, 2007). Potential management practices that can be used to mitigate soil waterlogging stress include the use of flood-tolerant varieties, adjusting management practices, and improving drainage (Gurpreet *et al.*, 2019). In this case, for Di Baldassare (2010), the introduction of early warning systems is, therefore, urgently needed.

2.3. Tests statistics

For any form of scientific procedure where a rigorous exploitation of a time series is in view, it is essential to verify the authenticity of the variable in a random variable context. Statistical tests (or hypothesis tests) allow clear, mathematically rigorous conclusions to be drawn from the data to be analyzed. A typical situation is to test whether or not the data support a hypothesis. The statistical test is useful when a decision must be made between two hypotheses:

H_0 : null hypothesis, corresponding to a status quo situation.

H_1 : alternative hypothesis, corresponds to the hypothesis that we want to demonstrate.

Compare at a significance level of $\alpha=5\%$, the null hypothesis is rejected when the p-value is less than the α value, implying an acceptance of the alternative hypothesis.

Statistical analysis of time series of hydrometeorological data is one of the tools for identifying climate variations. These tests will provide accurate insights into the state of the distribution of the variables involved.



Tests of homogeneity (Wilcoxon)

The Wilcoxon test is a non-parametric test for comparing the means of two independent samples. The Wilcoxon distribution is defined as follows:

Let X_1, \dots, X_n be independent and identically distributed from a sample X and Y_1, \dots, Y_m from a sample Y . The corresponding Wilcoxon statistic is defined as follows:

$$UU = \sum_{i=1}^n \sum_{j=1}^m S(X_i, Y_j) \text{ with } S(X_i, Y_j) = \begin{cases} 1, & \text{if } X > Y \\ \frac{1}{2}, & \text{if } X = Y \\ 0, & \text{if } X < Y \end{cases} \text{ (Eq:1)}$$

Tests of independence (Kolmogorov-Smirnov)

For the test of the independent nature of the distribution of the samples several statistical tests exist, however, according to Magel *et al*, (1997), the test of Kolmogorov-Smirnov is more robust. Indeed, the Kolmogorov-Smirnov test allows to compare two distributions. This test is used for tests of fit of a distribution to compare an empirical distribution determined from a sample to a known distribution. It can also be used to compare two empirical distributions.

Let be a sample E_1 , including n_1 observations, and F_1 the corresponding empirical distribution function. Let be a second sample E_2 , comprising n_2 observations, and F_2 the corresponding empirical distribution function.

The null hypothesis of the Kolmogorov-Smirnov test is defined by:

$H_0: F_1(x) = F_2(x)$ (H_0 : Both samples follow the same distribution)

$H_1: F_1(x) \neq F_2(x)$ (H_a : The distributions of the two samples are different)

2.3.1. Stationarity test (Dickey-Fuller & KPSS)

The purpose of a stationarity study is to show a non-random behavior of the time series of measurements. A time series X_t ($t=1,2,\dots$) is said to be stationary if its statistical properties such as expectation, variance, and autocorrelation do not vary in time.



More importantly, it will allow us to determine whether a state is stationary or not. To this end, identifying that a series is not stationary then allows us to study what type of non-stationarity it is. A non-stationary series can, for example, be stationary in difference: X_t is not stationary, but difference but $X_t - X_{t-1}$ is stationary.

However, there are two different approaches: tests for which the null hypothesis H_0 is that the series is stationary (Leybourne and McCabe's KPSS test), and those for which the null hypothesis is, on the contrary, that the series is not stationary (Dickey-Fuller test, Augmented Dickey-Fuller (ADF) test, Phillips-Perron test, DF-GLS test).

Dickey-Fuller test

This test was developed by Dickey and Fuller (1979) to identify a unit root in a time series for which it is believed that there is a first-order autoregressive term and possibly a time-related trend term.

As a reminder, the autoregressive model of order 1 noted AR (1)), can be written $X_t = \rho X_{t-1} + \varepsilon_t$ $t=1, 2, \dots$, where ε_t is a sequence of independent and identically distributed variables following a normal distribution $N(0, \sigma^2)$.

The series is stationary if $|\rho| < 1$. It is not stationary and corresponds to a random walk if $\rho = 1$.

If we add a constant and a time trend, the model is written

$X_t = \rho X_{t-1} + \alpha + \beta t + \varepsilon_t$ $t=1, 2, \dots$, where ε_t is a sequence of independent and identically distributed variables following a normal distribution $N(0, \sigma^2)$.

Dickey and Fuller have chosen to take the null hypothesis $\rho = 1$ because it has an immediate operational implication: if the null hypothesis is not rejected, then in order to analyze the series and eventually make predictions, it will be necessary to transform it by differentiation.

The two alternative hypotheses proposed are:

$H_0: |\rho| < 1$, the series is stationary

$H_1: |\rho| > 1$, the series is explosive.



Fuller (1976) had already shown that this approach can be generalized to an AR(p) model to determine whether there is a unit root without identifying whether the non-stationarity comes from a particular term.

KPSS stationarity test

KPSS stationarity test takes its name from its authors (Kwiatkowski, Phillips, Schmidt and Shin, 1992). Unlike the Dickey-Fuller tests, this test allows us to test the null hypothesis that the series is stationary. Let the model be:

$Y_t = \delta X_{t-1} + r_t + \varepsilon_t$ $t=1, 2, \dots$, where ε_t is a stationary error, and r_t is a random walk defined by $r_t = r_{t-1} + \mu_t$, where r_0 is a constant and where μ_t are independent and identically distributed with mean 0 and variance σ^2 .

The series Y_t will be stationary in the case where the variance σ^2 is zero. It will then be stationary in trend if δ is not zero and in level (around r_0) if $\delta = 0$.

Let n be the number of time steps available for the series. Let e_t be the residuals of the linear regression model of y_t on time and a constant when we want to test the stationarity in trend, and the deviations from the mean for the stationarity in level.

We define

$$s^2(l) = \frac{1}{n} \sum_{n=1}^n e^2 + \frac{2}{n} \sum_{s=1}^l w(s, l) \sum_{t=s+1}^n e_t e_{t-s} \quad (\text{Eq:2})$$

with

$$w(s, l) = 1 - s(l + 1) \quad (\text{Eq:3})$$

2.3 Forecasting and [Hydrologic Engineering Center's for River Analysis System] HEC RAS Modeling





Many studies (Lins & Slack, 1999; Déry & Wood, 2005; Petrow & Merz, 2009; Di Baldassarre & Montanari, 2009; Blöschl & Montanari, 2010) prove that it is difficult to separate the effects of natural climatic fluctuations and human activity like land management practices, urbanization, deforestation, river training and embankment on flooding. Some options for reducing the impact of flooding with new technology are to use computer models, remote sensing, flexible and focused warning systems for prediction and monitoring, and permanent or temporary flood–reduction systems (Hunt, 2002). The accuracy of models used for any flood forecasting and warning system is critical since an accurate flood forecast with sufficient lead time can provide advanced warning of an impending flood early enough so that flood damages can be reduced significantly (Adamowski, 2008). Indeed, according to the forecasting model, the numerical outputs provide a probable idea of future values over a confidence interval. The particular role itself is the rightful exploitation of the values predicted by the models. This is where hydraulic modeling comes in with HEC RAS. In the past, the model has been used in flood prediction contexts (Hicks *et al.*, 2005; Prafulkumar *et al.*, 2011; Habtamu *et al.*, 2021). Machine learning applied in areas of hydrologic processes is a recent approach and has been applied in rainfall-runoff modeling (Riad *et al.*, 2004), extreme hydrologic event analysis, streamflow computation (Veintimilla-Reyes *et al.*, 2016). The specificity here however is to determine the discharge and rainfall for the defined return periods necessary for the hydraulic modelling. Those results will be evaluated in the future with the best forecasting models for the observations of the study environment. In a univariate monthly variable context, the Holt Winters Smoothing Exponential (HWES), Autoregressive Integrated Moving Average (ARIMA), and Seasonal Autoregressive Integrated Moving Average (SARIMA) models are often used for their performance (Mansor *et al.*, 2021; Mbugua *et al.*, 2021; Jere *et al.*, 2023). These models are selected among other methods because they take into account trend and seasonality components (Mansor *et al.*, 2021).

Holt winters smoothing exponential forecasting model

Holt-Winters models, whether additive or multiplicative, allowed for forecasting a time step in the future. At the expense of simple or exponential smoothing methods, the Holt-Winters method allows us to take into account the notions of trend and seasonality (Teg *et al.*,2021). This method allows for a time-varying trend and a seasonal component of period p. The forecasts take into account the trend and the seasonality. This model involves three parameters (α , β , and γ). It is called additive when the seasonal component is stable over time. And multiplicative when the seasonal component varies over time. The larger the differences between observations, the larger the seasonal component. The equations of the model are given by:

$$L_t = \alpha \left(\frac{Y_T}{S_{T-M}} \right) + (1 - \alpha)(L_{t-1} - T_{t-1}) \quad (\text{Eq:4})$$

The trend estimate is given as:

$$T_t = \beta(L_t - L_{t-1}) + (1 - \beta)T_{t-1} \quad (\text{Eq:5})$$

The seasonality estimate is developed as:

$$S_t = \gamma \left(\frac{Y_T}{L_t} \right) + (1 - \gamma)S_{t-s} \quad (\text{Eq:6})$$

The forecast for m periods into the future is written as:

$$F_{t+m} = (L_t + mT_t)S_{t-s+m} \quad (\text{Eq:7})$$

Here; we have the following:

Y_T :is the new observation

L_t :is the current level estimate of series

L_{t-1} :is the previously smoothed level

α : is the smoothing constant for the level

β : is the smoothing constant for trend estimate

T_t : is the current trend estimate

T_{t-1} : is the previously smoothed trend



γ : is the smoothing constant for the seasonality estimate

S_t : is the seasonal component estimate

S_{t-s} : is the previous seasonal component

m: is the number of seasons in a year

s: is the length of seasonality (number of periods in the season)

t: is the time period

$0 \leq \alpha \leq 1$; $0 \leq \beta \leq 1$; and $0 \leq \gamma \leq 1$ (Teg *et al.*, 2021)

ARIMA & SARIMA forecasting model

ARIMA models are capable of representing both stationary and nonstationary time series data.

Seasonal Auto Regressive Integrated Moving Average = SARIMA (p, d, q)(P, D, Q)_s

Auto Regressive Integrated Moving Average = ARIMA (p, d, q)

Where:

p is the order of the non-seasonal autoregressive model,

q is the order of non-seasonal moving average model,

P is the order of seasonal autoregressive model,

Q is the order of seasonal moving average model,

d is the number of non-seasonal differences,

D is the number of seasonal differences

s is the periodic term (Mohammad, 2015)

The four important steps required for identifying the correct forecasting model are stationary test, identification of model, model fitting and finally performance evaluation (Mohanad *et al.*, 2018). The degree of differencing d (and D) will be determined using ACF and PACF followed by the Augmented Dickey-Fuller Test (ADF). For the different variables p, q, P and Q, the AIC



& BIC minimization criterion will be used to obtain the best parameters (identification of model, model fitting and finally performance evaluation).

2.4.Plant Selection and Land Management

Floods are a major threat to agriculture, as they can cause significant crop losses and soil damage. To minimize these losses, farmers can opt for flood-tolerant crops, adapted agricultural practices, or preventive land management.

A work conducted in India by Singh *et al.* (2019) showed that some plants were able to withstand flooding. They observed that rice cultivation was often affected by floods, resulting in lower yields. So, they sought to identify plants that could withstand flooding and provide high yields. After a series of tests, they concluded that some rice and maize varieties were able to grow even during floods, which could help farmers preserve their crops and maintain their production levels (Singh *et al.*, 2019).

A work conducted by Islam *et al.* (2020) on the effect of rice cultivation on flooding shows that for example rice cultivation can increase the vulnerability of flood-prone areas, but the use of flood-tolerant rice varieties can reduce crop losses and improve the resilience of farming communities. Outside of rice in another work, conducted by Mohanty *et al.* (2019) on the effectiveness of using cover crops to reduce crop losses caused by flooding. The researchers found that the use of cover crops such as sorghum and millet can reduce crop losses and improve soil quality. Finally, a work by Liu *et al.* (2021) examined the effectiveness of using flood-adapted plants to restore river ecosystems. The researchers identified several species of plants adapted to flood-prone areas and found that the use of these plants can improve the biodiversity and resilience of river ecosystems. In addition to flood-tolerant crops, there are also agricultural practices that can help prevent or mitigate flooding. For example, a work done by Sarker *et al.* (2020) examined the effect of different agricultural practices on reducing flood risk in a watershed. The results showed that a good practice (strip cropping, live hedge planting,



agroforestry) can help reduce flood risk by improving the capacity of soils to absorb water, reducing erosion, and regulating stream flow.

In conclusion, there are different approaches to preventing and mitigating the effects of flooding in agricultural areas. Selection of flood-tolerant crops, agricultural practices such as strip cropping and agroforestry, and land use planning based on landscape characteristics can all help reduce flood risk. Ecosystem-based approaches can also be effective, although they are subject to additional limitations and considerations (Jonkman & Kelman, 2005).



CHAPTER THREE:

3.1. Study Area

The study area is located in the tropics, more precisely in the Gulf of Guinea. It is a region governed by the intertropical front and is located between Helene High in the South and Azores High in the North. Thus, the climatic forces at play are the Harmattan (from North to South) and the Monsoon (from South to North).

The district of Adjohoun is in the region of Ouémé located in the south-eastern part of Benin. It is located between latitudes 6°60' and 6°80' N and longitudes 2°42' and 2°58' E and covers an area of 315,713 km² (Figure 3-1).

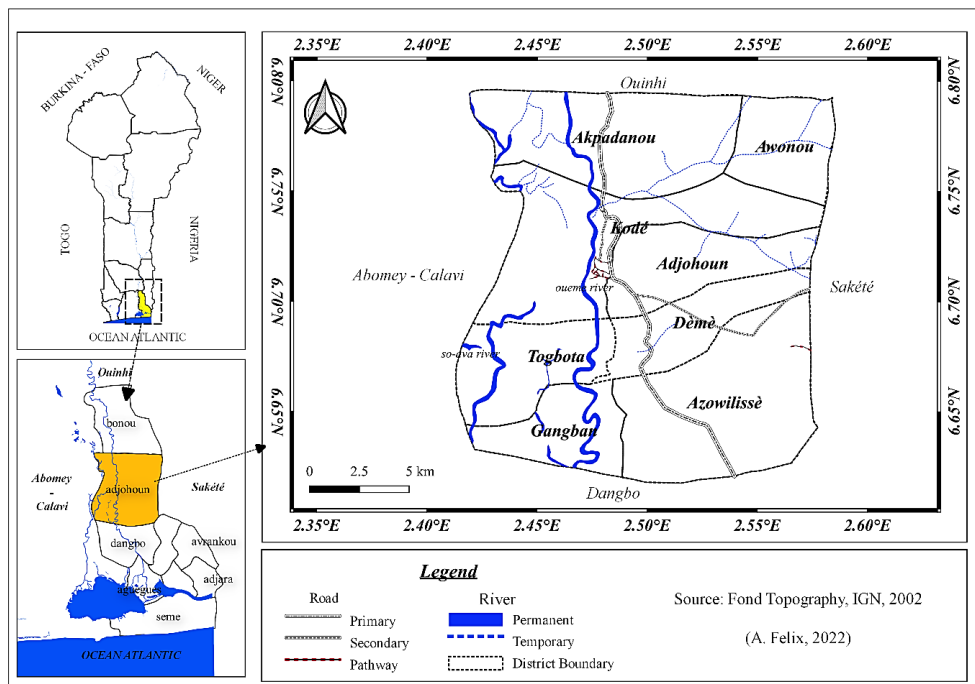


Figure 3-1: Study area map

Hydrographically (Figure 3-1), the district is mainly crossed by the Ouémé River over a length of 24.97 km from North to South and partially by the Sô-Ava River (10.09km). The average annual rainfall is 1121mm (Totin *et al.*, 2016). It is distributed in, two rainy seasons from April to July and from September to August when rain floods occur especially from June to July. Two (2) dry seasons are from December to March and from July to August when a river flood is

observed by the overflow of the Ouémé River during September with the contribution of rainfall from the North of the country (Totin *et al.*, 2016).

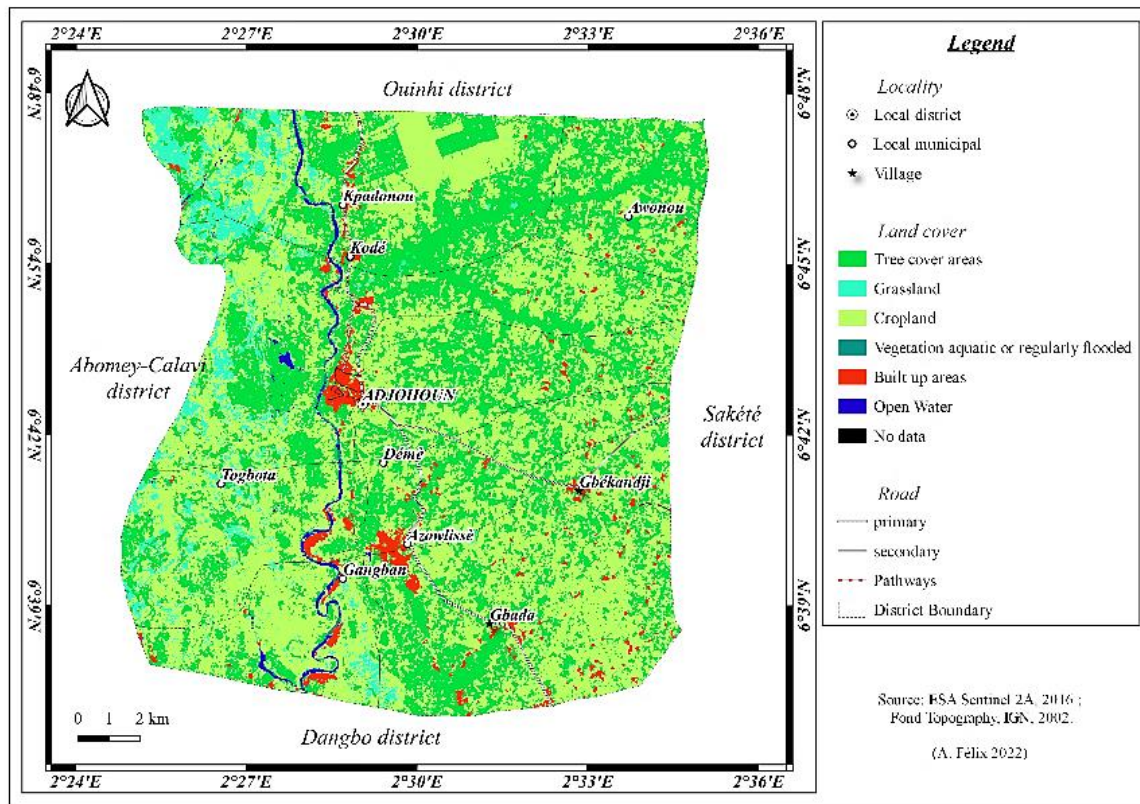


Figure 3- 2: Land cover of study area, (source: European Spatial Agency, Sentinel 2A)

On land cover (Figure 3- 2), considering the 2016 satellite data from the European Space Agency (ESA, 2016), the district is dominated by the classes of "Tree cover areas" on 128.15km² and "Cropland " on 106.25km²(

Table 3- 1). Although the agricultural areas are heterogeneous, most of them take place in the West Valley. A cartographic assessment of the topography however shows that the valley of the district is an aggregation of topographic elevation below 10m (Figure 3- 4).

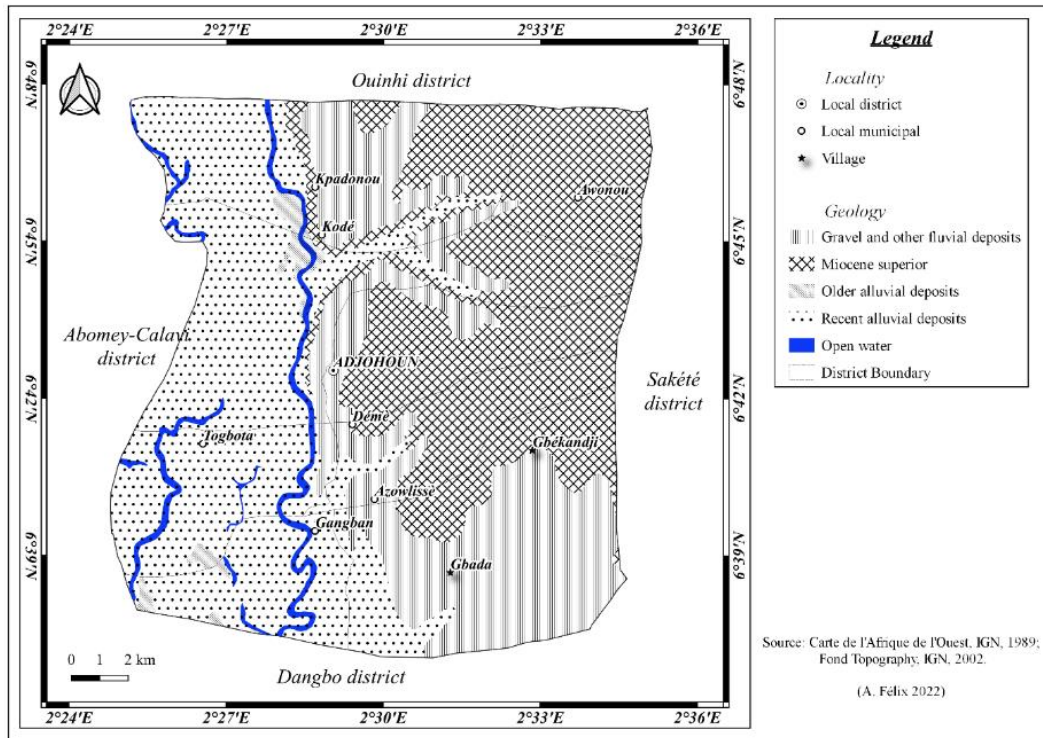


Figure 3- 3: Geology map study area

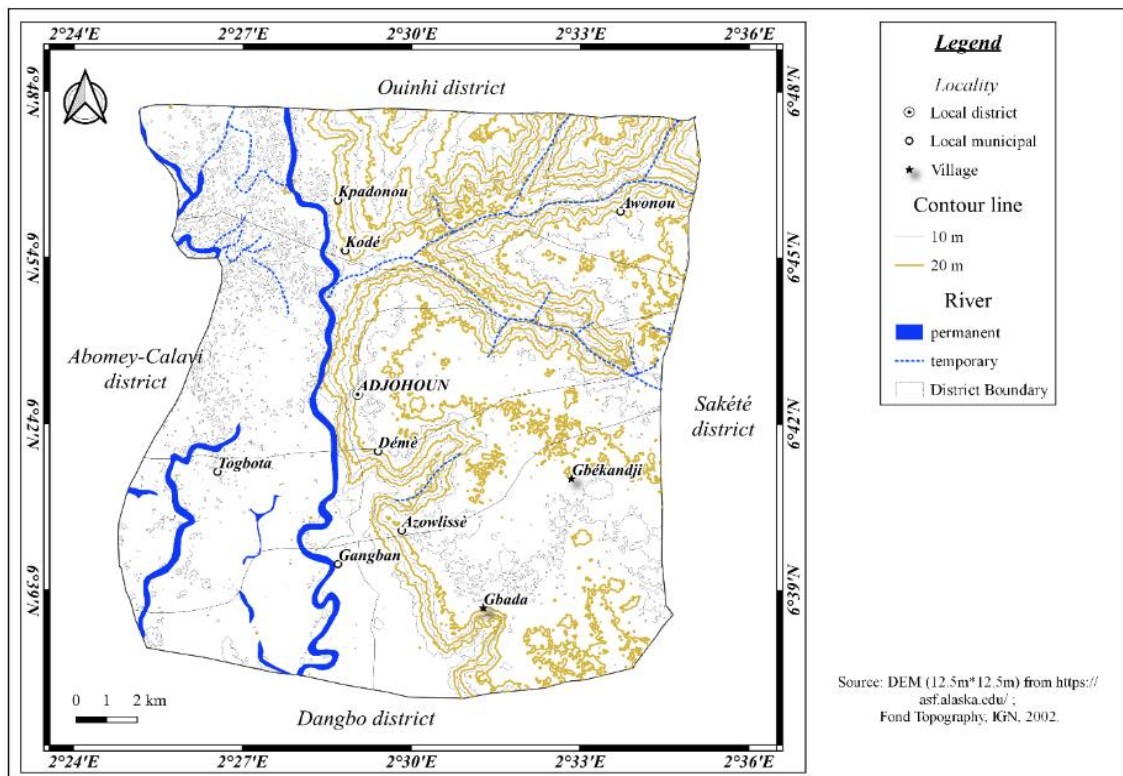


Figure 3- 4: Contour line map study area

Table 3- 1: Land cover class statistic year 2016 (source: European Spatial Agency, Sentinel 2A)

Description	Area (km ²)
Tree cover areas	128.15
Shrubs cover areas	0.11
Grassland	15.23
Cropland	106.35
Vegetation aquatic or regularly flooded	0.61
Built up areas	8.89
Open water	2.35
No data	0.01

On the geological level, the geological of the district is dominated by recent alluvial deposits, gravel and other fluvial deposits and Miocene Superior (Figure 3- 3). These deposits promote soil renewal, supply rich organic matter, and makes water available for irrigating the fields. It is for this reason that the West River region of the district is in high demand for agriculture.

With a population clearly negligible compared to the main Ouémé region (Figure 3- 5 & Figure 3- 6), the district of Adjohoun is classified as a region with great agricultural potential, with its valleys crossed by the Ouémé River (PCM, 2015). A total of 74,956 inhabitants according to the fourth General Population and Housing Census (INSAE, 2013), the growth rate is 2.54% between 2002 – 2013. The district is subdivided into eight (8) subdistricts namely: Akpadanou, Azowlissè, Adjohoun, Awonou, Dèmè, Kodé, Gangban and Togbota. Although the Adjohoun sub-district is the economic center of the region, it is Azowlissè sub-district (22,057 inhabitants, 2013) which concentrates a large population, followed by Gangban (15,602 inhabitants, 2013) and Dèmè in last position with its 2337 inhabitants (Figure 3- 7). Throughout the territory, the density is 269 inhabitants/km² (INSEA, 2013).



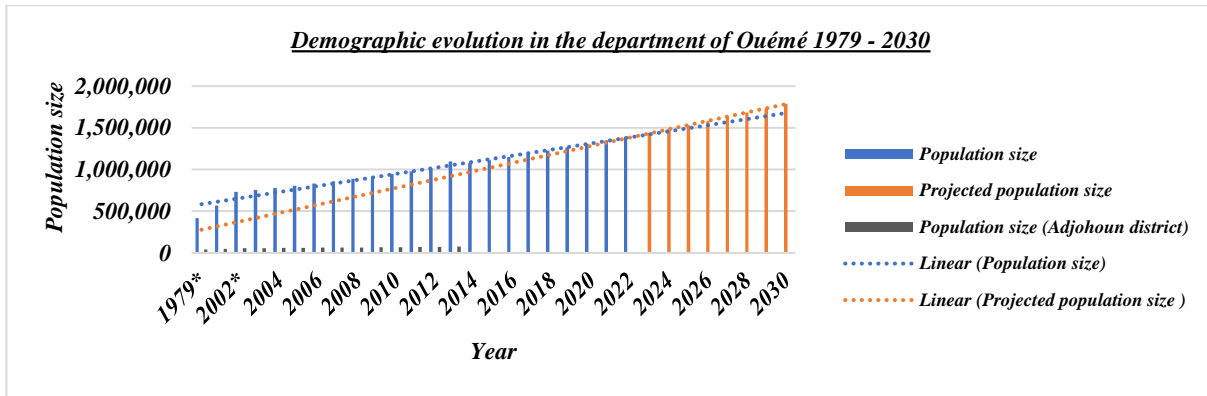


Figure 3- 5: Ouémé region population size 1979 – 2030 (source : INSAE, 2013)

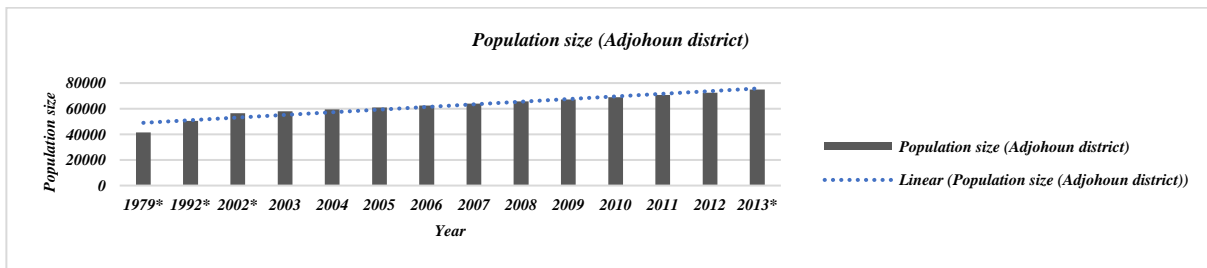


Figure 3- 6: Adjohoun district population size (source: INSAE, 2013)

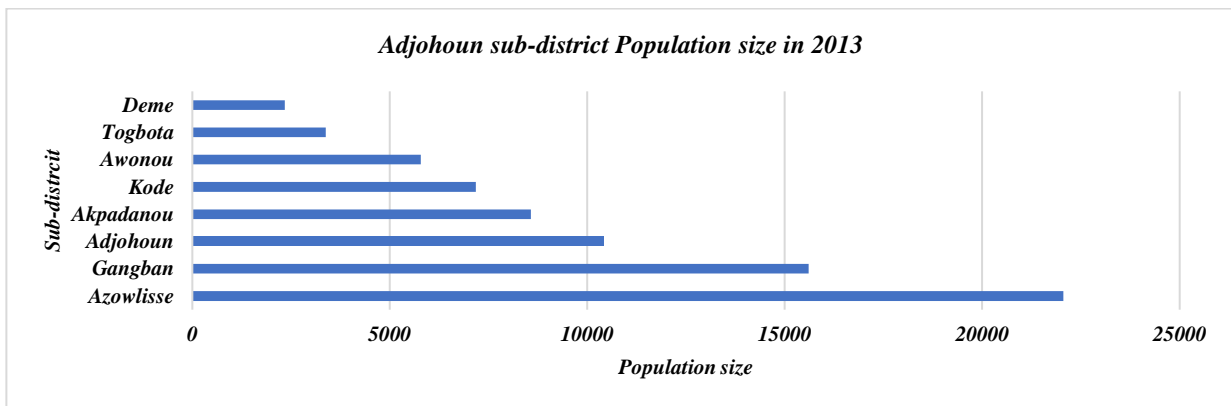


Figure 3- 7: Adjohoun sub-district population size (source: INSAE, 2013)

3.2.Data Used and Methods

This section presents the different methods of collecting and processing data. This study used, meteorological data including rainfall, temperature, and evapotranspiration; hydrological data such as discharges and spatial data (digital elevation model, satellite images, etc.). QGIS, HyFRAN plus, HEC RAS, R and Python are the software packages used for the study.



3.2.1. Data collection

The daily climatic data was provided by the Agency for the Safety of Air Navigation in Africa and Madagascar (ASECNA), and the hydrological data was provided by the DG-Eau (General Directorate of Water) Benin. Rainfall and temperature data concerns the synoptic station of Cotonou from 1922 to 1984 and 1990 to 2017 is collected. For hydrological data, the streamflow and water level (from the Bonou station) at the entrance of Adjohoun district are used, from 1948 to 2017 with years 2006, 2009, and 2013 without measurement. The district is not equipped with a rainfall station, so the data from the nearest synoptic station (Cotonou synoptic station) is considered for this study. Cotonou synoptic station is 45km away from the study area. A synoptic station can represent range of 200 km in vast plains (Hatem *et al.*, 2012, Hubbard 2001).

These data are relatively complete for the temperature and rainfall series but unfortunately have very significant gaps for the series of water discharges and heights, during the years 2006, 2009, and 2013. In addition, data from the geographic is collected. Those data concerning the valley administrative boundary and river path are from the National Institute of Geography (IGN) and a Sentinel 2A of 2016 and 2020 from the European Space Agency "ESA" (European Spatial Agency) available on www.esa.int/ESA_Multimedia/Images/2017/10/African_land_cover and www.esa.int/Applications/Observing_the_Earth/Space_for_our_climate/ESA_global_land_cover_map_available_online) with a spatial resolution of 20 m * 20 m. The Digital Elevation Model (DEM) of 12.5m × 12.5m pixel size downloaded from <https://asf.alaska.edu/> (Li, 2010) covering the study area are used.

3.2.2. Data corrections

The concentration of these missing data over several months during the years 2006, and 2009 and concerning the gaps from 1885 to 1889 forced us to ignore them. Also, with the discharges,



the years without measurements have been ignored. The purpose of ignoring its missing values is to take into consideration only values actually observed and not approximate.

3.5. Data Processing Methods

In order to achieve the specific objectives formulated, a research methodology was adopted. Each specific objective corresponds to its own research methodology.

3.5.1 Characterize the hydroclimate (rain & streamflow) events of the study environment and the occurrence of exceptional phenomena (2-year and 5-year)

Rainfall and hydrometric indices allow characterizing the temporal heterogeneity of climatological variability and identifying major trends in hydroclimatic series (El Aoula, 2021). To better visualize the periods of deficit and surplus on an annual scale, these indices were centered and reduced using the following formula:

$$\varphi = \frac{\gamma - \rho}{\sigma} \quad (\text{Eq:1})$$

Where φ is the Reduced Centered Variable (Rainfall Index (RSI) or Hydrometric Index (HSI) depending on the variable under study), γ is the cumulative value of the variable over a given period t , ρ is the smoothed moving average of the time series over the study period, and σ is the standard deviation of the series over the study period (Hallouz *et al.*, 2013). Here, the emphasis is put on wet years and dry years. Furthermore, to weigh the hydroclimatic extremes of the study environment, the descriptive rank statistic is applied to the rainfall and discharge data. Extreme hydroclimatic events are often evaluated through the 95th and 99th percentiles respectively (Sadio *et al.*, 2020, Kodja, 2018, Amoussou, 2014).

In frequency analysis, the observations must be independent and identically distributed (El Adlouni, 2008). For this, a global assessment of the time series with statistical tests of homogeneity and independence at the prime is necessary. A frequency analysis can be described as the search for the frequency of occurrence of a particular event with an associated probability of non-exceedance. In the framework of this study, the evaluation concerns extreme



flooding events. Therefore, a flood situation on a daily scale, hence the consideration of the maximum daily annual values. From the chronology of precipitations (P) and discharges (Q) an extraction of the maximum daily annual rainfall the maximum daily P_{jmax} as well as the annual maximum daily discharge rates Q_{jmax} was carried out to serve as the basis for the frequency analysis in our context. An extensive analysis is done to evaluate the correlation between the variables flow, water level and precipitation. The correlation matrix is evaluated by considering the temporal chronology of the flow series in order to have a uniform correspondence of the days of observation given the character of shift of the days of different measurements.

Calculation of empirical frequencies and characterization of return periods

A study of frequency analysis allows to highlight the distribution law of daily maximum rainfall and discharge in our case. The maximum daily data obtained from the Cotonou station (P_{jmax}) and Bonou (Q_{jmax}) was subjected to a frequency analysis. To realize it, we used the computer program HYFRAN (Hydrological FRequency Analysis PLUS).

The initialization to a frequency analysis is to estimate the values related to exceptional floods. According to the occurrence of an event, an inverse probability is associated with it. In one particularity, the higher the return period, the lower the probability of occurrence. Similarly, a high probability of occurrence is associated with a low return period ($P_{<} = \frac{1}{1-T}$). The main goal of this section was to characterize the probabilistic occurrence of extreme events in each series in play.

It was considered return periods T of 2 years and 5 years with maximum daily data (P_{jmax} & Q_{jmax}) of each year, which were adjusted with adjustment laws of the extreme values.



After an ascending order of a sample of maximum rainfall or discharge of size n , the expression of the empirical or experimental frequency of non-exceedance of Hazen for a value x of rank i is noted:

$$f(x) = \frac{i-0.5}{n} \quad (\text{Eq:8})$$

where n is the size of the sample considered.

The determination of the parameters of each adjustment model and the choice of the best model representing the distribution of the annual daily maximums based on the criteria previously outlined allow us to determine with confidence the associated value for the 2 and 5-year return period floods. Determining a flood for a return period of 2 years is equivalent to estimating the chance of occurrence of a flood of 50% annual occurrence. At the not exceeding, it is determined by the formula below:

$$T = \frac{1}{1-F} \quad (\text{Eq:9})$$

where T : return period (year); F : non-exceedance frequency

The purpose of the frequency analysis is to determine the annual probabilistic occurrence of an exceptional flood value likely to generate rare floods. The values resulting from this analysis were used for the hydraulic modeling whose outputs were mapped and correspond to critical thresholds of abnormal events. However, in order to increase the chance of apprehending these hydroclimatic events, a statistical forecast is necessary. The forecast allowed us to predict future events with a confidence interval of about 95% of cases. On this numerical evidence, and with the availability of frequency extrema, it will be possible to have a margin of maneuver, by comparing the predictions to the critical threshold of disasters.

Within this framework, for the variable's precipitation and discharge, the maximum daily values are extracted and thus constitute a new database to which tests of hypotheses of homogeneity



and independence was applied. For this purpose, the HyFRAN software has been used as well as for the determination of the defined return periods.

Among these laws are the GEV, Gumbel, and Weibull fitting laws (Hounkpè *et al.*, 2015, Bacharou *et al.*, 2013). The more values tend to follow the distribution of values of the mean-to-extreme fitting law, the more likely this fitting law is to estimate rainfall and discharge extremes. In search of a certain assurance of the best fitting law for daily maxima, in addition to critical graphical analysis, two numerical evaluation criteria were used. These are the AIC and BIC criteria, the more their values are minimal for a law, the better it is.

Law of adjustment: GEV, Gumbel, Weibull

In hydrology, the GEV, Gumbel, and Weibull distributions are among the most widely used in the analysis of extremes (Katz *et al.*, 2002; Stedinger *et al.*, 1993). For a random variable, distributed according to a GEV distribution, the distribution function is written as:

$$f(x) = \frac{1}{\alpha} \left[1 - \frac{k}{\alpha} (x - \mu) \right]^{\frac{1}{k}-1} \exp \left\{ - \left[1 - \frac{k}{\alpha} (x - \mu) \right]^{\frac{1}{k}} \right\} \text{ (Fisher and Tippet (1928)) (Eq:10)}$$

For a random variable, distributed according to a Gumbel distribution, the distribution function is written as:

$$f(x) = \frac{1}{\alpha} \exp \left[- \frac{x-\mu}{\alpha} - \exp \left(- \frac{x-\mu}{\alpha} \right) \right] \text{ (in Kouassi *et al.*, 2018) (Eq:11)}$$

For a random variable, distributed according to a Weibull distribution, the distribution function is written as:

$$f(x) = \frac{k}{\alpha} \left(\frac{x}{\alpha} \right)^{k-1} \exp \left[- \left(\frac{x}{\alpha} \right)^k \right] \text{ (Weibull W., 1951) (Eq:12)}$$



With $\mu (\in \mathbb{R})$, $\alpha (> 0)$ and $k (\in \mathbb{R})$ are the position, scale, and shape parameters determined by the likelihood method, respectively.

Validation of the statistical model: AIC, BIC and graph

The validation of a model is based on the evaluation of the deviations of the estimates compared to the observations. The two standard methods are often a graphical and numerical analysis. A graphical analysis corresponds to the evaluation of the superposition or mean deviation of the values predicted by the model from the actual observations. It is a method qualified as rudimentary but which proves its worth. In addition, we have a numerical approach through the AIC and BIC criteria. These two criteria allow us to choose the best-fitting distribution by taking into account the estimation error and parsimony (number of parameters to be fitted) (Kouassi *et al.*,2018). The distribution for which the values of the two criteria are the lowest is the one selected.

The expression of the Akaike Information Criterion (AIC) is as follows (Goula *et al.*,2010; Ague & Afouda, 2015; Kouassi *et al.*,2018):

$$AIC = -2\text{Log}(L) + 2n_p \quad (\text{Eq:13})$$

where L : likelihood and n_p : number of parameters

The Bayesian Information Criterion (BIC) expression is as follows (Goula *et al.*,2010; Ague & Afouda, 2015; Kouassi *et al.*,2018):

$$BIC = -2\text{Log}(L) + 2n_p\text{Log}(N) \quad (\text{Eq:14})$$

where L : likelihood; n_p number of parameters; N sample size.

3.5.2 Delimit the cultivation and flooding areas according to the occurrence of extreme floods events (2-year and 5-year)

Trend of spatial repartition of land use in the study





The goal is to extract the cropland class in order to know where the population and the spatial cultivation tendency in the district. Overall, a spatial distribution is often based on the natural resources of the environment capable to meet the expectations of the community. According to Brown *et al.* (2005), land use trends affect a variety of changes in ecological systems around the world. Agricultural activities being the main source of socio-economic development in the region has a direct or indirect impact on the distribution of conurbation (Tcheignon & Guidibi, 2006). Although the swollen Ouémé River is a source of fertilization for agricultural land (Yabi, 2019; Mouritala, 2018), it is also sometimes a source of disasters due to its overflow. Spatial mapping is used to assess the distribution of land use classes vulnerable to hydroclimatic problems. As such, the important classes facing hydroclimatic issues are mainly human habitats and agricultural areas (Bani *et al.*, 2016; Koumassi 2014).

A sentinel 2A data for the years 2016 and 2020 available on the European Space Agency platform are used. Those satellite data sets are validated by sixteen experts with more than three thousand (3 000) reference land cover zone, with 73% overall weighted accuracy by zone. Twenty-two (22) main classes were established by using the United Nations Food and Agriculture Organization's (FAO) Land Cover Classification System (LCCS) (ESA, 2021) as the legend.

The study area comprises seven main land cover classes namely; water, built up areas, herbaceous wetlands, shrubs cover areas, grassland, cropland and tree covers areas. From these classes, an extraction of shapefiles related to the built-up areas and cropland classes was done and mapped, followed by a description of their distribution in space and some related summaries statistics. This result offered the possibility of cross-referencing it with the results of hydraulic modeling in terms of water levels and submerged areas for the land management aspect.

Hydraulic modelling

Hydrologic Engineering Center's River Analysis System (HEC RAS), is an open-source software (<https://www.hec.usace.army.mil/software/hec-ras/>). In this work, the latest version 6.3 was used. HEC RAS was developed by US Army and classified as the most used software for 1D or 2D hydraulic calculations (Hydrologic Engineering Center, 2016a). It is used also to analyze constructed or natural network channels, levee-protected areas, overbank/floodplain areas, etc (Hydrologic Engineering Center, 2016b).

It has four main components: (a) steady flow water surface profiles, which is used for calculating water surface profiles; (b) unsteady flow simulation, to simulate one-dimensional (1D), two-dimensional (2D), and combined one/two-dimensional (1D/2D) unsteady flow on a full network of open channels and floodplains; (c) sediment transport computations, which is applied for the simulation of 1D sediment transport/movable boundary calculations resulting from scour and deposition; and (d) water quality analysis; which is intended to allow the user to perform riverine water quality analyses (Hydrologic Engineering Center, 2016a, 2016b). Standard applications of this model include flood wave routing and flood inundation studies (Arturo *et al.*, 2016). The HEC-RAS model was developed to perform full 2D computations and solves both the 2D St Venant equations and the 2D diffusion wave equations through an implicit finite-volume solution (Luliia S. *et al.*, 2019). To run the model, data like the geospatial data, hydrograph data (river flooding), hyetograph data (precipitation data), Maning coefficient table, soil infiltration rate, and the digital elevation model of the region are required. To complete the models, a two-dimensional (2D) unsteady flow simulation was run to propagate flow and precipitation from the return period (2 and 5 yrs) quantiles values.

The unsteady flow component can be used to perform subcritical, supercritical, and mixed flow regimes (subcritical, supercritical, hydraulic jumps, and drawdowns) calculations in the unsteady flow computations module (Hydrologic Engineering Center, 2016b). To proceed, spatial (Digital Elevation Model, land use, administrative boundary) data is required. In this



way, the study zone extends largely than the Adjohoun district and was drawn with an applied 50m*50m grid on the DEM. Then the request boundary condition is affected based on the type of modeling. Two boundary conditions were assigned for rainfall flooding like the hyetograph as the propagate precipitation and a normal depth at the downstream. While for river flood modeling, a hydrograph is defined as the upstream boundary condition, and a normal depth is computed and assigned for downstream. However, inasmuch as an unsteady flow, a data transformation is needed to meet the times series format for modeling. In this case, a Gauss function was used to distribute during a time t the calculated value of each return period in order to approach the hydrograph/hyetograph shape. It considers that the rainfall (hyetograph) duration is daily (24 hours) with a peak at 9:45. For the return period value of streamflow, a Gauss function distribution is applied and transform it into cumulative time series. Using the cumulative time series let us to fit the normal estimated value from frequential analysis. The defined time steps are set to 15min.

The expected outputs from this modeling are inundation map and databases. Inundation visualization is accomplished in the HEC-RAS Mapper portion of the software. Inundation maps were animated, with multiple background layers (terrain, aerial photography, etc...) to assess the flooding behavior for some land management purposes as recommendations. The final result was exported and converted into spatial data to compute some statistics like: water area submersion and water level submersion. The main output for some identified regimes flows or rainfall was processed to achieve the last specific objective. But it's very important to specify the seasonality and/or stationarity of rainfall events and flow rates in the study area for statical forecasting. The importance of this seasonal forecast is to provide farmers and planners with vital information on the risk and extent of flooding for the next (future) growing season. This information, applied to submergence water level references, gives an idea of the occurrence of



flooding in the next cropping season, and thus defines the flood zones and the submergence water level for crops, to enable a judicious choice of the type of crop or the type of development that is most suitable. The following paragraphs discuss the methodology for seasonal forecasting and optimal crop selection.

3.5.3. Identifying the best fitting flood forecasting models for the study region

Forecasting makes use of various techniques, whether through simple, double, or triple smoothing, machine learning, or through an autoregressive mechanism to predict possible future observations. A common fact between all existing forecasting models is the exploitation of past and present observations for forecasting (Teg *et al.*, 2021). Among many others, models such as Holt-Winter smoothing exponential, ARIMA, and SARIMA forecasting models are used. These three statistical prediction models are used using monthly maximum flow values as input data. These extracted values were subjected to stationarity, seasonality and autocorrelation tests in order to identify the type of regime. Thus, the particularity is to identify the best statistical prediction according to the type of regime. The best model will be selected on the basis of a graphical assessment and a numerical evaluation (MAE, RMSE and MAPE).

The evaluation criteria: MAE, RMSE, MAPE, graphic

In a context of multiple forecasting through various models, the choice of the best model will relate to evaluate the performance of the forecasts. In this perspective, the database is divided into two (2) distinct parts of which one part will be used for calibration and another for validation. In other words, on the observations, one year will be ignored and used as a reference for the evaluation of the performance of the models. On this, in addition to a graphical appreciation, the statistical criteria of evaluation of deviations such as: mean absolute error (MAE), mean squared error (MSE), root mean square error (RMSE), and mean absolute percentage error (MAPE) will be used.

- Mean absolute error (MAE)



The mean absolute error (MAE) measures the accuracy of fitted time series values. MAE expresses accuracy in the same units as the data, which helps conceptualize the amount of error and is calculated by the following formula:

$$\text{MAE} = \frac{1}{\text{Number of observation}(n)} \sum_{t=1}^n |\text{Observation}_t - \text{Predicted}_t| \quad (\text{Eq:15})$$

➡ mean squared error (MSE)

The mean squared error (MSE) is a more sensitive measure of a substantial forecast error than MAE, and the following formula estimates it:

$$\text{MSE} = \frac{1}{n} \sum_{t=1}^n (\text{Observation}_t - \text{Predicted}_t)^2 \quad (\text{Eq:16})$$

➡ mean square error (RMSE)

The root mean square error (RMSE), like the MSE, penalizes significant errors but has the same units as the forecast, so its magnitude is easily interpreted:

$$\text{RMSE} = \sqrt{\text{MSE}} \quad (\text{Eq:17})$$

➡ mean absolute percentage error (MAPE)

The mean absolute percentage error (MAPE) measures the accuracy of fitted time series values. MAPE expresses accuracy as a percentage, and the following formula estimates it:

$$\text{MAPE} = \frac{1}{n} \sum_{t=1}^n \frac{|\text{Observation}_t - \text{Predicted}_t|}{\text{Observation}_t} \quad (\text{Eq:18})$$

After the analysis for errors, we compare the accuracy measures of the forecast models. Less MAPE and less RMSE often are the best way to define the best forecast (Teg *et al.*, 2021).

3.6 Develop a dynamic early warning decision-making tool for crop selection and land management

In order to link modeling results to plant selection, a synthesis of previous scientific research was carried out, with priority given to local crops. In the Adjohoun district, several crops are grown, including maize (*Zea mays*), sorghum (*Sorghum bicolor*), rice (*Oryza sativa*), sweet potato (*Ipomoea batatas*), cassava (*Manihot esculenta*), yam (*Dioscorea species*), cowpea



(*Vigna unguiculata*), soyabean (*Glycine max*), mango (*Mangifera indica*), orange (*Citrus sinensis*), avocado (*Persea americana*), tomatoes (*Solanum lycopersicum*), okra (*Abelmoschus esculentus*), chili pepper (*Capsicum species*) and teak (*Tectona grandis*), palm tree (*Phoenix dactylifera*) (Akpadda *et al.*,2016; Basile A., 2017). By considering these plants, information was synthesized on their (a) height class, (b) maximum water level tolerated by the crop, (c) optimal soil type and (d) infiltration rate of the soil hosting the crop. This information is vital for assessing the potential for selecting a preferred crop type for an agricultural area. Consequently, a proven knowledge of (e) soil type, (f) infiltration rate (mm/h), maximum submergence height of the plant and its own height enables a clear decision to be taken on the insurance and potential risk incurred in the event of flooding in the said area. And so, the primary outcome of this section is the minimization of the risk of loss and damage in the event of flooding, through the optimal selection of a type of agricultural crop in a hydraulically stable environment ("crop capable of withstanding the height of downstream water submersion for a time t before total infiltration"). The secondary outcome is that of reference and decision-making support in the district's construction and land-use planning projects.

For this purpose, it would be very useful to put the results online in google earth's ".kmz" format for direct access to the information. Initially, reference values close to probabilities of 20% (5yrs) and 50% (2yrs) were chosen. For each reference value, the hydraulic model outputs were compressed in Keyhole Markup Language (Qref.kml) format and edited in Quantum (QGIS). Editing enabled us extract and add the necessary information (water depth (ft), conversion unit(cm), Municipal, Crop-maximum water level (m), Sol-infiltration rate(mm), etc) to each pixel unit (50m*50m). At the end of the process, these "Qref.kml" files were converted into compressed "Qref.kmz" files for 3D visualization in Google Earth with smartphones and/or computers.



To access this data, all the information was compiled and saved on Google Drive. On this platform, a website has been set up and will be deployed for unlimited access to the administrative staff and population of Adjohoun for use. Beyond these aspects, the web platform will be used to share and publish seasonal forecast results (*Qpredict*). In action, for any *Qpredict* prediction or observation event less than or equal to a *Qiref*, the corresponding *Qref.kmz* file is downloaded and used. However, it should be stressed that these files have been broken down by locality to enable very rapid reading by smartphones.



CHAPTER FOUR:

RESULTS AND DISCUSSION

4-1. Hydroclimate (Rain & Discharge) Events of the Study Environment

In the study area, the results showed a bimodal rainfall regime with two rainy seasons and two dry seasons against a unimodal hydrometric regime (Figure 4- 1). Distinctly, we notice:

- high rainfalls in the major rainy season from April to July
- low rainfalls in the minor rainy season from mid-November to October
- high dry spells in the dry season from December to March
- low dry spells in the dry season from August to September.

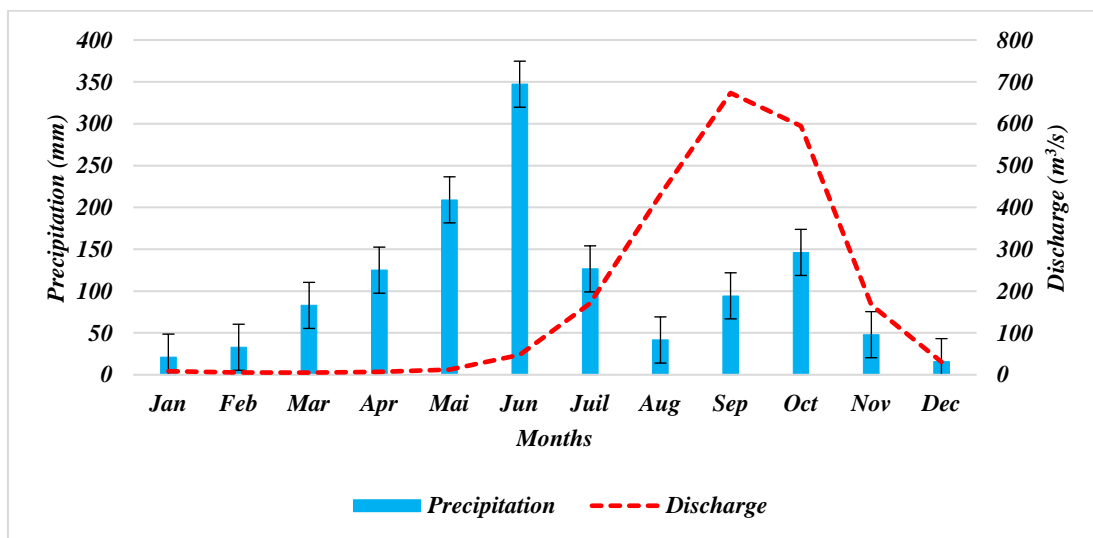


Figure 4- 1: Monthly average of precipitation and discharge at Adjohoun district

As for the unimodal trend character of the water flow and a peak in the flow of the Ouémé River during the period of the season, it is due to the waters of the basin coming from the north. The end of the monsoon season coincides with the only rainy season in the north of the basin, drained by the Ouémé River (Totin *et al.*, 2016).



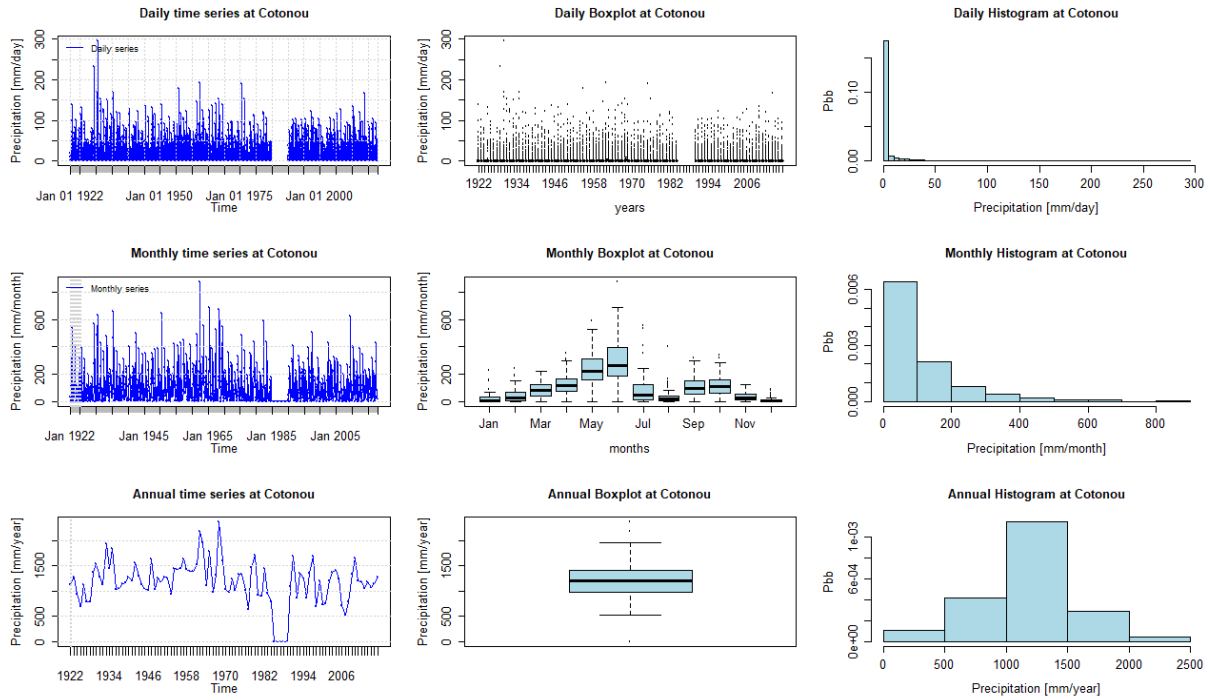


Figure 4- 2: Precipitation daily/monthly/annually Cotonou time series plots

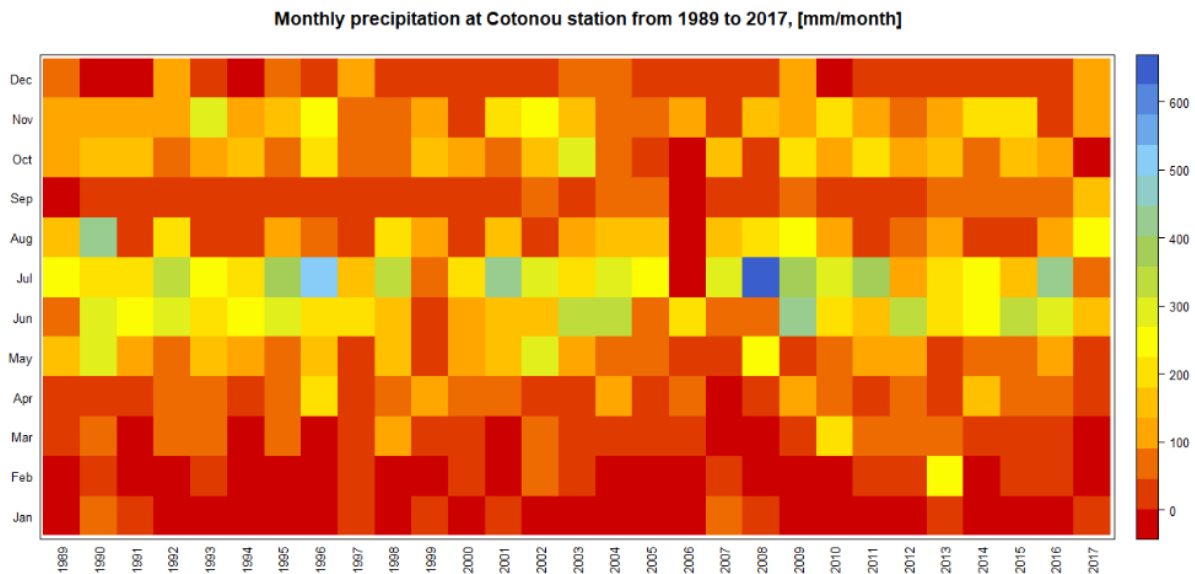


Figure 4- 3: Monthly precipitation matrix at Cotonou from 1989 to 2017

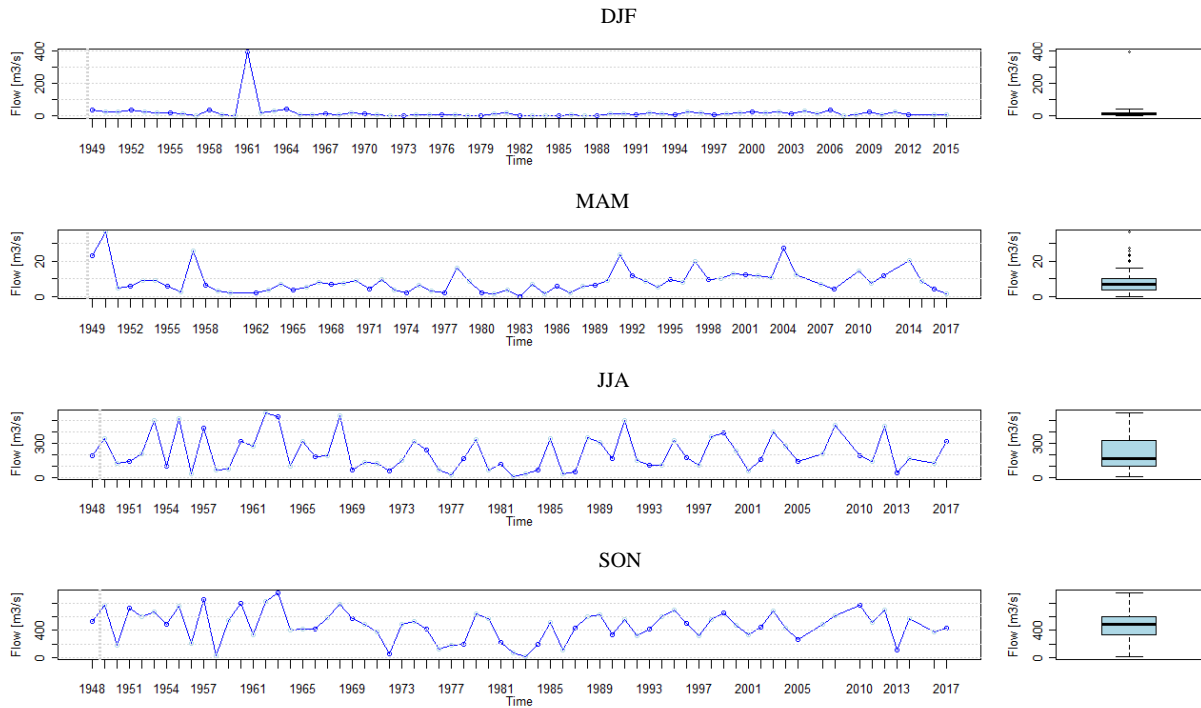


Figure 4- 4: Seasonal flow variation at Bonou station

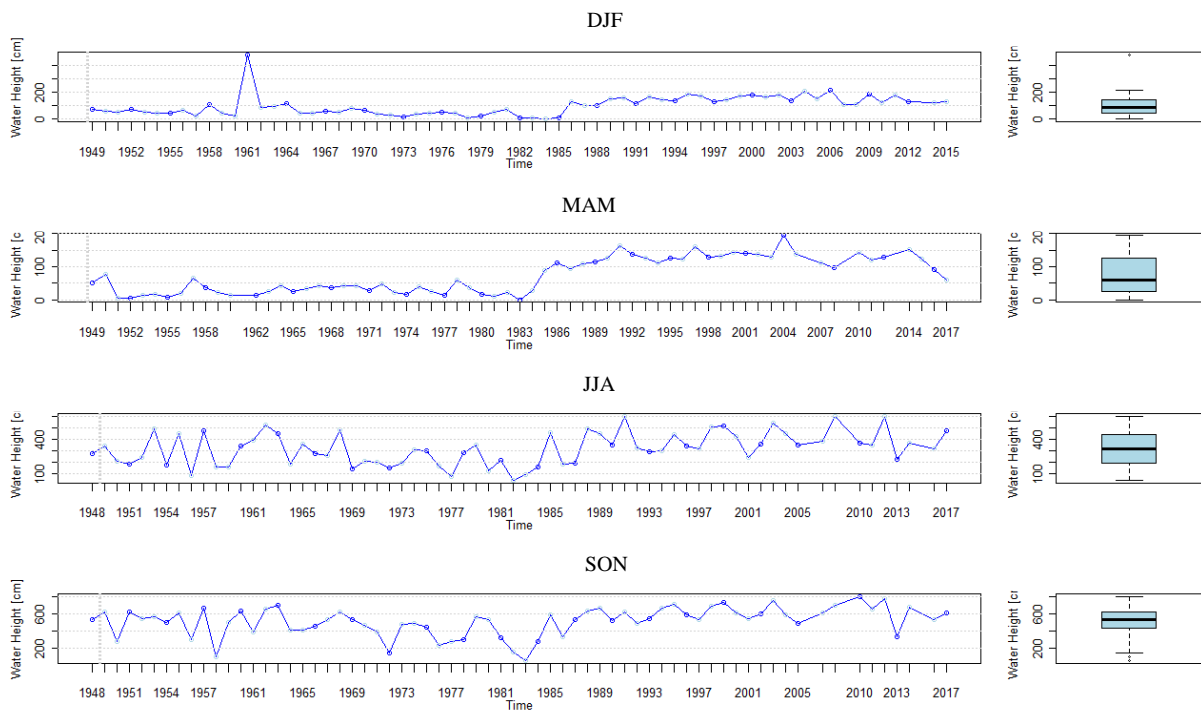


Figure 4- 5: Seasonal water level variation at Bonou station

An in-depth analysis of the rainfall and hydrometric (discharge and water level) time series highlighted several facts about the behavior of these parameters. As a result, according to the group of graphs above (Figure 4- 2), the average monthly rainfall in June shows a high average



total, making it the wettest month. However, if we look at the monthly rainfall matrix from 1989 to 2017 (Figure 4- 2), we find that there are rainfall surpluses in April (125.03mm), May (209.01mm), June (347.23mm), July (125.52mm), September (94.32mm) and October (146.23mm). However, we can notice that June is the month of high rainfall. Based on Figure 4- 2, especially on the monthly boxplots, we can see that June has a large extent against a small extent for July. In addition, the extreme monthly values (July), showing high values. In Adjohoun, June can be described as a very rainy month, with sequences of light rain and a rainy July with very heavy showers. Consequently, the months of June and July are those in which the probability of rainfall flooding is highest. In this sense of probability, always considering the Figure 4- 1, it is important to emphasize that a very high probability of occurrence of scenarios of daily observations of 1mm/day, monthly cumulative less than 100 mm/month and an annual cumulative between 1000 and 1500mm/year. Extreme daily values of more than 50mm/day, monthly values of more than 200mm/month and annual values of more than 2000mm/year have a low or very low probability of occurrence in the study area.

Moreover, concerning the river discharge, the reference of flood is situated in the interval of August to November (Figure 4- 7). However, a peak in discharge was noted during the month of September. From the seasonal decomposition of the discharge and water level analysis, it appears that the behavior of the water level and the discharge varies from one season to another. From the Figure 4- 4 and Figure 4- 5, we can clearly see an almost similar behavior in terms of evolution of discharge and water level over time. In this respect, a clear increase in the series variation is observed from 1985 onwards. In fact, from 1985 onwards, we notice a strong increase in water level for a small increase in flow. This translates into a high-water level for a low discharge, which a priori results from a change in the section of the river. Specifically, during the winter season (December-January-February [DJF]), over the 59 years of the study,



we observe a very low variation of the discharge ($\leq 100 \text{ m}^3/\text{s}$) for a water level average lower than 1.5m. During the spring season (March-April-May [MAM]) the water level and the discharge vary enormously with an upward trend. From the summer season (June-July-August [JJA]) to Autumn season (September-October-November [SON]) the water level and the discharge increase preponderantly to reach a water level averaging over 3.5m (JJA) and 5m (SON). The table below presents the statistics on the hydropluviometric extremes.

Table 4- 1: Extreme statistical summary

Variables	Mean	95th percentile	99th percentile	Max
Precipitation (mm/d) and date	- -	22 -	61.125 -	295 (6/13/1930)
Streamflow (m^3/s) and months of occurrence	202.8 -	915.21 7 th /9 th /10 th months	1068 8 /9 th /10 th months	1401 9/15/1963 6:00 PM
water Level (m) and months of occurrence	2.74 5 th /6 th /7 th /8 th /9 th /11 th /12 th months	7.99 8 /9 th /10 th months	8.74 8 /9 th /10 th months	9.53 9 th months

The 95th and 99th percentile values correspond to very rainy events and very heavy rainfall events. The percentile statistics show values of 61.125mm as a very rainy daily event and 295mm (6/13/1930) as a very heavy rainy event recorded so far at the station. Concerning the streamflow, the average daily observable discharge is about $202.8 \text{ m}^3/\text{s}$, the streamflow of about $915.21 \text{ m}^3/\text{s}$ and $1068 \text{ m}^3/\text{s}$ correspond respectively to 95th and 99th percentiles. The maximum streamflow recorded so far is $1401 \text{ m}^3/\text{s}$ on 9/15/1963. These extreme values are usually observed during the 7th, 8th, 9th and 10th month of the year. In addition, the average water level in the stream at the station is notable 2.74m from the month of May. The 95th and 99th percentile values corresponding to the catastrophic and very catastrophic flooding events recorded at Bonou are 7.99m and 8.74m. However, the maximum water level is about 9.53m.

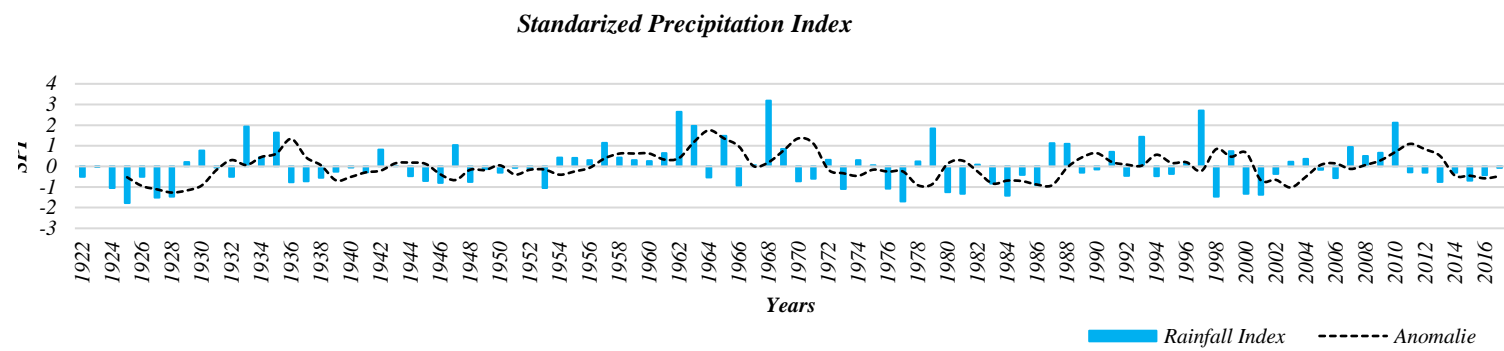


These maxima are generally observed during the 9th months of each year. Consequently, the month of September appears to be the month where there is a greater chance of flooding in the Ouémé basin.

In addition, Figure 4- 6 on standardized indices offer a possibility of analyses of the succession of the climate (wet or dry) of the environment and the flow regime (surplus or deficit). From 1922 to 2017, the climatic regime experienced a succession of wet and dry years. Overall, the study area has experienced more dry years than wet years (Figure 4- 6-A), 55 years in the dry class and 41 in the wet class. However, the runoff is in surplus in 26 years and in deficit in 32 years (Figure 4- 6-B). An interpretation of the sub-plot (C) allows to underline a possible correlation between rainfall and runoff. The presence of a dephasing between the rate of water flow in the river and the rate of precipitation was noted. This allows us to emphasize that the amount of precipitation does not explain the discharge rate of water in the river.

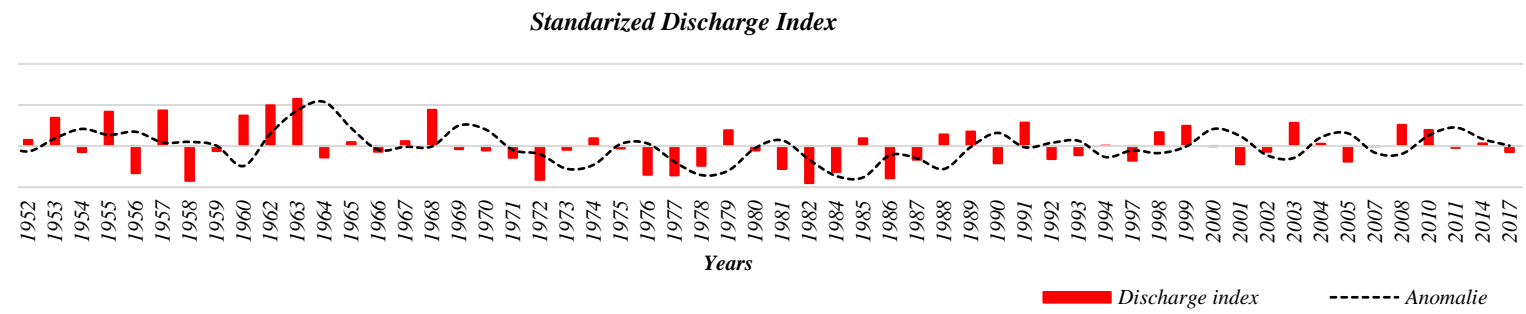


A



B

SDI



C

Standardized Index

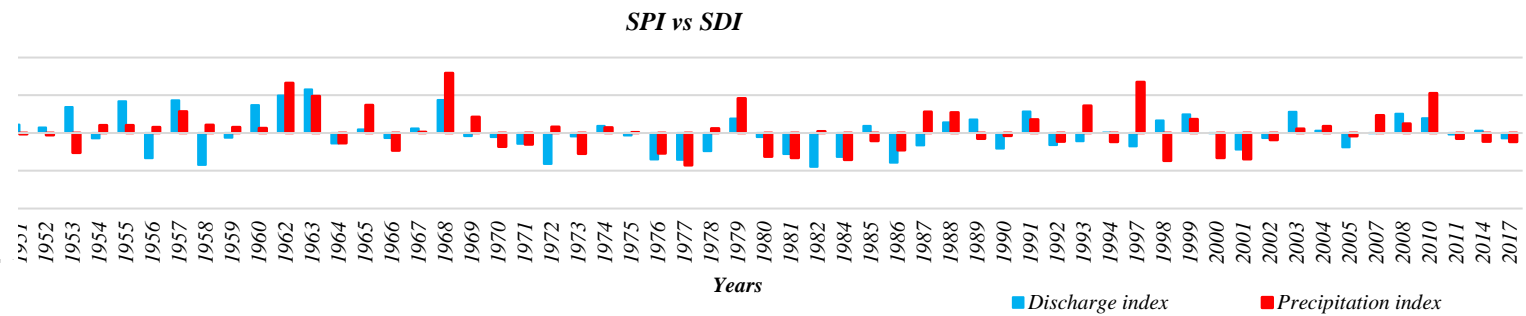


Figure 4- 6:(A)-Standardized Precipitation Index (SPI) from 1922 to 2017, (B)-Standardized Discharge Index (SDI) from 1949 to 2017, (C)- SPI & SDI for Adjohoun region from 1949 to 2017

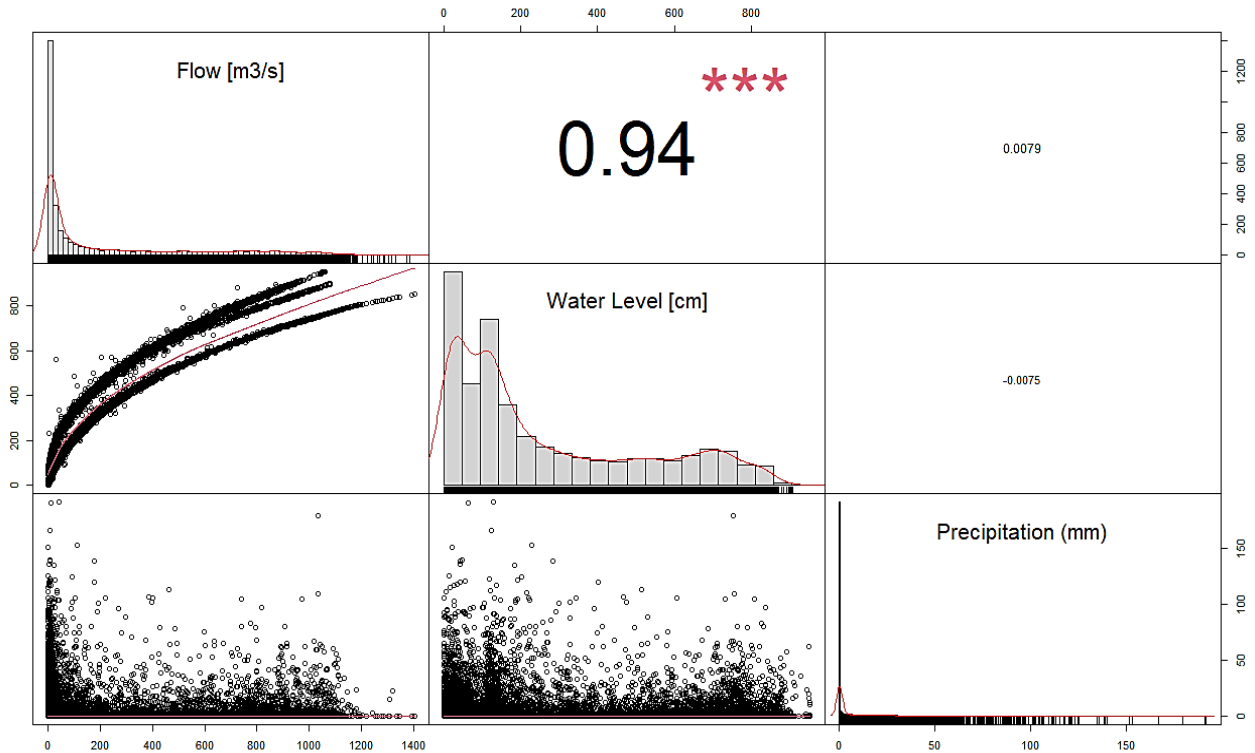


Figure 4- 7:correlation matrix between daily variable (flow, water level, precipitation)

The correlation matrix (Figure 4- 6) allows us to conclude that the precipitation in Cotonou does not explain either the water level or the observed discharge at the Bonou station. This is due to the insignificant and negligible quality of the correlation coefficient. Between the variable precipitation and the water level, it is -0.0075, and 0.0079 between precipitation and discharge. However, a very strong and significant correlation emerges between the variables discharge and water level. The correlation rate is about 94%, suggesting that the water level values can be explained by the flow values with a margin of error of only 6%. Thus, globally, the distribution of the discharge time series as a function of the water level time series shows an exponential type of distribution with $\lambda = 0.5$. Hence for a high-water flow corresponds to a high-water level and vice versa.

In terms of characterization of hydro-rainfall events in the study area (Adjohoun), it should be noted that the environment is marked by a bimodal rainfall regime and unimodal for the flow rate, with the rainfall peak observed during the months of June (high rainy season) and October

(low rainy season) with a flow rate peak during the month of September. The month of June is qualified as a very rainy month with sequences of rain of short intensity and a rainy month of July with very consequent showers. It also appears from the standardized indices (Figure 4- 6- A) that Adjohoun has had more dry years than wet years.

According to DGEC (2022), flooding in Benin is ranked as the country's second biggest natural disaster after epidemics. In terms of the characterization of hydro-pluviometric events in Adjohoun, our research results show that the environment is dominated by a bimodal precipitation regime and a unimodal flow regime. These results are in line with those of authors such as Totin *et al.*, (2016) and Evariste *et al.*, (2018). They showed that the flood season starts in July and reaches its peak in September, with the risk of flooding but the joy of fishing in the region. It was also pointed out that in the study environment, there are more dry season years than humid years through the standardized PSI and SDI indices (Amoussou *et al.*, 2017). Authors such as Issa (1995) and Ogouwalé (2006) have also highlighted this aspect, going even further than our analyses by showing a declining trend in rainfall since the 1960s, but with occasional years of very high rainfall. On a related theme, N'Tcha *et al.*, (2017) had worked on the whole watershed, analyzing future climate trends with RCP4.5 and RCP8.5 scenarios using a global regional model called REgional Model (REMO) for the period 2015–2050. On the trends of extreme daily rainfall indices over the Ouémé basin, despite observing a reduction in the number of rainy days and climatic extremes, they informed the community to prepare for an uncertain future climate.

4-2-Characteristics of extreme events

4-1-1. Precipitation adjustment

The Cotonou station, which is more representative of rainfall distributions in Adjohoun, is used for the determination of the 2- and 5-year return floods. A distribution of the maximum annual



daily rainfall on the Hazen probability (Figure 4- 8) shows a low distribution of observations for low (0.0050) and very high (0.9950) probabilities of non-exceedance. This allows to conclude partially that, the advent of the extreme daily rains very high is certain but for a very high return period is, approximately, 200 years ($P_{jmax}=295\text{mm}$ in 1930). For a probability of not exceeding 0.5 (2 years) and close to immediate, we note an important distribution of observations for a P_{jmax} averaging 100mm. Thus, the study area can be identified as an area dominated by daily maximum annual rainfall with a return period of 2 years. These results are of the same order of observation as those of Amoussou *et al.*, (2022) and Meylan *et al.*, (2012).

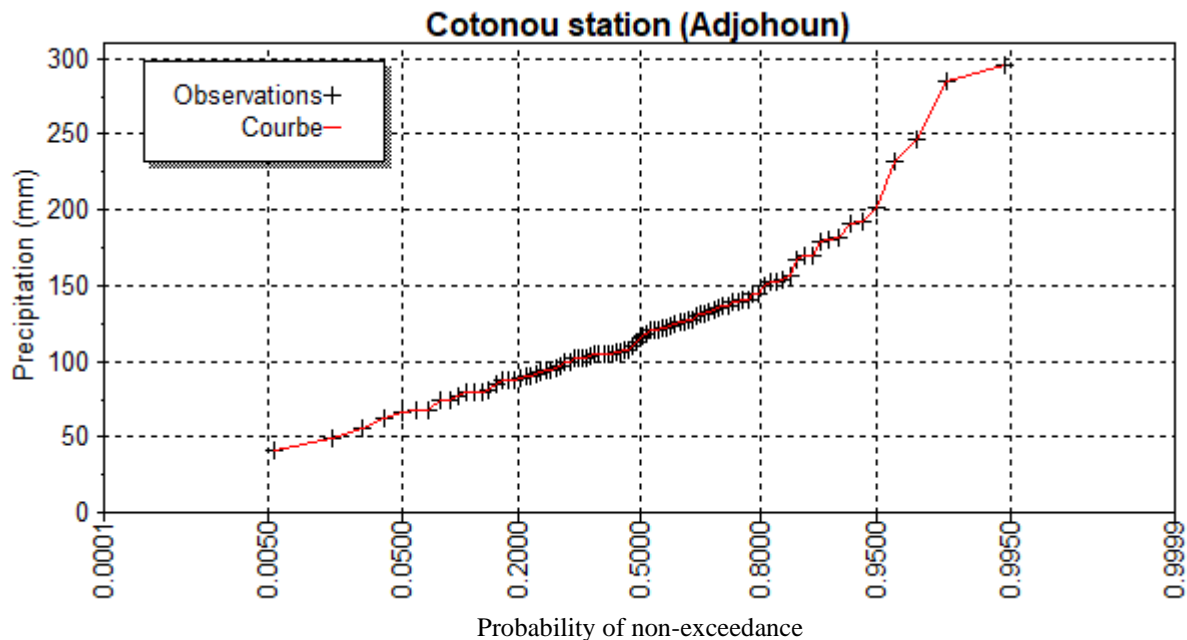


Figure 4- 8: Distribution of the maximum annual daily rainfall on the Hazen probability paper To fit the data to the defined fitting laws such as GEV, Gumbel and Weibull, a hypothesis test on the independence, stationarity and homogeneity of the series is done. The results of the test are shown in the Table 4- 2 below.

Table 4- 2: Results of test hypothesis

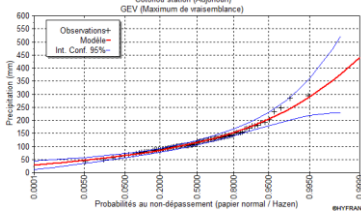
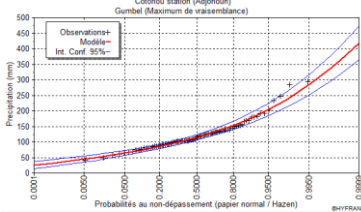
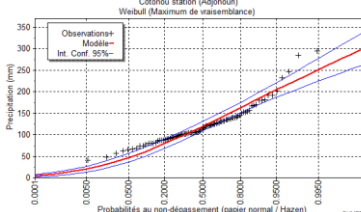
	Test hypothesis	Statistical value	p-value	Conclusion
Precipitation	Wald-Wolfowitz	$ U =2.00$	0.0458	We have to reject H_0 at the 5% significance level, but we accept it at the 1% significance level.

test of independence			
Kendall's stationarity test	$ K = 2.57$	0.0103	We have to reject H0 at the 5% significance level, but we accept it at the 1% significance level.
Wilcoxon homogeneity test	$ W = 3.13$	0.0018	We must reject H0 at the 1% significance level, The two subsamples are not homogeneous.

From Table 4- 2, we conclude that the data are independent (1%), stationary (1%), and homogeneous (1%). Being a sufficient condition, Table 4- 3 summarizes on the treatment outputs. Very briefly, an acceptance at a 5% level of significance for laws such as GEV and Gumbel. But a rejection for the Weibull adjustment law at a 1% significance level. Thus, we are 95% confident that the annual maximum daily rainfall values follow either a GEV distribution or the Gumbel distribution. A graphical appreciation of the three (3) graphic laws, allows to confirm the assertions formulated previously. We can easily notice a shift of the Weibul curve from the observations against a tendency of the two other laws to follow the real values of observations.



Table 4- 3: D ng to GEV, Gumbel and Weibull laws

Adjustmen laws	Chi- quare	p-value	Hypothesis	Conclusion	Graphic
GEV	0.35	0.3135	H0: the sample comes from a GEV law H1: the sample does not come from a GEV law	At the 5% level, H0 is accepted.	
Gumbel	0.14	0.3390	H0 : the sample comes from a Gumbel distribution H1: the sample does not come from Gumbel	At the 5% level, H0 is accepted.	
Weibull	16.23	0.0019	H0: the sample is from a Weibull distribution H1: the sample does not come from Weibull	At the 1% level, H0 is rejected.	



Since it is difficult to recognize the best fitting law, BIC and AIC evaluation criteria were used for this purpose. The search for minimization of these criteria was met for the Gumbel fitting law (Table 4- 4).

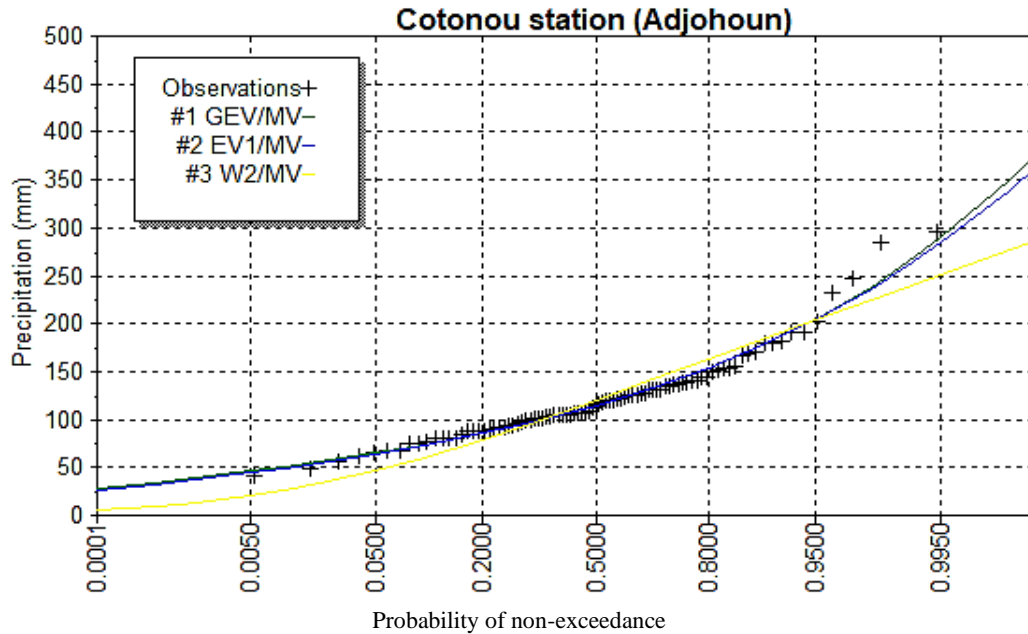


Figure 4- 9: Graphical comparison of the fitting laws

Table 4- 4: Assessment of the laws of adjustment to the AIC and BIC criteria

Law	BIC	AIC
Gumbel	938.401	933.379
GEV	942.827	935.294
Weibull	958.458	953.436

Finally, regarding the best fitting law for the annual maximum daily rainfall, it turns out that Gumbel's law best fits the observations. For this purpose, the observations will be fitted with the Gumbel law (Table 4-5).

Table 4- 5: Estimation of the maximum daily rainfall of return period 2 years and 5 years (Gumbel)

T (i yrs)	Pjmax (i) in mm	Confidence interval (mm)	Annual probability
5	153	141 - 166	20%
2	115	106 - 123	50%

Consequently, each year we estimate a 50% chance of recording a daily rainfall of about 115mm or between [106mm, 123mm]. While, there is a 20% chance of having a five-year rainfall of about 153mm or between [141mm, 166mm]. These values are the source of rainfall flooding in the study area. The results obtained are partly in line with those of Agbazo (2016) or Badou *et al.*, (2023), based on the law of adjustment of rainfall extremes, but they were preferably based on hourly rainfall data.

4-1-2. Discharge adjustment

The observations of annual maximum daily discharge are distributed on a Hazen non-exceedance paper (Figure 4- 10). It can be seen that the majority of the annual daily discharge values are located around the probability of non-exceedance of 0.5. However, the range of probability of occurrence of the maximum annual daily values is between 0.2 and 0.8 with more than 60% of the observations. Until now, bi-centennial (T=200 yrs) floods have been recorded at the Bonou station.

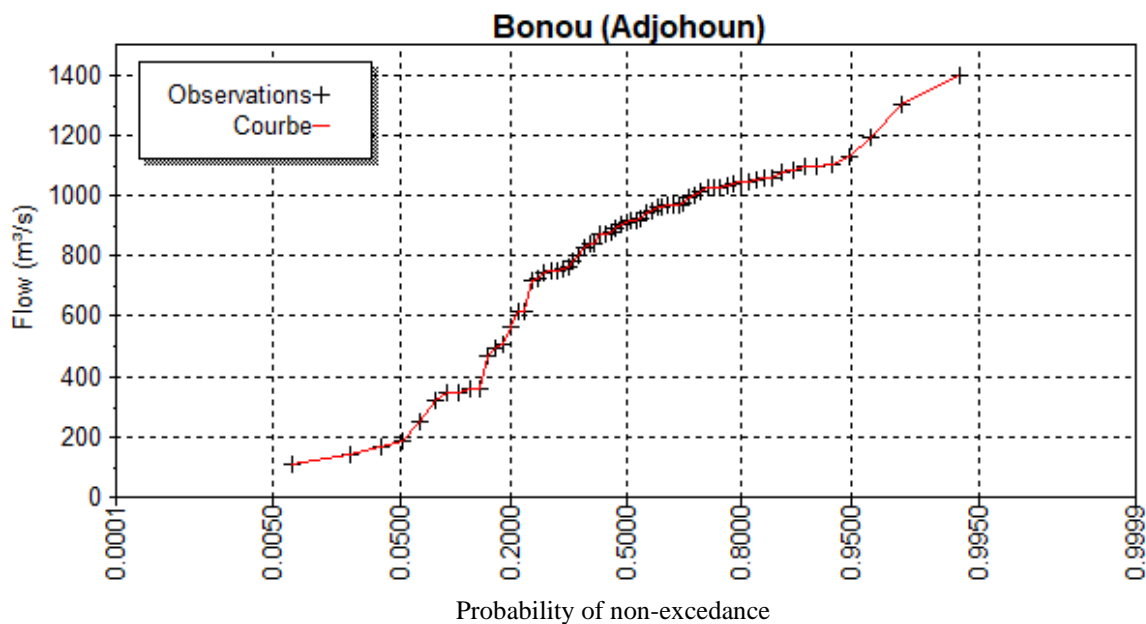


Figure 4- 10: Distribution of Qjmax on Hazen probability paper



The results compiled in Table 4- 6, show that the annual maximum daily streamflow data are independent, stationary and homogeneous. The tests of homogeneity, stationarity and independence are all accepted at the 5% significance level. These necessary and justified conditions allowed for frequency analysis of the annual maximum daily streamflow series.

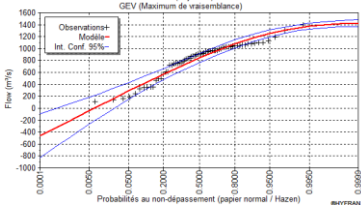
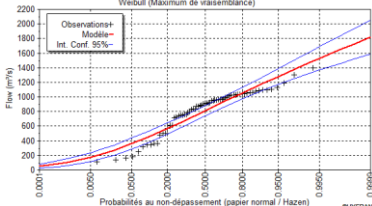
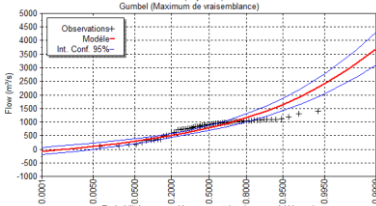
Table 4- 6: Results of test hypothesis

	Test hypothesis	Statistical value	p-value	Conclusion
	Wald-Wolfowitz test of independence	$ U = 0.758$	0.449	We can accept H_0 at the 5% significance level
Streamflow	Kendall's stationarity test	$ K = 1.82$	0.0690	We can accept H_0 at the 5% significance level
	Wilcoxon homogeneity test	$ W = 1.32$	0.186	We can accept H_0 at the 5% significance level

Then, in order to determine the best fit to the observations, fit tests, graphical trend analysis and BIC and AIC evaluation on the annual maximum daily streamflow data through GEV, Gumbel and Weibull laws were initiated.



Table 4- 7: T f annual maximum daily streamflow data to GEV, Gumbel and Weibull laws

Adjustmen laws	Chi- quare	p-value	Hypothesis	Conclusion	Graphic
GEV	6.13	0.0131	H ₀ : the sample comes from a GEV law H ₁ : the sample does not come from a GEV law	H ₀ accepted at 1% threshold	
Weibul	13.60	0.0013	H ₀ : the sample comes from a Gumbel distribution H ₁ : the sample does not come from Gumbel	H ₀ rejected at 1% threshold	
Gumbel	19.27	0.0000	H ₀ : the sample is from a Weibull distribution H ₁ : the sample does not come from Weibull	H ₀ rejected at 1% threshold	



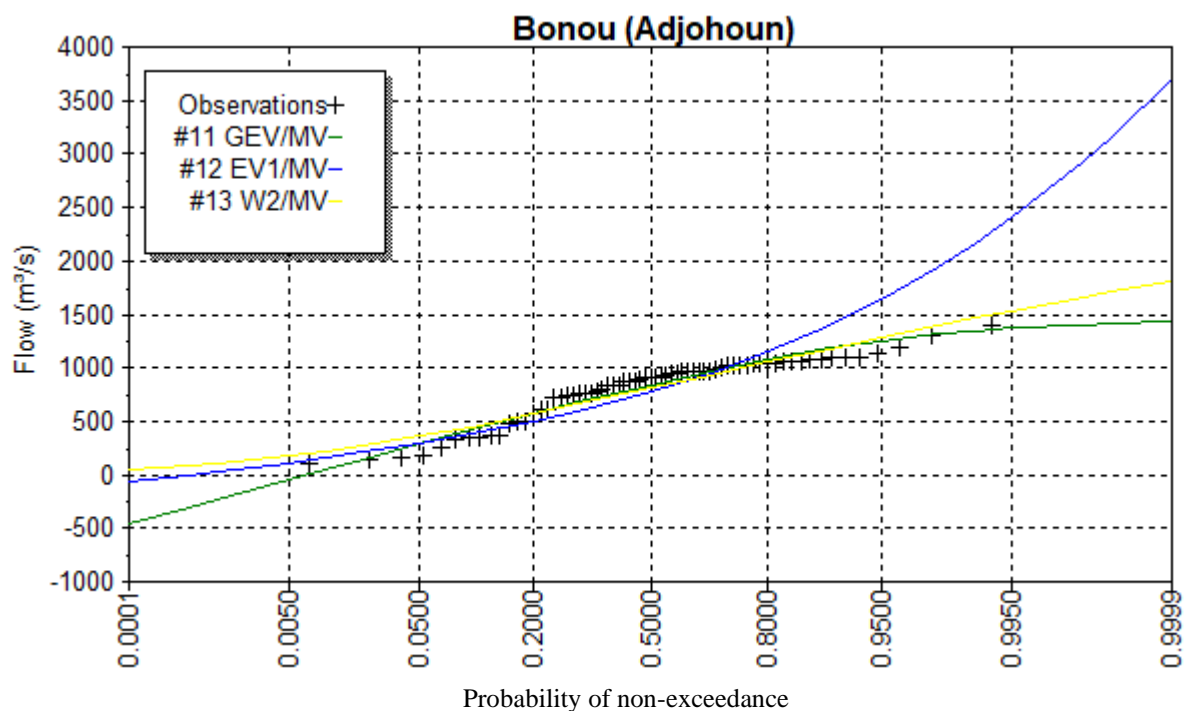


Figure 4- 11: Graphical comparison of the fitting laws

Table 4- 8: Assessment of the laws of adjustment to the AIC and BIC criteria

Law	BIC	AIC
Gumbel	957.693	951.079
Weibull	962.379	957.970
GEV	982.368	977.958

From tables Table 4- 7, Table 4- 8 and Figure 4- 11, we deduce that the law that best fits the trend of the annual maximum daily streamflow is the Gumbel law. The streamflow estimates for the 2-year and 5-year return periods are shown in Table 4- 9 below.

Table 4- 9: Results of the estimation of the maximum daily rainfall of return period 2 years and 5 years (Gumbel)

T (i yrs)	Q _j max (i) in m ³ /s	Confidence interval (m ³ /s)	Annual probability
5	1150	1010 - 1300	20%
2	780	688 - 873	50%

The streamflow values for the 2-year and 5-year return periods are $780\text{m}^3/\text{s}$ and $1150\text{m}^3/\text{s}$ respectively. However, we estimated that, there is a 20% chance of recording discharges between $[1010\text{m}^3/\text{s}, 1300\text{m}^3/\text{s}]$ and a 50% chance of $[688\text{m}^3/\text{s}, 873\text{m}^3/\text{s}]$ at the Bonou station. In sum, the analysis of the occurrence of rainfall and hydrometric events shows that the maximum annual daily values potentially follow a Gumbel distribution. A biennial rain flood is $115\text{mm}/\text{day}$ and a five-year flood $153\text{mm}/\text{day}$. For a biennial river flood the value is around $780\text{m}^3/\text{s}$ and $1150\text{m}^3/\text{s}$ for the quinquennial one. These return flood data were used as discharge data for the hydraulic modeling whose results are presented in the following section.

With regard to frequency analysis, Ogouwale *et al.*, (2022), in researching the manifestation of extreme hydroclimatic events in the lower valleys of the Ouémé, extreme values were analyzed under Gumbel, Pearson III and Goodrich laws. The comparative study shows a 16-12% recession in rainfall extremes between 1951-1970 and 1971-1990, compared with a 10% increase over the 1990-2019 period. In his opinion, we can expect an 11% increase in the frequency of rainfall extremes by 2050 in the lower valleys.

4-2- Delimit the Cultivation and Flooding Areas According to the Occurrence of Extreme Floods Events (2-Year And 5-Year)

4-2-1 Trend of spatial repartition of land use in the study

The fundamental aim of spatial analysis is to see the spatial arrangement of the population around the river.



Land use diagram - Adjohoun district (years 2020)

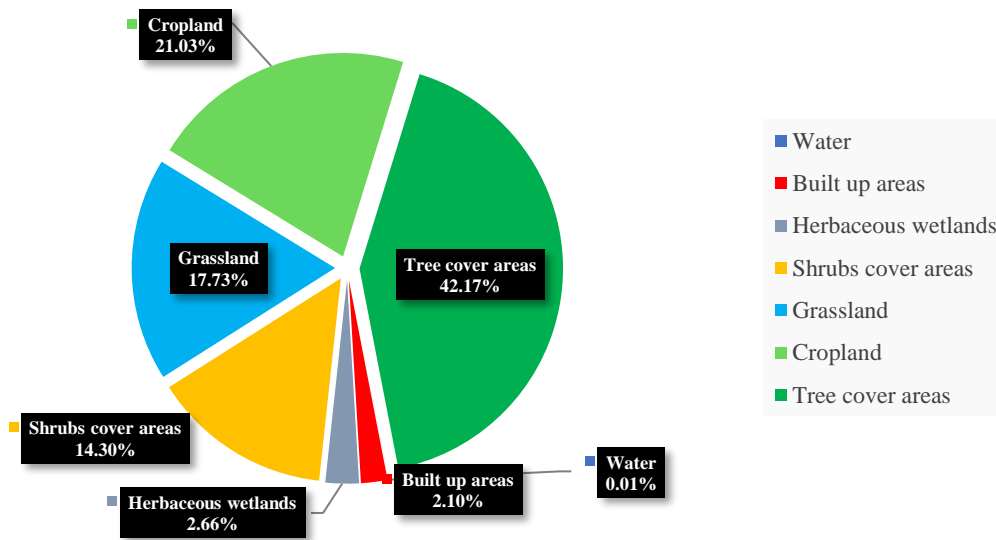


Figure 4- 12: Land use diagram

The important classes identified for this purpose are seven distinct classes and include: water, built up areas, Herbaceous wetlands, shrubs cover areas, grassland, cropland and tree covers areas. A geographical analysis of the land use shows a heterogeneous territorial exploitation dominated by a large concentration of built-up area mainly along the Ouémé River. With a percentage of about 2.10% for a surface area of 6.36 km², built up areas serving as human settlement is located east of the river. Vegetation cover is also fairly extensive, with trees, farmland and meadows. On the territorial level, the tree cover areas are about 133.23 km² or 42.17% of the total area. While the cropland (21.03%) and grassland (17.73%) classes dominate the western part of the Ouémé River (Figure 4- 12). Indeed, the western part of the river represents the low valley often fertilized by the overflow of the Ouémé from its bed in high water. As pointed out by Tchegnon & Guidibi (2006) the fertile hydromorphic soils offer a wide range of agricultural possibilities in the area. It is a source of fertilizer for food crops, mainly maize, manioc, rice, etc. Banana, palm and sugar cane plantations also dominate the region. Banana, palm and sugar cane plantations also dominate the region. However, one of the strong remarks through the extraction of land use layers (A) such as built-up areas (B), cropland (C) and grassland (D) shows a strong tendency of population settlement on the banks of the Ouémé



River. Furthermore, associated with the sentinel images, the valley is juxtaposed by temporary water zones to the west and southeast of the Ouémé River. According to the Figure 4- 13 (C and D), a strong dominance of agricultural activities is evident in the valley west of the river against a strong tendency for shrub plantations in the east. Similar patterns have been documented by Lawin *et al.*, (2018) in the northern part of the Ouémé catchment. Also, comparable situations have been noted in India, with the population settling on the banks of the Vishwamitri River (Kaulgud *et al.*, 2015). It has been shown that there is a common effect of population relocation or migration following river erosion or flooding (Zaman, 1989; Islam *et al.*, 2010; Pramantha, 2012). In some cases, displaced people may suffer from loss of land, livelihoods, increased poverty, food insecurity, lack of sanitation facilities and drinking water (Haque, 2023; Majumdar *et al.*, 2023). All settlement on riverbanks can be beneficial in terms of ecological services such as fishing, as highlighted by Shrestha et al, (2022).



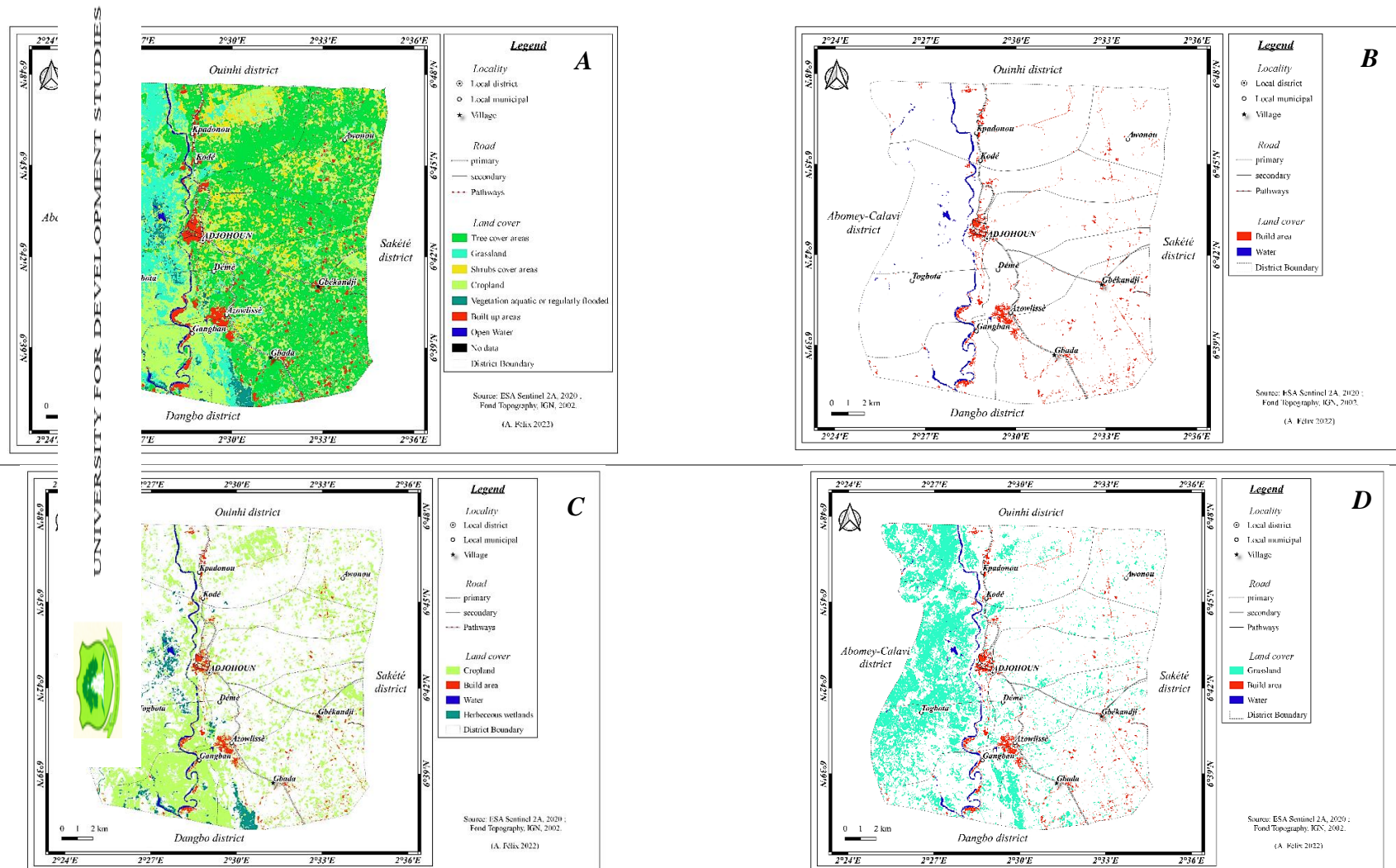


Figure 4- 13: Cover data extraction. (A)-LULC of Adjohoun district year 2020, (B) Built up areas of Adjohoun district, (C)-Cropland of Adjohoun district, (D)- Grassland of Adjohoun district

4-2-2 Hydraulic modeling

The hydraulic modeling process in the study area allowed to analyze the hydrodynamic behavior of the environment. This was done in order to assess the flood risks, the extent of each type of flooding, the likely impacts on agriculture, goods and services of the district. This section reports the output of two distinct hydraulic models: a fluvial model focusing on the overflow of the Ouémé River, and a pluvial model focusing on an exceptional rainfall. As presented in Figure 4- 14, the hyetograph of rainfall flood scenario considered is a distribution of 115mm and 153mm of rainfall over 24 hours following a Gaussian function. This operation transforms the unit values from the frequency analysis into a time series. This operation was performed on the 2-year ($780 \text{ m}^3/\text{s}$) and 5-year ($1150 \text{ m}^3/\text{s}$) return period discharge entities whose cumulative series is considered as an upstream boundary condition (Figure 4- 15) for modelling. The behavior and hydraulic response of the valley to an increase in river flow are studied. The target values correspond to the quantiles estimated from the frequency analyses. It is therefore important to be able to recover information on the evolution of the submergence heights of fields and infrastructures at different flow quantiles until the target values $Q=780 \text{ m}^3/\text{s}$ and $Q=1150 \text{ m}^3/\text{s}$ are reached (Figure 4- 15). Apart from hydraulic modelling, the Gaussian function was used by Bogner *et al.*, (2012) for an application in a flood forecasting system by combining extreme value analysis and non-parametric regression methods. These transformations have proven their importance in the field of flood and water resource management based on extreme quantiles (Kelly & Krzysztofowicz, 1997; Lang & Renard, 2007; Bogner *et al.*, 2017).



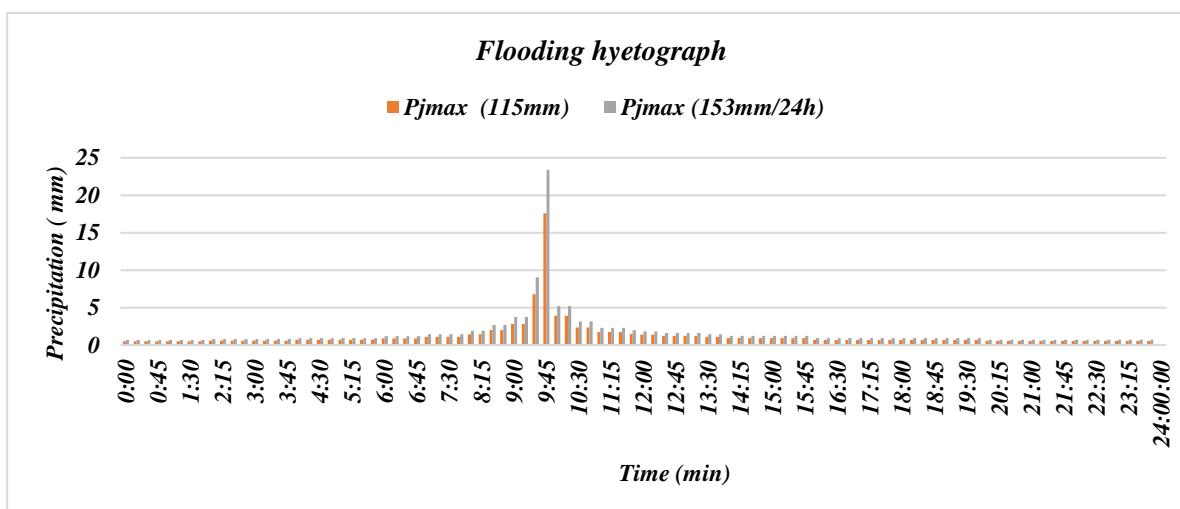


Figure 4- 14: Rain flood hyetograph input

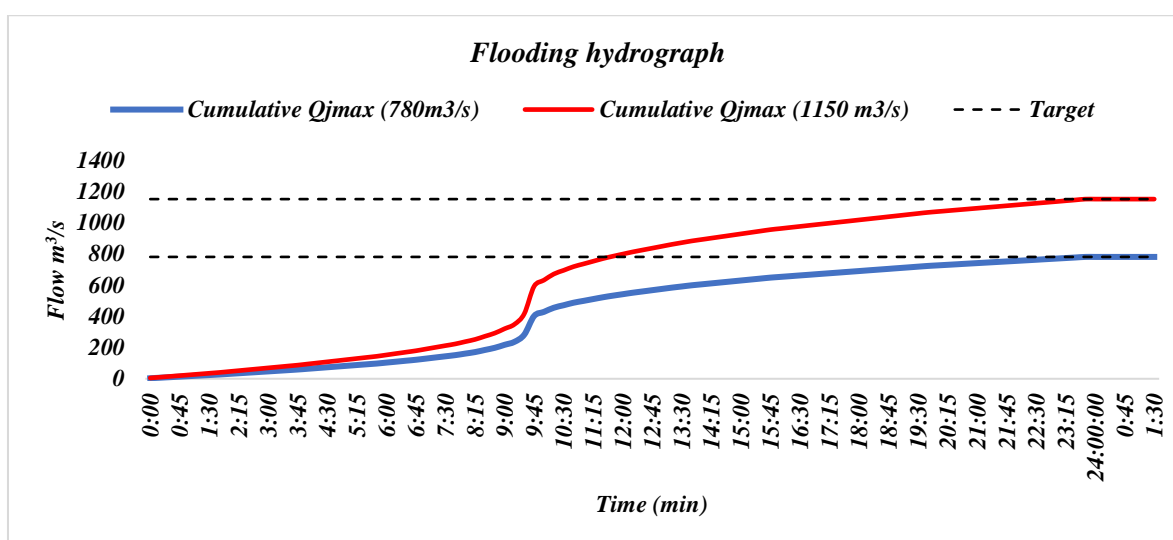


Figure 4- 15: Cumulative River flood input

Table 4- 10 presents the crops, their respective height classes, the maximum water level they can tolerate, the type of crop, the suitable soil type, infiltration rate and reference for the major crops cultivation practice in the Adjohoun district.

Table 4- 10:summary on crops and soil characterization

Crop characterization			Soil characterization			Reference
Crop	Height class	Maximum water level (m)	Crop type	Suitable soil type	Infiltration rate (mm/h)	
Maize	>2m	1.2	Cereal	Loam, clay	100	Malekian <i>et al.</i> , (2012); Benjamin <i>et al.</i> ,(2015); Yang <i>et al.</i> ,(1998)
Sorghum	>2m	1.2	Cereal	Sandy loam, clay	90	Promkhambut <i>et al.</i> , (2010); Sher <i>et al.</i> ,(2013)

Rice	0.5m-1.5m	0.8	Cereal	Clay	60	Doni <i>et al.</i> , (2014) ; Abdul <i>et al.</i> , (2018)
Cassava	2.0-4.0m	1.5	Root	Sandy loam	30	El-Sharkawy. <i>et al.</i> , (2002); Sri, <i>et al.</i> , (2021); Wasonga <i>et al.</i> , (2020)
Sweet potato	0.5m-1.0m	1.2	Root	Sandy loam, clay	20	Asa <i>et al.</i> , (2021) ; Nwanne <i>et al.</i> , (2020)
Yams	>2m	1.5	Root	Loam, sandy loam	50	Charles <i>et al.</i> , (2019), Schiwachi <i>et al.</i> , (2016)
Mango	>2m	1.5	Fruit	Loam, clay	50	https://www.ikisan.com/ap-mango-soils-and-climate.html , Hahn <i>et al.</i> , (2022)
Avocado	>2m	1.2	Fruit	Sandy loam	40	Cantuarias. <i>et al.</i> , (2019); Christopher (2014)
Orange	>2m	1.5	Fruit	Loam, sandy loam	50	Salama (2017); Sandra (2012)
Tomatoes	0.5m-1.5m	0.8	Vegetable	Sandy loam, clay	30	Evy <i>et al.</i> , (2019) ; Tareq <i>et al.</i> , (2020); Tujuba <i>et al.</i> , (2020)
Cowpea	0.5m-1.5m	1	Legume	Sandy loam, clay	20	Bisikwa <i>et al.</i> , (2014) ; Olorunwa <i>et al.</i> , (2023)
Soybean	0.5m-1.0m	1	Legume	Loam, sandy loam	40	Kim <i>et al.</i> , (2018), Khadeja <i>et al.</i> , (2022)
Okra	1.0m-2.0m	1.5	Vegetable	Loam, clay	40	Vwioko <i>et al.</i> , (2019), Ahmet <i>et al.</i> , (2009)
Palm tree	>2m	1.5	Tree	Sandy loam, clay	10	Parolin <i>et al.</i> , (2010)
Chili pepper	0.5m-1.5m	0.9	Vegetable	Sandy	20-30	Suh, <i>et al.</i> , (1987) ; Garcia <i>et al.</i> , (2017)
Smaller crops (Lettuce)	<=0.2m	0.2	Legume	Sandy	20-30	Islam <i>et al.</i> , (2021), Dan (2020)



Under this synthesis of information, seven (7) categories of water level ranging from 0.2m to more than 2.5m emerge for the plants. On the other hand, the maximum tolerable water level, varies from 0.2m to 1.5m. With this information, the final outputs of the two possible sources of flooding in the Adjohoun district are processed via the HEC RAS tool. The results are discussed in the paragraphs below.

Rainfall flood events

An analysis of the outputs of the simulation results shows a similarity of observations in terms of spatial distribution of areas affected by the presence of water. Spatially, there is a homogeneous distribution of water stagnation areas in the district (Figure 4- 16). However,

two distinct zones emerged from the observations. Based on the water level classes, we note that the western part of the Ouémé River is mainly characterized by moderately low water levels as opposed to a moderately high in its eastern part. This difference may be partly due to the variable topography where a plateau rises in the East (Adjohoun Valley) while on the other side of the river there are ridge lines well defined by a cadence of altitude. This allows for water recharge of the Ouémé River. In terms of potential damage, rainfall flooding for events of 50% and 20% chance of occurrence, the impact remains low overall. Statistically, considering a biennial rainfall event (T=2yrs), about 53.92km² (17.08%) of the territory of Adjohoun is affected against 160.61km² (50.87%) for a five-year rainfall flood (T=5yrs) for a variation in water height from 0.25m to 3.9m. A more detailed analysis shows that a very important distribution of water level lower or equal to 30.48cm against a very weak distribution for high water level. For a rainfall of 115mm/24h about 42.84km² (13.57%) of the total area of the district presents a water level lower or equal to 30cm against about 92.58km² (29.32%) for 53mm/24h. However, there are classes of high water level including 304.8cm (46.04m²) for a rainfall of 115mm/24h and 396.24cm (55.04m²).

Table 4- 11: statistics summary on rainfall events for 2yrs and 5yrs return periods

Water level class area plots	<div> <div>Rainfall events of 115mm/24h</div> </div> <div> <div>Rainfall events of 153mm/24h</div> </div>												
	<table border="1"> <thead> <tr> <th>Rainfall</th><th>115mm/24h</th><th>153mm/24h</th></tr> </thead> <tbody> <tr> <td>Total flood area (km²)</td><td>53.917</td><td>160.610</td></tr> <tr> <td>Percentage</td><td>17.08%</td><td>50.87%</td></tr> <tr> <td>High water level (cm)</td><td>304.8</td><td>396.24</td></tr> </tbody> </table>		Rainfall	115mm/24h	153mm/24h	Total flood area (km ²)	53.917	160.610	Percentage	17.08%	50.87%	High water level (cm)	304.8
Rainfall	115mm/24h	153mm/24h											
Total flood area (km ²)	53.917	160.610											
Percentage	17.08%	50.87%											
High water level (cm)	304.8	396.24											

Consequently, in the Adjohoun valley, in terms of flood heights, the risks related to large losses are potentially low for events with return periods of 2 years and 5 years. However, some areas have water levels that exceed the maximum tolerable water level for planting certain types of crops. For example, 1.81% (3.72km²) are not recommended for the production of crops that do not tolerate a maximum water level below 0.9m (Tomatoes, Rice, Chili pepper) like suggested by Garcia *et al.*, 2017).

Table 4- 12: statistics on the distribution of water level classes for 115mm and 153mm scenarios

Water level (cm)	Rainfall of 115mm/24h		Rainfall of 153mm/24h	
	Percentage in district area	Area (km ²)	Percentage in district area	Area (km ²)
<=30.47	13.57%	42.84602	29.32%	92.57901
60.96	2.54%	8.01808	3.82%	12.06363
91.44	0.69%	2.17142	1.18%	3.71596
121.92	0.20%	0.62092	0.40%	1.26027
152.4	0.06%	0.19497	0.14%	0.44838
182.88	0.02%	0.05026	0.05%	0.15063
213.36	0.00%	0.01180	0.02%	0.04792
243.84	0.00%	0.00306	0.01%	0.01808
274.32	0.00%	0.00061	0.00%	0.00461
304.8	0.00%	0.00005	0.00%	0.00151
335.28	0.00%		0.00%	0.00090
365.76	0.00%		0.00%	0.00039
396.24	0.00%		0.00%	0.00006

Thus, from the above table, it appears that the Adjohoun district is not plagued by large-scale crop loss disasters. However, the limits here are drawn around the return periods and the associated rainfall. It is not to be neglected, the presence of areas with a high water flooding potential whose farmers of the district must well define an agricultural scheme capable of managing the excess of water or opt for a judicious future choice of a type of crop capable of withstanding at the advent of floods the excess of water during a given time t. In sum, the



Adjohoun district is potentially free of serious losses and damage related to biennial and five-yearly rainfall floods.



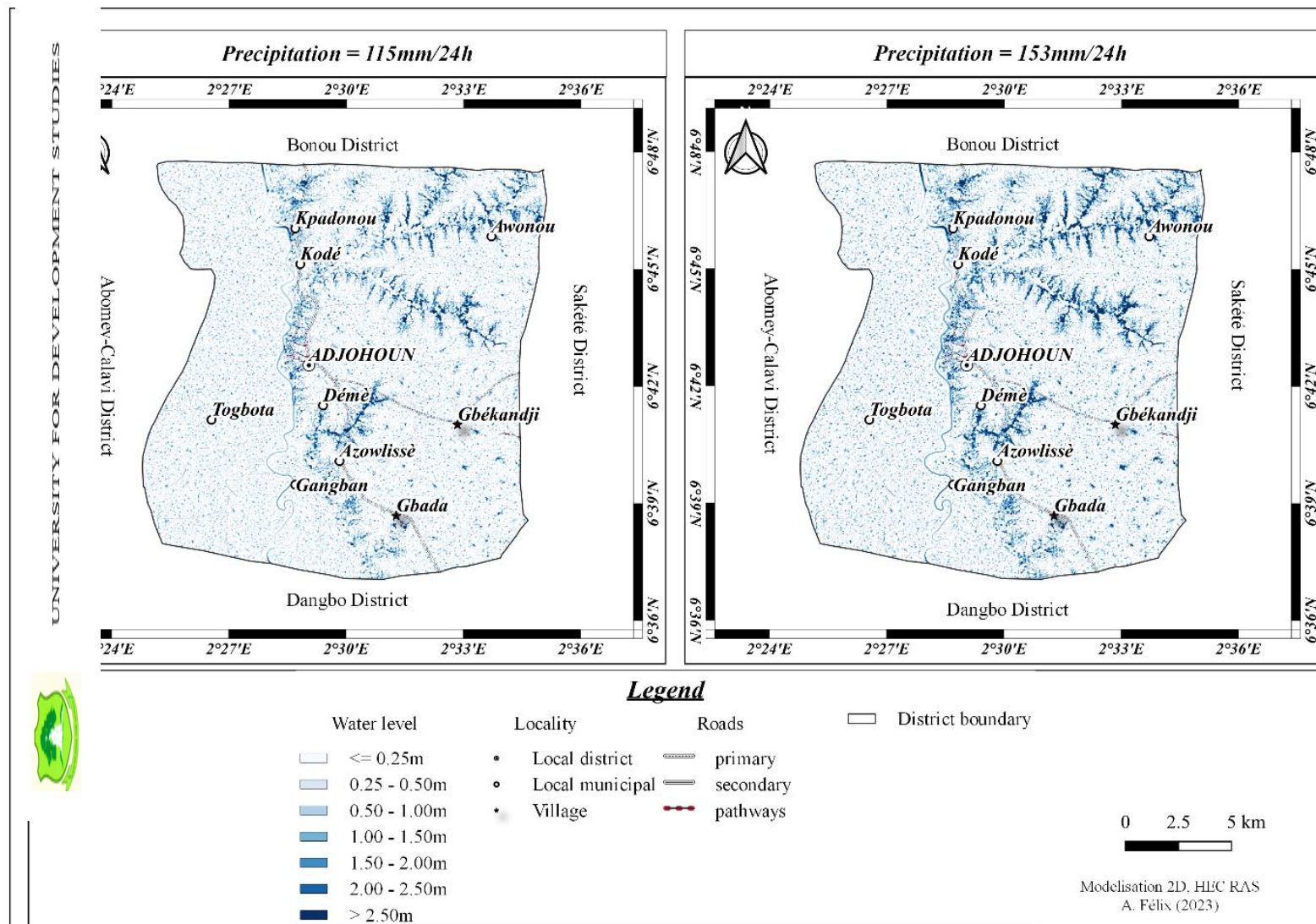


Figure 4- 16: Map of flood zones under a 2-year and 5-year return period rainfall

River flood events

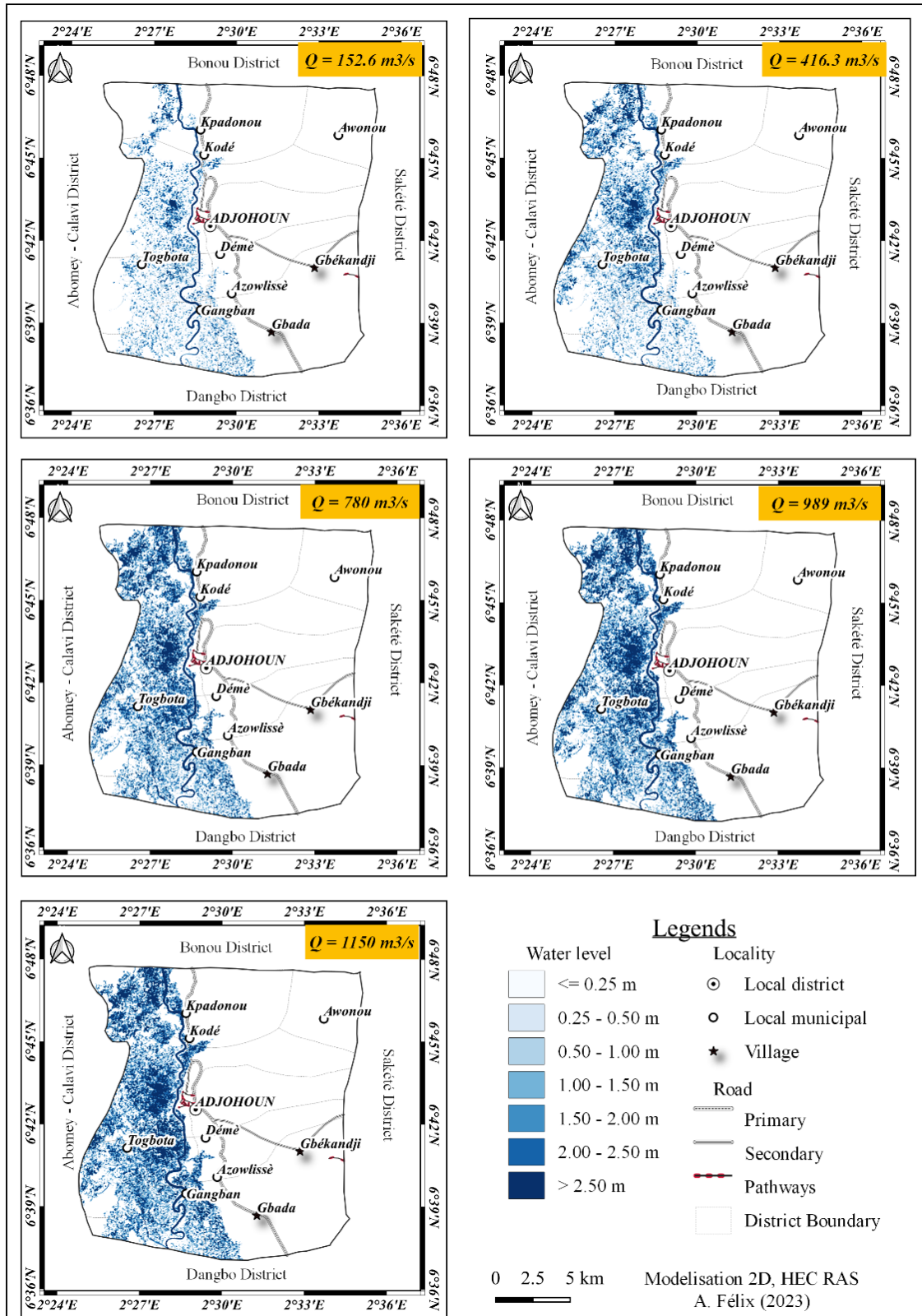


Figure 4- 17: Map of flood zones under different discharge

The scenario is, however, contradictory in a context of fluvial flooding related mainly to the overflow of the Ouémé River. First, the analysis shows that the river overflows to the west of the Ouémé River. Secondly, the height of water submersion is proportional to the water discharge. These results are in line with the work carried out by Ernest *et al.*, (2022) and by Houngué (2020) on a primary valley located further upstream from Adjohoun.

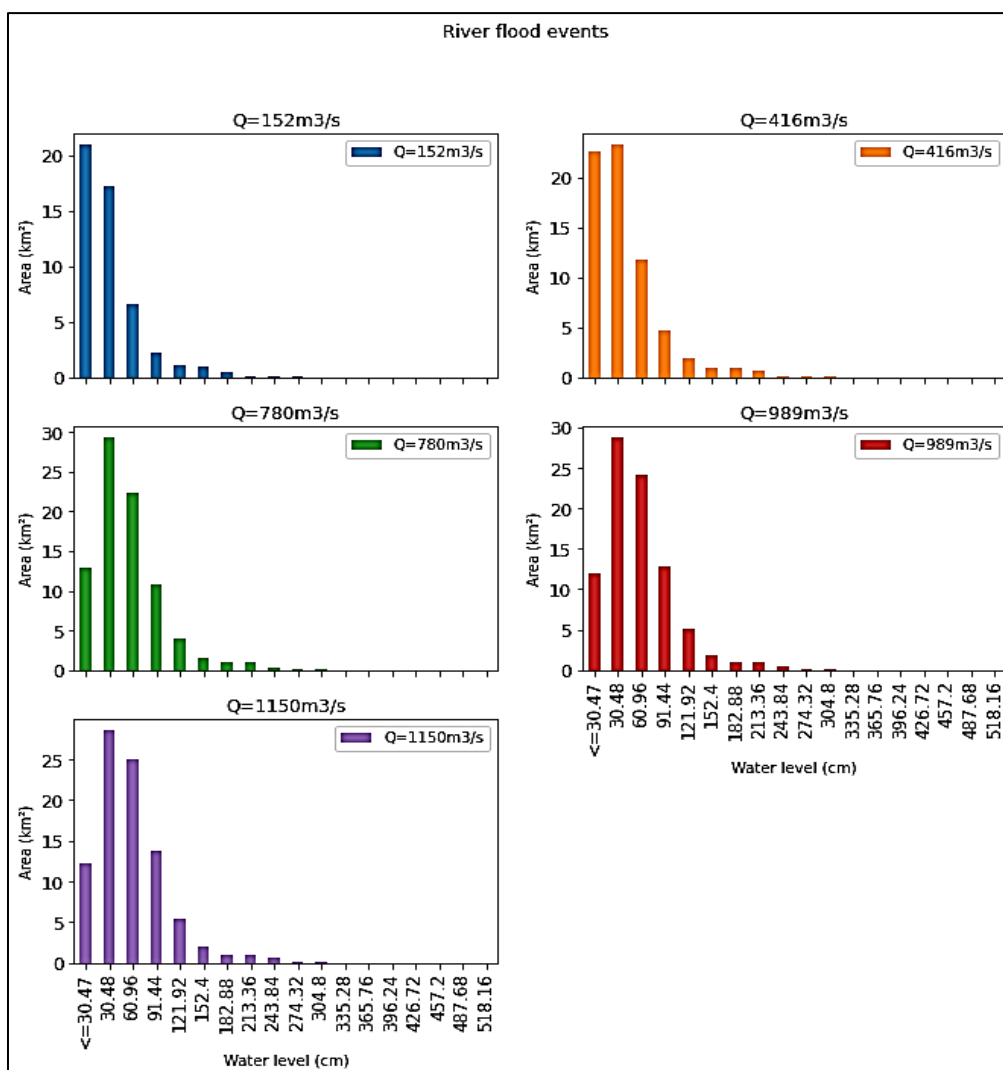


Figure 4- 18:- summary plots water vs Area (km²) for each discharge

Table 4- 13: statistics summary on river flood

			T=2yrs		T=5yrs
	Q=152 m ³ /s	Q=416 m ³ /s	Q=780 m ³ /s	Q=989 m ³ /s	Q=1150 m ³ /s
Total flooded area (km²)	49.584	66.796	83.360	87.359	89.817
Percentage	15.63%	21.06%	26.28%	27.55%	28.32%

High water level (cm)	457.2	487.68	487.68	487.68	518.16
----------------------------------	-------	--------	--------	--------	--------

Specifically, it can only be noted that at most 30% of the total area of the sector is likely to be flooded during the rise of water in the river. Considering the above table (Table 4- 13), maximum water level heights of about 487.68cm and 518.16cm can be reached in the study area. However, these water level classes are still lower than the water level classes of 30.48 cm, 60.94 cm, 91.44 cm, 121.92, 152.4 cm, 182.88, 213.36 cm and 243.84 cm. Considering Figure 4- 17 and Figure 4- 18, as the discharge increases, a minimization of the water level classes around 30.48cm is observed at the expense of the high-water level classes. A direct consequence of this increase is a reduction of the window of wide possibilities of choice of plants tolerating a given water level. On the other hand, it demonstrates the vulnerability of the district to fluvial type floods. Thus, losses and damages are potentially related to fluvial floods.



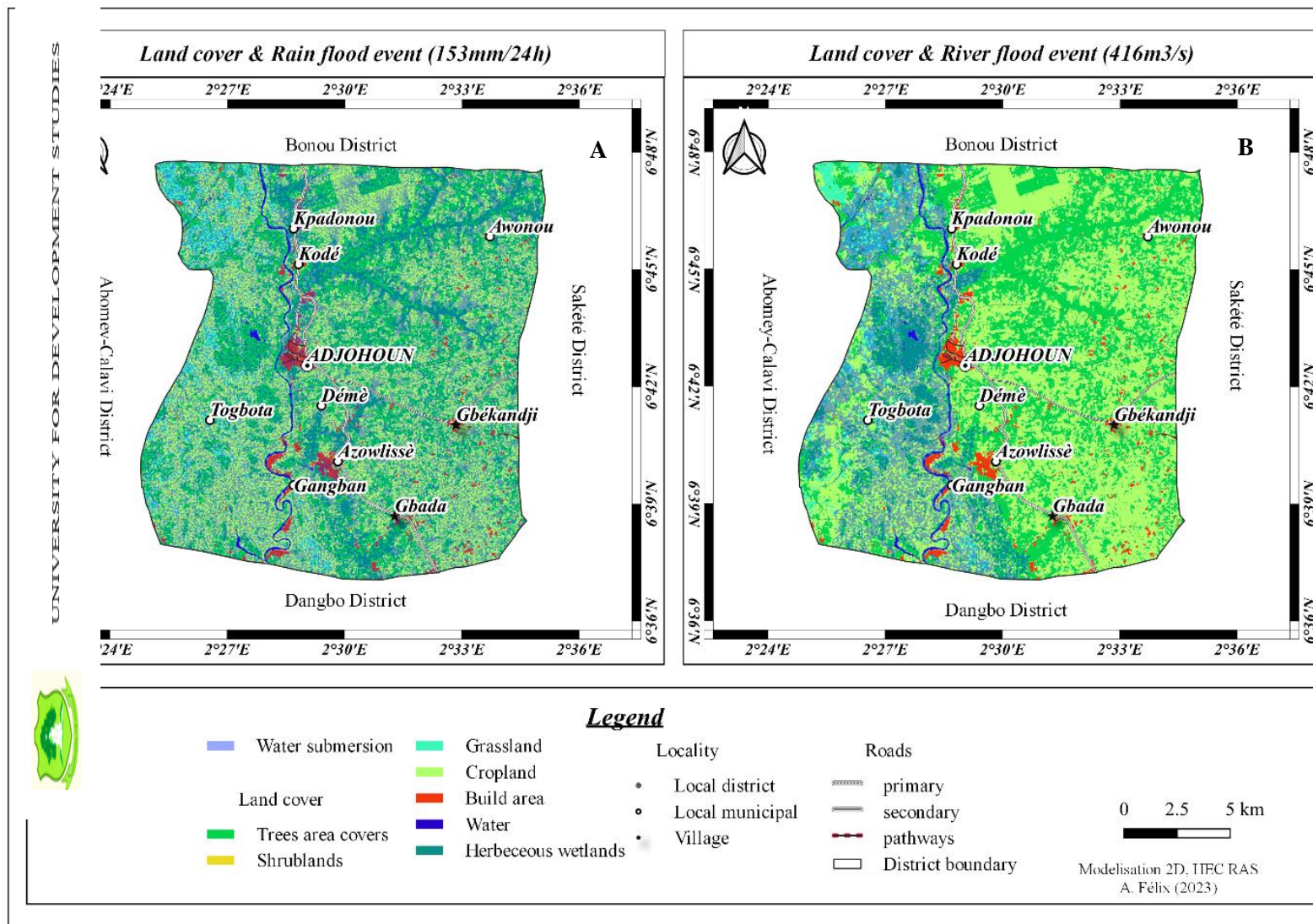


Figure 4- 19: Land cover & flood (rain, river) events



In sum, a comparison with the results of hydro-rainfall behavior analysis evaluated in the Adjohoun district highlights the following facts. The months of May-June-July are known as months with a high probability of observing showers capable of generating rainfall floods and those of August-September-October for the occurrence of riverine floods. Therefore, similar scenarios can be observed as shown in Figure 4- 19 (A) in the months of May-June-July or the one in Figure 4- 19 (B) in the months of August-September-October in a case of river overflow. In these cases, we can observe crop areas, houses, roads or infrastructures inundated by water. However, the intensity of impact is nevertheless low for a rainfall flood against a river flood capable of inundating the eastern sector of the district, known as an area of high agricultural activity. But according to Loc *et al.*, (2020), in the State of Thailand, rainfall contributes more than 73.77% over 76 km² in terms of flooding of the plains. Furthermore, according to the results obtained by Moncoulon *et al.*, (2014), river overflow could be a combined effect of slope, heavy rainfall and catchment size. Olanrewaju *et al.*, (2017), on the contrary, argue that the effect is due to the lack of water drainage infrastructure. Thus, the potential source of losses and damages is related to river floods that severely affect the population and much of the agricultural sector, which is the western part of the Ouémé River. Consequently, a particular focus is placed on the discharge series in a context of seasonal forecasting of river floods in the study area in an approach to identify the best forecasting model. The following paragraphs discuss the results on seasonal forecasting, the dissemination of the results of this study online with the aim of exploiting the results of this research.

4-3. Identify the Best Fitting Flood Forecasting Models for The Study Region

4-3-1. Seasonal forecasting of river floods

Seasonal flood forecasting predicts a future event calibrated to a confidence interval. The forecasting methodology varies from one forecasting model to another. In our case, the Holt-Winters, ARIMA and SARIMA forecasting models were chosen. As a precursor, tests of seasonality, stationarity and autocorrelation of the series were performed, followed by the evaluation and validation of the best river flood forecasting model.

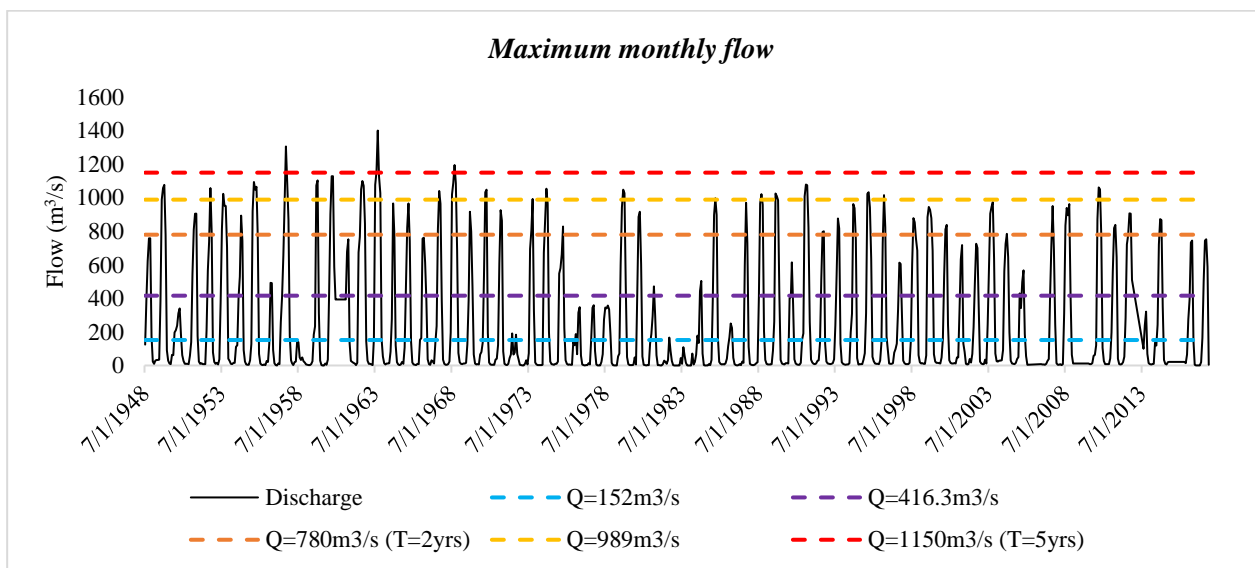


Figure 4- 20: Time series used for seasonal forecasting

As part of the effectiveness of seasonal forecasting, the daily inflows to the Adjohoun district (Bonou station) were processed and transformed into monthly maximum flows (Figure 4- 20). A seasonal forecast based on the monthly maximum values will make it possible to predict the monthly maximum daily value likely to be observed - for the coming season. A forecast equivalence of monthly maximum flows in the ranges 152 m³/s, 416.3 m³/s, 780 m³/s (T=2years), 989 m³/s or 1150 m³/s gives an idea of the risk and range of probable flood heights for plantation fields, infrastructure, etc. Furthermore, for the evaluation and validation of the best forecasting model, the time series was divided into two parts, one part for testing and the second part for the assessment of the quality of the forecast.

Tests on seasonality, stationarity and autocorrelation

In order to ensure the stationarity in time of the raw observations, a study on the detection of stationarity and seasonality break was conducted. This particular attention allowed us to see the evolution in time of the seasonality as well as the stationarity of the flow regime through the observations.

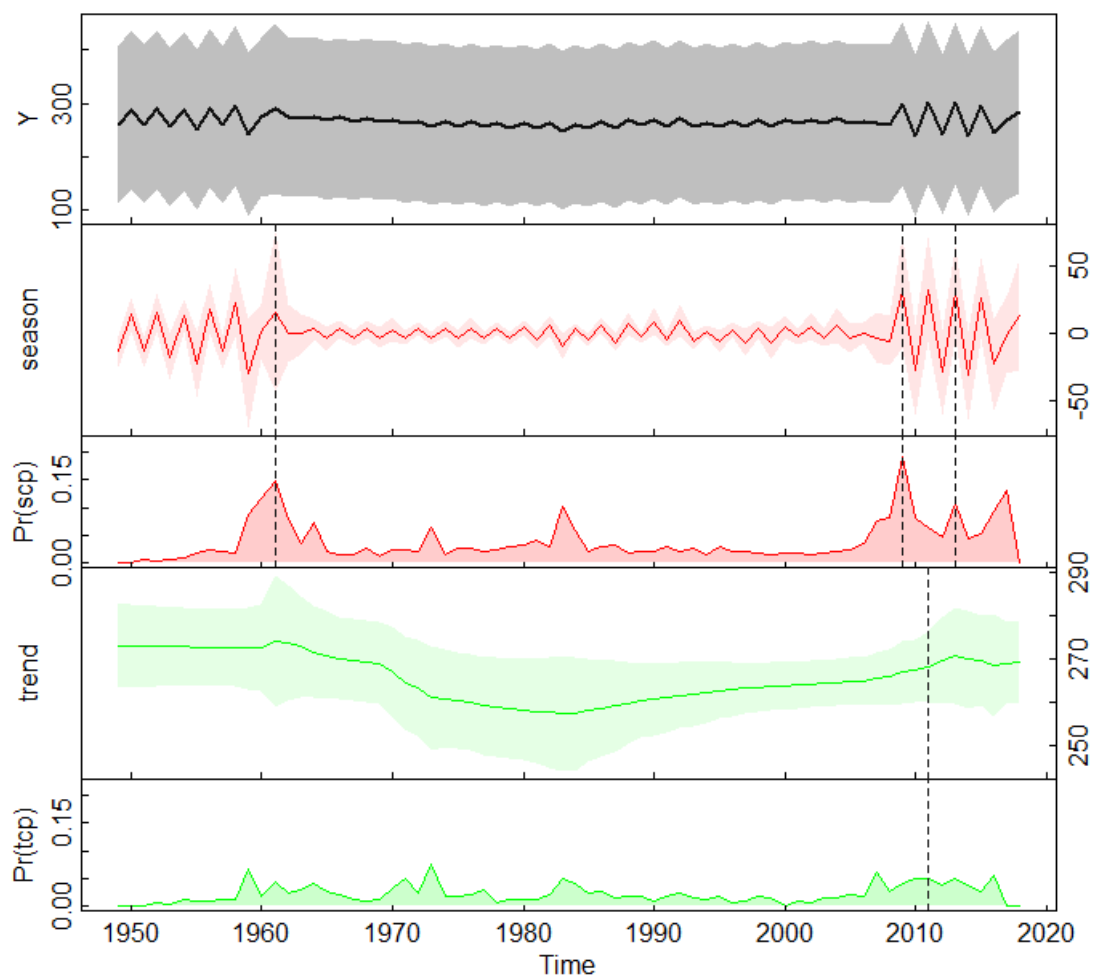


Figure 4- 21: Break in stationarity on the chronology of raw observations

From the above graph, three (3) periods of change in the state of seasonality can be noticed including 1949-1960 (high amplitude), 1961-2008 (low amplitude) and 2009-2017 (high amplitude) (Figure 4- 21). Concerning the stationarity graphically (Figure 4- 21), from 1949 to 1960 (stable trend) we notice a stability of the flow regime. However, this trend changes through a decreasing behavior of the flow regime of the river from 1961 to 1987 (decreasing

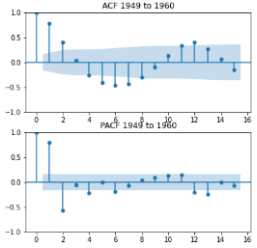
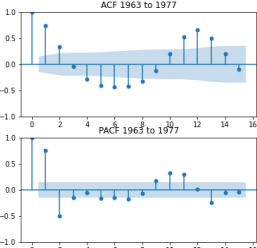
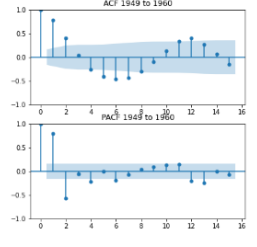


trend) and a resumption of the flow regime from 1989 until 2010 (increasing trend). From 2010 onwards, a return to a stable flow regime was observed. Thus, for a better appreciation of the predictive capacity of monthly maximum discharges under different discharge regimes, two (2) time ranges were considered such as 1949-1959 (stable trend & high amplitude seasonality), 1963-1978 (decreasing trend & low amplitude seasonality) and 1980-2004 (increasing trend & high amplitude seasonality).

Evaluation of forecasting models

The table below shows the results of the statistical tests on the defined data samples.

Table 4- 14: summary on ADF, PP and KPSS tests and ACF & PACF

Period	Discharge behavior	Statistical tests			Decision	Autocorrelation & Partial Autocorrelation Function (ACF & PACF)
		Augmented Dickey-Fuller (ADF) test	Phillips-Perron (PP) test	Kwiatkowski-Phillips-Schmidt-Shin (KPSS) test		
1949-1959	Stable trend & strong seasonality	Stationary (p.value = 0.01)	Stationary (p.value = 0.01)	Non-stationary (p.value = 0.1)	Stationary	
1963-1977	Downward trend & low amplitude seasonality	Stationary (p.value = 0.01)	Stationary (p.value = 0.01)	Non-stationary (p.value = 0.1)	Stationary	
1980-2004	Upward trend & strong seasonality	Stationary (p.value = 0.01)	Stationary (p.value = 0.01)	Non-stationary (p.value = 0.1)	Stationary	



The values of each series as presented in the table above (Table 4- 14) is evaluated the predictive capacity of each model as well as the robustness of the model through the variation of the discharge regime over time. Figure 4- 22, Figure 4- 23 and Figure 4- 24 below allow a graphical appreciation of the prediction quality of the three (3) models under evaluation for the prediction of discharges in the study area. Initially, considering a regime with a stable flow tendency and a strong seasonal amplitude, two models emerge promptly. These are the SARIMA and HWES models (Figure 4- 22). The prediction of monthly maximum flows from these models fits the measured values as well as possible. In contrast, the ARIMA model struggles to predict monthly maximum flows, tending to overestimate the minimum and underestimate the maximum. Then, in the context of a downward flow regime and a low amplitude seasonality (Figure 4- 23), the ARIMA model performs better than its competitors. However, it still overestimates the minimum observations, a factor that increases the forecast error of the model.

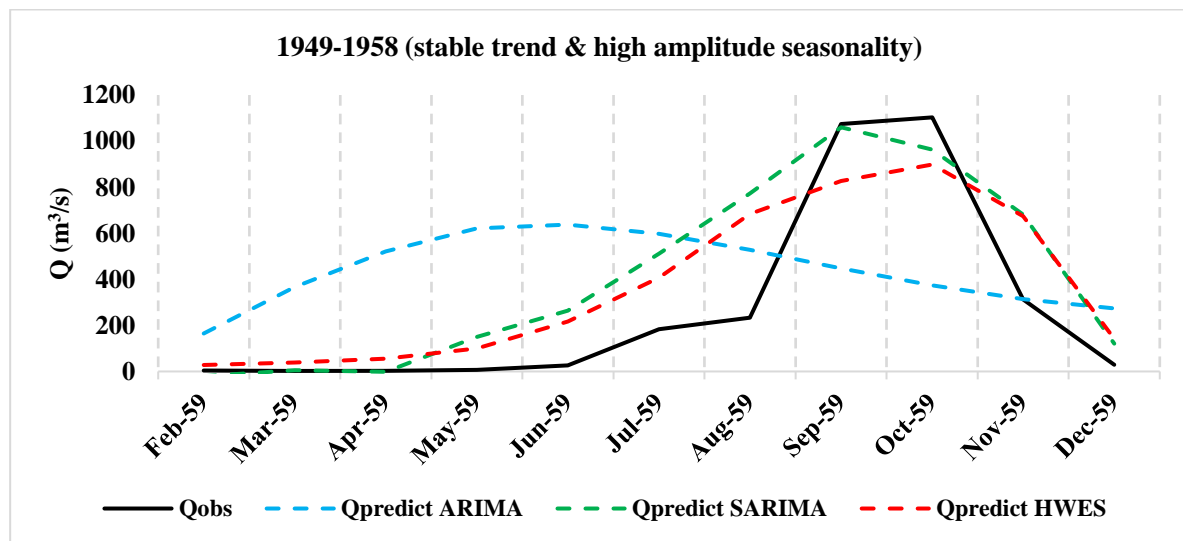


Figure 4- 22: Flow prediction for the year 1959 under a stable regime with a strong seasonal amplitude

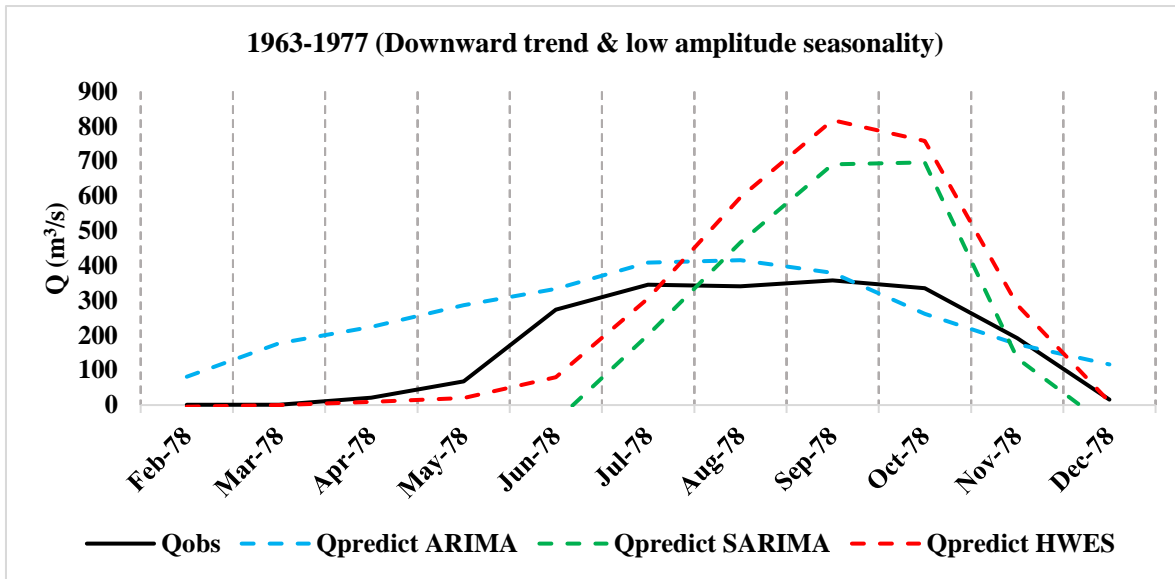


Figure 4- 23: Flow prediction for 1978 under a declining regime & low amplitude seasonality

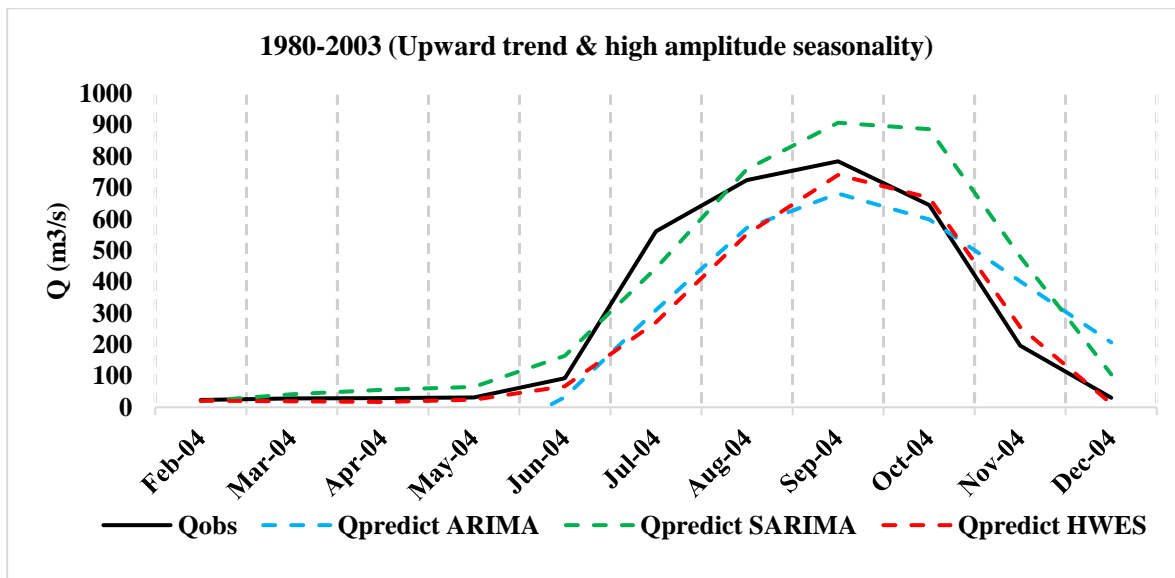


Figure 4- 24: Flow prediction for 2004 under an increasing regime & high amplitude seasonality

Evaluating the performance of the forecast models under an upward trend flow regime and increasing seasonality, graphically all three models perform better. However, further analysis under numerical criteria such as RMSE, MAE and MAPE allow for a stricter judgment. Presented by the table below, in search of the minimization of the values of the criteria for each flow regime, a SARIMA (2,0,1) (1,1,1) model [12] performs well under a regime with a stable trend and strong amplitude. Under a regime of decreasing trend and low amplitude, the ARIMA

(6,0,3) model is very efficient. In our era, under an upward-trending, high-amplitude flow regime, the HWES model performs well especially under the evaluation criteria.

Table 4- 15: Performance evaluation of forecasting models under RMSE, MAE and MAPE criteria

Predicted period	Model	Criteria			Flow regime	Best fitting forecasting model
		RMSE	MAE	MAPE		
1959	HWES	223.27	181.47	629.65	Stable trend & high amplitude seasonality	SARIMA
	SARIMA (2,0,1) (1,1,1) [12]	241.19	172.20	413.91		
	ARIMA (2,0,4)	469.03	416.17	4594.58		
1978	HWES	214.68	140.05	122.00	Downward trend & low amplitude seasonality	ARIMA
	SARIMA (1,0,1) (2,1,2) [12]	194.57	156.01	958.54		
	ARIMA (6,0,3)	119.15	99.10	2509.86		
2004	HWES	104.97	60.13	27.70	Upward trend & high amplitude seasonality	HWES
	SARIMA (1,0,2) (2,1,1) [12]	128.58	93.08	74.15		
	ARIMA (5,0,2)	149.10	135.95	236.79		

In sum, under this section of evaluation of monthly maximum discharge forecasting model capable of causing flooding in the Adjohoun district, the models under study according to the flow regime present weaknesses, limitations and acceptable performances. Consequently, we conclude that depending on the flow regime, a method of forecasting maximum monthly flows must be chosen. Currently, in the study area the trend of the flow regime is increasing with a strong amplitude of seasonality and therefore the best statistical model for flood forecasting is the Holt Winter Exponential Smooth (HWES). This model can be used for future floods of current years while making an analysis on the trend and seasonality of historical data, thus adapting the best model accordingly. It should be noted that the HWES model has proven its performance in studies conducted by Jere *et al.*, (2019) for forecasting annual international tourist arrivals in Zambia. However, the model has also proven its performance in forecasting wholesale prices of exotic vegetables in Kenya (Mbugua *et al.*, 2021). On the other hand,



compared to other forecasting models, the HWES model may be less efficient, as demonstrated by Mansor *et al.*, (2021) in Malaysia, where SARIMA performs well in forecasting medium-term electricity load demand. However, Munim *et al.*, (2023) have shown that for forecasting monthly container throughput data from the ports of Shanghai, Busan and Nagoya in Asia, the models studied perform less well than the prophet model.

4-4. Early Warning Decision-Making Tool for Crop Selection and Land Management

First, the spatial heterogeneity of the reported flood water height classes makes it difficult to map each type of crop. Also, from the analyses made it is found that the water level and the flooded area vary from one maximum value to another. These two facts exclude the uniformity and uniqueness of potential damage (crops/plantations, infrastructure, etc.) related to flooding in Adjohoun.

Therefore, for accessibility of the outputs of this work, and the consideration of the spatio-temporal variability of floods, a database was developed and mounted online. The platform is mounted on Google Site and made available to the public. It provides information on the seasonal forecast of monthly maximum flows (Q_{predj}). Q_{predj} compared to the values of fictitious reference flows (Q_{ref}) 152 m³/s, 416 m³/s, 780 m³/s, 989 m³/s and 1150 m³/s allows to take curative and preventive measures against potential future floods. The second crucial information is the availability of informative data on the fictitious flow, water height (cm), plant tolerance height, infiltration rate, etc. in *.kmz format for a 3D visualization on Google Earth from smartphones and/or computers.

The website created is accessible via the following link <https://sites.google.com/view/adjohoun-zero-perte>. It presents on the home page the key information about my personality, the study area, the objectives and some results. It provides links to a portal for downloading the Google earth application, and other links to a page for publishing information related to the Q_{pred} seasonal forecast and Q_{ref} databases. Figure 4- 25



below, shows the home interface of the site on a smartphone. For optimal use, the user can log in to the site and access the seasonal forecast page to get information on the futuristic Qpred values. With this information, users will be able to :

- Compare Qpred to reference flow values Qref (152 m³/s, 416 m³/s, 780 m³/s (T=2years), 989 m³/s and 1150 m³/s (T=5years),
- Connect to the Zero Loss platform==> River Flood==> Qref (of your interest)==> Download the *.kmz file of your area,
- Open the download file in google earth with your smartphone/computer,
- Select plants wisely and design your space to reduce loss and damage.

To know the time needed for the total infiltration of the water height in your area, do:

"(Depth*30.48*100) /Infiltration rate".



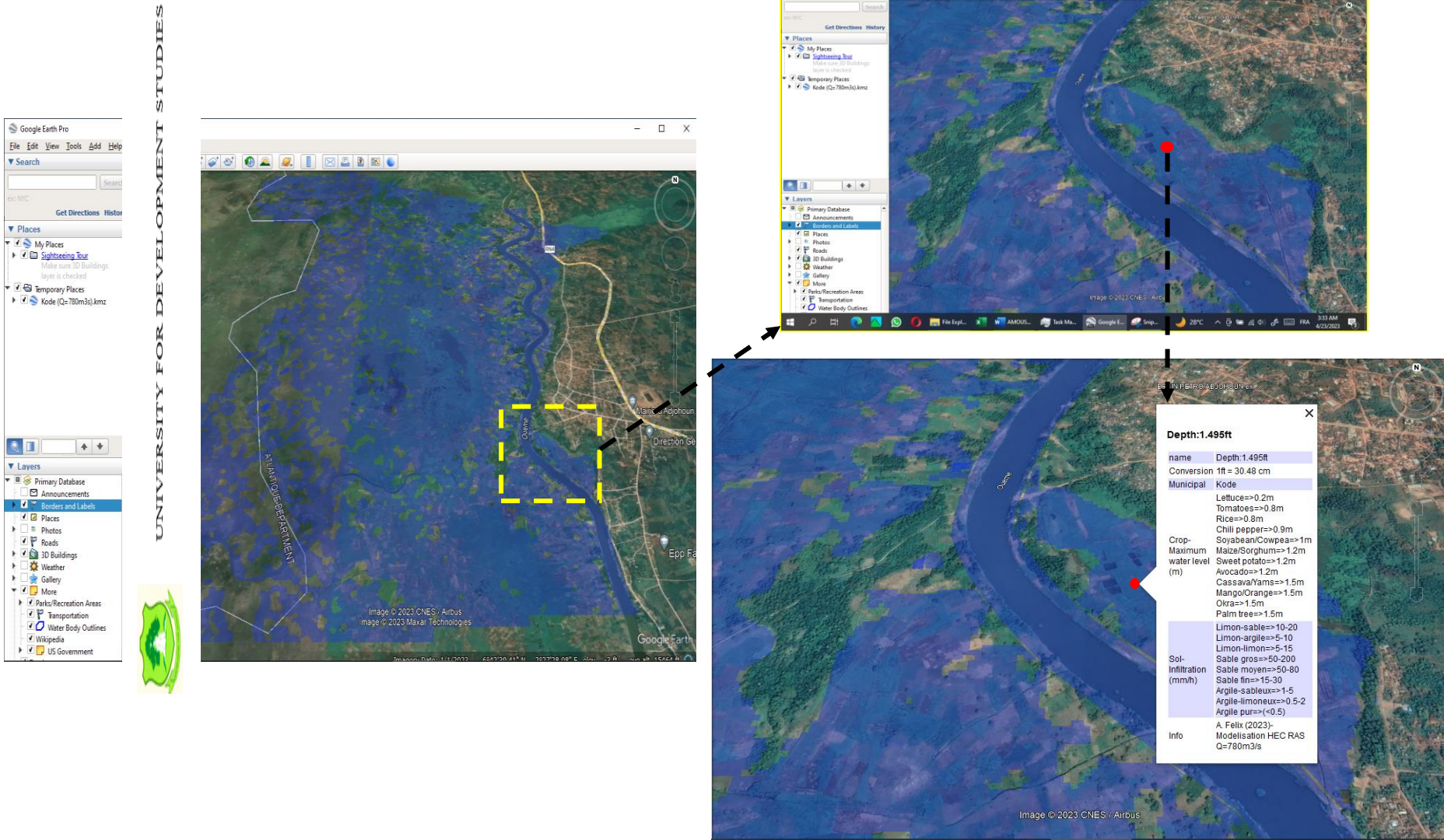


Figure 4- 25: Display of the page on a smartphone

The download of the *.kmz file is done according to the forecast value and the concerned municipality. Once downloaded, the opening must be done under Google earth for a 3D visualization, or other Geographic Information System (GIS) tool that can support *.kml/kmz format files. Figure 4- 26 below shows an example of opening under Google earth. In this case, a reference flow of $780 \text{ m}^3/\text{s}$ for the Kodé municipality has been chosen. We see a very clear 3D graphic rendering, with distinction of crop fields, houses, infrastructures, etc., and of course the flood limits marked by the polygons with transparent blue colors. However, in order to have relative information about an area of interest, as shown below (Figure 4- 26) it is necessary to move, zoom in on the area and click on the place in question. Then a pop-up window will open

presenting information about the water level (ft) in the area under the reference flow. It will also present, an assistance about the Crop-Maximum water level tolerable (m) for the majority of the local plants, the infiltration rate (mm/h) under each type of soil. With this information, the farmer will be able to intelligently choose a plant capable of overcoming the trials of flooding. A field trip gives an idea of the type of soil, and knowing the type of soil, one has an idea of the infiltration rate, which in turn, when related to the water level, gives an idea of the time needed for complete infiltration of the water.





On the other hand, information on the maximum height of the water level tolerated by a plant assists farmers in selecting resistant plants that can survive the projected disasters.

Codjo *et al.*, (2015) worked on the adaptation of the Adjohoun farming population to climate change, have explained the adaptive measures implemented by these populations with a model of crop association and use of short-cycle crops. Others apply to ridge cropping (Waïdi, 2020). Also, in almost the same context, in Cameroon, beyond a selection of short-cycle crops, the population opted for crops that are resistant to climatic hazards (Chimi *et al.*, 2022). Faced floods, people opt to abandon the site, reseed or use the most suitable crops or plants. However, the authors point out that these measures are applied insignificantly (Chimi *et al.*, 2022).

A research study by Zhang *et al.*, (2018) examined the strategies used to select flood-resistant rice varieties. The researchers identified several genes associated with flood tolerance and used this information to develop new, more flood-resistant rice varieties. A study carried out in India also showed that certain plants were capable of resisting flooding. After a series of tests, Zhang *et al.*, (2018) and Singh *et al.*, (2019) concluded that certain rice and maize varieties were able to grow even when flooded, which could help farmers preserve their crops and maintain their production levels. The study by Kamara *et al.* (2019) highlighted the contribution of plants to community resilience in the event of flooding. The authors analyzed farmers' agricultural practices in flood-prone areas of Sierra Leone and found that farmers use plant varieties that are more flood-resistant and have shorter ripening times. These articles can be a good resource for delving deeper into the problems of flooding and crop losses in the Adjohoun region of Benin, and for finding solutions to deal with them.



CHAPTER FIVE:

CONCLUSION AND RECOMMENDATIONS

5.1. Conclusion

At the end of this research, a number of conclusions has been drawn. These are oriented towards each specific objective. Generally, this study was to identify the flood zones for plant selection and land management according to the occurrence of hydroclimatic events adjusted with numerical predictions. Then the first objective aims to characterize the hydroclimate (rain & flow) events and occurrence of exceptional phenomena for the return period of 2-year and 5-year. In this respect, it was found that rainfall does not explain 100% of the flow measured in the river, while 94% of the flow in the river is significantly explained by the value of the water level in the river. In Adjohoun, the regime is bimodal, with a cumulative peak in June for precipitation and unimodal for discharge, with a peak in September. However, July can be considered a month with a high probability of heavy rainfall causing flooding.

Over the 79 years of river discharge observations, maximum daily values only occur in the month of September. There is therefore a high probability of crop and property losses due to river flooding in September. To this end, for the occurrence of extreme phenomena, the maximum annual daily values of precipitation and discharge were evaluated using three extreme value distributions, including Gumbel, GEV, and Weibull. In this regard, Gumbel's is the best distribution to describe the observations. For a return period of 2 years (50% annual probability), daily of 115mm and 780 m³/s are expected, compared with 153mm and 1150 m³/s for a return period of 5years (20% annual probability).

With regard to the second specific objective dealing with hydraulic modeling, the results show that the Adjohoun Valley is more vulnerable to river flooding than to rainfall. In the case of rain-fed floods, approximately 17.08% or 53.92km² of the surface area is likely to be affected





for a return period of 2years, with a maximum water height of 304.8cm (50m²). In the event of a 5 years flood, this will rise to 396.24cm (60m²), and half the area will be covered by water. However, this represents only 1.81% (3.72km²) of the valley's surface area, which is not suitable for the production of plants that do not tolerate a maximum water level below 0.9m (Tomatoes, Rice, Lettuce, Chili pepper). For river flooding, the situation is different. Only about 28.32% (89.817km²) is subject to flooding, with a submersion height of up to 518.16cm. Most of the flooding occurs on the right bank of the Ouémé River, a highly cultivated area. This may explain the crop losses often reported by the authorities. The most predominant flood height classes are 30.48cm (~30km²); 60.96cm (~29km²), 91.44cm(~15km²), and 121.92cm (~5km²), where a careful choice of crop types is essential.

The third objective is to find the best statistical model for the seasonal prediction of maximum monthly discharge. Depending on the trend and seasonality of the discharge regime, three sub-periods have been detected, with each varying in accuracy. For current discharge observation, in the study area, the trend of the flow regime is increasing with a strong amplitude of seasonality and therefore the best statistical model for flood forecasting is the Holt Winter Exponential Smooth (HWES) model [RMSE=104.97, MAE=60.13, MAPE=27.70].

Finally, the last objective responds to the overall aim of this research by combining the results of the previous objectives into a platform. The platform provides information on seasonal and flood height forecasts for each crop plot, enabling optimal crop selection and land management.

5.2. Recommendations for management policy

For the local population,

- For their own safety, we recommend that they live on non-flooded land located at the east of the river and 150m faraway from the bank;
- For those who have their land in the river's main bed, a maximum above-ground foundation height of around 5m should be allowed for any losses;

- Growers of small-scale vegetables (lettuce, carrots, legumes, etc.) in the main or minor riverbed should avoid growing them from mid-August to the end of October. They can take a risk by opting for resistant crops (rice, taro plants) or large-scale crops (trees), with a suitable layout for water drainage if possible;
- Those farming in valleys should exclude the months of September and October in their cropping calendar;
- In the case of continuous exploitation of the valley, depending on the nature of the soil (infiltration capacity) and the maximum submersion height, choose the most suitable farming system.

To district authorities,

- Encourage the population to leave flood-prone areas for secure habitat areas, and promote intelligent agriculture (resistant crops);
- Implement hydraulic structures to manage annual floods by building a small dam or artificial flood control lake.

5.3. Further research

Human life is very precious, and in the context of sudden night-time flooding, national early warning and monitoring systems are less effective in providing rapid response and assistance to disaster victims. So, for future research, we plan to explore the technology of networked connected objects to develop an IT tool for direct, real-time monitoring of the state of rising waters in Adjohoun.



References

1. Abdul Halim NS, Abdullah R, Karsani SA, Osman N, Panhwar QA, Ishak CF, (2018). Influence of Soil Amendments on the Growth and Yield of Rice in Acidic Soil. *Agronomy*. vol 8(9):165. <https://doi.org/10.3390/agronomy8090165>.
2. Adamowski Jan F. (2008). Development of a short-term river flood forecasting method for snowmelt driven floods based on wavelet and cross-wavelet analysis, *Journal of Hydrology*, Vol 353, Issues 3–4, pp.247-266, <https://doi.org/10.1016/j.jhydrol.2008.02.013>.
3. Adejuwon, J.O., & Adejuwon, M.A. (2014). Flooding and crop losses in Nigeria: The way forward. *Journal of Agricultural Science*, 6(4), 143-152. <https://doi.org/10.5539/jas.v6n4p143>.
4. Aderonmu, A. T. (2015). Assessing the impact of changing climate on agriculture in Missouri and the use of crop insurance as an adaptation strategy (1980–2010). (Doctoral dissertation). University of Missouri-Kansas City, Kansas City, KS.
5. Adjakpa T. T., 2016. *Gestion des risques hydro-pluviométriques dans la basse vallée du Niger au Bénin : cas des inondations des années 2010, 2012 et 2013 dans les communes de Malanville et Karimama*, Université d'Abomey-Calavi, thèse de doctorat, 279p.
7. Agbazo, M (2016). Estimation of IDF Curves of Extreme Rainfall by Simple Scaling in Northern Oueme Valley, Benin Republic (West Africa). *Earth Sci. Res. J.*, vol.20, n.1, pp.1-7. ISSN 1794-6190. <https://doi.org/10.15446/esrj.v20n1.49405>.
8. Aghakouchak, A., Chiang, F., Huning, L. S., Love, C. A., Mallakpour, I., Mazdiyasni, O., Moftakhari, H., Papalexiou, S. M., Ragno, E., & Sadegh, M. (2020). Climate Extremes and Compound Hazards in a Warming World, *Annual reviews*, <https://doi.org/10.1146/annurev-earth-071719-055228>.



9. Ague A.I. and A. Afouda (2015). Analyse fréquentielle et nouvelle cartographie des maxima annuels de pluies journalières au Bénin. *Int. J. Biol. Chem. Sci.*, 9, 121-133.
10. Ahmet Kurunç & Ali Ünlükara (2009) Growth, yield, and water use of okra (*Abelmoschus esculentus*) and eggplant (*Solanum melongena*) as influenced by rooting volume, New Zealand. *Journal of Crop and Horticultural Science*, 37:3, 201-210, DOI: [10.1080/01140670909510265](https://doi.org/10.1080/01140670909510265).
11. Ahouangan M., Bakary D., Pierre O. and Y. C. Hountondj (2014). Adaptation et résilience des populations rurales face aux catastrophes naturelles en Afrique subsaharienne. Cas des inondations de 2010 dans la commune de Zagnanado, Bénin. *Presses de l'Université d'Angers*, Angers, France, 265-278p, <http://www.openedition.org/9567>.
12. Akpla Canisius, Edouh T. Lucrèce, Agbangba E. Codjo, Oumorou Madjidou, Akodogbo Hervé, (2022). Amélioration de la gestion de l'inondation et de l'agriculture de décrue par la méthode de cartographie participative par drone dans la Commune d'Abomey-Calavi, *Ecole polytechnique d'Abomey-Calavi*, Mémoire, 62 pages, <http://biblionumeric.epac-uac.org:8080/jspui/handle/123456789/5342>.
13. Allen, T. and P. Heinrigs (2016). Emerging Opportunities in the West African Food Economy, *West African Papers*, No. 01, OECD Publishing, Paris. <http://dx.doi.org/10.1787/5jlvfj4968jb-en>.
14. Amangabara T. G., and Obenade M., 2015. Flood vulnerability assessment of Niger delta states relative to 2012 flood disaster in Nigeria. *American Journal of Environmental Protection*, vol. 3, no. 3, pp. 76–83.
15. Amegnaglo, J. (2016). Evaluation of the effects of floods on maize production in southern Benin using remote sensing and GIS techniques. *Journal of Applied Remote Sensing*, 10(1), 016017. <https://doi.org/10.1117/1.JRS.10.016017>.





16. Amoussou E., Camberlin P., Totin Vodounon S. H., Trambly Y., Houndenou C., Mahé G., Paturel J.-E. and Boko M. (2014). Evolution des précipitations extrêmes dans le bassin versant du Mono (Bénin-Togo) en contexte de variabilité/changement. Dijon : CRC, p. 343-349. *Colloque de l'Association Internationale de Climatologie*, 27., Dijon (FRA), ISBN 978-2-907696-20-3.
17. Amoussou E., Pierre Camberlin, V.S.H. Totin, and Jocelyne Pérard (2011). Événements hydroclimatiques et risque d'inondation au sud-ouest du Bénin. *24ème colloque de l'Association Internationale de Climatologie*, Sep 2011, Rovereto, Italie. pp.39-44. (hal-01116604)..
18. Amoussou, E., Ossen, A. A., Totin, V. S. H., Lange. U., & Preuss, S. (2017). Hydroclimatic variability and flood risk on Naglanou and Akissa forests areas in Mono River Delta (West Africa). *International Journal of Biodiversity and Conservation*, 9(6), 212-223, <https://doi.org/10.5897/IJBC2016.1061> .
19. Ansah S. O., Ahiataku M., AYorke C. K., F. Otu-Larbi, Bashiru Yahaya, P. N. L. Lamptey M. Tanu,(2020). Meteorological Analysis of Floods in Ghana. *Advances in Meteorology*, vol. 2020, Article ID 4230627, 14 pages, 2020. <https://doi.org/10.1155/2020/4230627>
20. Arnell, N.W., Brown, S., Gosling, S.N. *et al* (2016). The impacts of climate change across the globe: A multi-sectoral assessment. *Climatic Change* **134**, 457–474. <https://doi.org/10.1007/s10584-014-1281-2>.
21. Arturo S. L., and Goodell C., (2016). *Controlling HEC RAS using MATLAB, environmental modelling & software*, volume 48, pages 339-348, <https://doi.org/10.1016/j.envsoft.2016.06.026>.
22. Asa, Adedoyin, Ayobami, Ezelobe, Courage, Afegheze and Ajisola, Judge K., (2021). Growth and Yield Response of Sweet Potato (*Ipomoea batatas*) to Organic and

Inorganic Fertilizer on Degraded Soil of Southern Guinea Savanna of Nigeria.
International Journal of Environment, Agriculture and Biotechnology Vol-6, Issue-5;
DOI: [10.22161/ijeab](https://doi.org/10.22161/ijeab).

23. Atiah, W. A., Amekudzi, L. K., & Danuor, S. K. (2023). Mesoscale convective systems and contributions to flood cases in Southern West Africa (SWA): A systematic review. *Weather and Climate Extremes*, 39, 100551. <https://doi.org/10.1016/j.wace.2023.100551>
24. Bacharou T., Adjiboicha M., Gbaguidi G., Houinou G., Orlova E., (2015). Caractérisation de la pluviométrie du bassin versant de l'Ouémé au Bénin : établissement des courbes Intensité-Durée-Fréquence des précipitations, *Structural Mechanics of Engineering Constructions and Buildings*, n°4, 76-80p.
25. Bacharou, T., Houinou, G., Adjiboicha, M., Edmond, C. A., & Orlova, E. (2013). Estimation des pluies exceptionnelles journalières en zone tropicale : cas du bassin versant de l'oueme au benin par comparaison des lois de jenkinson et de gumbel. *Structural Mechanics Of Engineering Constructions And Buildings*, (4), 63-71, <https://journals.rudn.ru/structural-mechanics/article/view/11034>.
26. Badou Djigbo Félicien, José Hounkanrin, Jean Hounkpè, Luc Ollivier Sintondji, Agnidé Emmanuel Lawin, (2023). Assessing the Return Periods and Hydroclimatic Parameters for Rainwater Drainage in the Coastal City of Cotonou in Benin under Climate Variability, *Advances in Meteorology*, vol. 2023, Article ID 1752805, 10 pages, 2023. <https://doi.org/10.1155/2023/1752805>.
27. Bailey-Serres, J., Lee, S. C., and Brinton, E. (2012). Waterproofing crops: Effective flooding survival strategies. *Plant Physiology*, 160, 1698– 1709. <https://doi.org/10.1104/pp.112.208173>



28. Baldassarre G. D., A. Montanari, H. Lins, D. Koutsoyiannis, and L. Brandimarte, (2010). Flood fatalities in Africa: from diagnosis to mitigation. *Journal of Geophysical Research Letters*, vol. 37, no. 22. <https://doi.org/10.1029/2010GL045467>.
29. Bani S., and Yonkeu S., (2016). Risques d'inondation dans la ville de ouagadougou : cartographie des zones à risques et mesures de prévention. *Journal Ouest-Africain des Sciences de Gestion*, ISSN 2424-7413 : Vol.1, No1,1-109, 2016.
30. Basile A. Germain G., Toussaint V., (2017). Importance et contributions de la fete “wemexwe” dans le développement des communes de la basse vallée de l’Ouémé. *European Scientific Journal*, Vol.13, No.26 ISSN: 1857 – 7881. <http://dx.doi.org/10.19044/esj.2017.v13n26p136>.
31. Benjamin Ason, Felix Owusu Ababio, Enoch Boateng and Macarius Yangyuoru (2015). Comparative Growth Response of Maize on Amended Sediment from the Odaw River and Cultivated Soil. *World Journal of Agricultural Research*, Vol. 3, No. 4, pp 143-147. doi: 10.12691/wjar-3-4-5.
32. Benkhaled A. (2007). Distributions statistiques des pluies maximales annuelles dans la région du Cheliff. Comparaison des techniques et des résultats. *Courrier du Savoir*, 8, 83-91. Doi : [http://scholar.google.com/scholar?q=BENKHALED%20A.%20\(2007\).%20Distributions%20statistiques%20des%20pluies%20maximales%20annuelles%20dans%20la%20r%C3%A9gion%20du%20Cheliff.%20Comparaison%20des%20techniques%20et%20des%20r%C3%A9sultats.%20Courrier%20du%20Savoir,%208,%2083-91](http://scholar.google.com/scholar?q=BENKHALED%20A.%20(2007).%20Distributions%20statistiques%20des%20pluies%20maximales%20annuelles%20dans%20la%20r%C3%A9gion%20du%20Cheliff.%20Comparaison%20des%20techniques%20et%20des%20r%C3%A9sultats.%20Courrier%20du%20Savoir,%208,%2083-91). 10.3923/jas.2010.1684.1694
33. Betz U. A., Arora, L., Assal, R. A., Azevedo, H., Baldwin, J., Becker, M. S., Bostock, S., Cheng, V., Egle, T., Ferrari, N., Schneider-Futschik, E. K., Gerhardy, S., Hammes, A., Harzheim, A., Herget, T., Jauset, C., Kretschmer, S., Lammie, C., Kloss, N., . . . Zhao, G. (2023). Game



changers in science and technology - now and beyond. *Technological Forecasting and Social Change*, 193, 122588. <https://doi.org/10.1016/j.techfore.2023.122588>.

34. Biao Eliézer Iboukoun, Eric Adéchina Alamou & Abel Afouda (2016). Improving rainfall–runoff modelling through the control of uncertainties under increasing climate variability in the Ouémé River basin (Benin, West Africa), *Hydrological Sciences Journal*, 61:16, 2902-2915, DOI: 10.1080/02626667.2016.1164315
35. Bisikwa J, Kawooya, R., Ssebuliba J., Stanley Peter, Biruma Ms. and Kalule D., (2014). Effects of plant density on the performance of local and elite cowpea [*Vigna unguiculata* L. (Walp)] varieties in Eastern Uganda. *African Journal of Applied Agricultural Sciences and Technologies*, 28-41, <https://www.researchgate.net/publication/267027251>.
36. Blöschl G. and A. Montanari (2010). Climate change impacts-throwing the dice? *Hydrological Processes*, 24, (3) 374-381.
37. Bo R. & Döös, (2002). Population growth and loss of arable land. *Global Environment Change*, Volume 12, Issue 4, 303-311p, [https://doi.org/10.1016/S0959-3780\(02\)00043-2](https://doi.org/10.1016/S0959-3780(02)00043-2).
38. Bodian A. (2014) - Caractérisation de la variabilité temporelle récente des précipitations annuelles au Sénégal (Afrique de l'Ouest). *Physio-Géo - Géographie Physique et Environnement*, vol. VIII, p. 297-312. doi : 10.4000/physio-geo.4243.
39. Bogner, K., Liechti, K., and Zappa, M., (2017). Technical note: Combining quantile forecasts and predictive distributions of streamflows, *Hydrol. Earth Syst. Sci.*, 21, 5493–5502, <https://doi.org/10.5194/hess-21-5493-2017>.
40. Bogner, K., Pappenberger, F., and Cloke, H. L., (2012) Technical Note: The normal quantile transformation and its application in a flood forecasting system, *Hydrol. Earth Syst. Sci.*, 16, 1085–1094, <https://doi.org/10.5194/hess-16-1085-2012>.



41. Brown Daniel G., Kenneth M. Johnson, Thomas R. Loveland, & David M., (2005). Rural land-use trends in the conterminous united states, 1950–2000. *Ecological Applications*, Volume 15, Issue 6 p. 1851-1863, <https://doi.org/10.1890/03-5220>
42. Cantuarias-Avilés, T.; Silva, S.R. Da; Angolini, S.F.; Brogio, B. Do A.; Baptista, E.G. & Micheletti, L.B (2019). Water status and productivity of 'Hass' avocado trees in response to supplemental irrigation during winter. *Pesquisa Agropecuária Brasileira*, v.54, e00237, doi : <https://doi.org/10.1590/S1678-3921.pab2019.v54.00237>.
43. Capstick, S., Whitmarsh, L., Poortinga, W., Pidgeon, N., & Upham, P. (2014). International trends in public perceptions of climate change over the past quarter century. *Wiley Interdisciplinary Reviews: Climate Change*, 6(1), 35-61. <https://doi.org/10.1002/wcc.321>.
44. Charles Tortoe, Paa T. Akonor and Jemima Ofori, (2019). Starches of two water yam (*Dioscorea alata*) varieties used as congeals in yogurt production. *Food Science and Nutrition*, Volume7, Issue3, 1053-1062pp, <https://doi.org/10.1002/fsn3.941>.
45. Chauhan, R., Thakuri, S. and Pradhan, C. (2023), Disaster and Displacement: Opportunities and Challenges for Enhancing Resilience in Nepal, *Emerald Publishing Limited, Bingley*, pp. 143-162. <https://doi.org/10.1108/978-1-80455-448-720231008>
46. Chimi, P. M., Mala, W. A., Fobane, J. L., Essouma, F. M., II, J. A. M., Funwi, F. P., and Bell, J. M. (2022). Climate change perception and local adaptation of natural resource management in a farming community of Cameroon: A case study. *Environmental Challenges*, 8, 100539. <https://doi.org/10.1016/j.envc.2022.100539>.
47. Christopher M. Menzel, M.D. and Le Lagadec, (2014). Increasing the productivity of avocado orchards using high-density plantings: A review. *ScienceDirect, Scientia Horticultura*, vol 177, issu 2, Pages 21-36, <https://doi.org/10.1016/j.scienta.2014.07.013>.



48. Cissé, O., Diop Gueye, N. F., & Sy, M. (2005). Institutional and legal aspects of urban agriculture in French-speaking West Africa: From marginalization to legitimization. *Environment and Urbanization*. <https://doi.org/10.1177/095624780501700211>.
49. Coulibaly, O., Barry, M.A., & Kouadio, H.J. (2013). Impacts des inondations sur les productions agricoles et les revenus des producteurs dans la région de Gbôklé (Sud-Ouest de la Côte d'Ivoire). *Journal of Applied Biosciences*, 67, 5210-5219.
50. Dan Drost (2020). *Lettuce in the Garden*, Utah State University, Horticulture, 3 pages.
51. Degan Berenger Sêgnonnan, Sintondji Luc O., Karambiri Harouna, Kamagate Bamory, Gbaguidi Victor S., Alamou Eric Adéchina, Afouda Abel A., (2019). Impact de la variabilité climatique sur l'évolution des crues du fleuve Ouémé au Bénin de 1952 à 2011, *Ecole polytechnique d'Abomey-Calavi*, thèse de doctorat, 319p, <https://biblionumeric.epac-uac.org:9443/jspui/handle/123456789/2216>.
52. Dègla Herve KOUMASSI, A. Eric TCHIBOZO, Expedit Wilfrid VISSIN, and Christophe S. HOUSSOU (2014). Sig et télédétection pour l'optimisation de la cartographie des risques d'inondation dans le bassin de la sota au Bénin. *Rev. Ivoir. Sci. Technol.*, 23 (2014) 137 – 152, ISSN 1813-3290, <http://www.revist.ci>.
53. Déry, S. J., & Wood, E. F. (2005). Decreasing river discharge in northern Canada. *Geophysical Research Letters*, 32(10). <https://doi.org/10.1029/2005GL022845>
54. DGEC, (2022). *Communication relative à l'adaptation du Bénin au titre de la convention cadre des Nations unies sur le changements climatiques (CCNUCC)*, Ministère du cadre de vie et du développement durable, République du Bénin, 131p.
55. Di Baldassarre, G. and Montanari, A. (2009) Uncertainty in River Discharge Observations: A Quantitative Analysis. *Hydrology and Earth System Sciences*, 13, 913-921. <https://doi.org/10.5194/hess-13-913-2009>



56. Di Baldassarre, G. D., Montanari, A., Lins, H., Koutsoyiannis, D., Brandimarte, L., and Blöschl, G. (2010). Flood fatalities in Africa: From diagnosis to mitigation. *Geophysical Research Letters*, 37(22). <https://doi.org/10.1029/2010GL045467>
57. Dibi-Anoh, P.A., Koné, M., Gerdener, H. *et al*, (2023). Hydrometeorological Extreme Events in West Africa: Droughts. *Surv Geophys* **44**, 173–195, <https://doi.org/10.1007/s10712-022-09748-7>.
58. Dickey D. A. and Fuller W. A. (1979). Distribution of the estimators for autoregressive time series with a unit root. *Journal of the American Statistical Association*, 74 (366), 427-431.
Doi:10.4314/ijbcs.v9i1.12
59. Doni, F., Isahak, A., Che Mohd Zain, C.R. , (2014). Physiological and growth response of rice plants (*Oryza sativa* L.) to *Trichoderma* spp. inoculants. *AMB Expr* 4, 45. <https://doi.org/10.1186/s13568-014-0045-8>.
60. Eba, A.O., Arokoyu, S.B., and Daramola, S.A. (2016). A review of the impacts of flood on agriculture in Nigeria. *International Journal of Development and Sustainability*, 5(7), 393-408.
61. Ekwezu, C.S., Ezech, C.U, (2020).. Regional characterisation of meteorological drought and floods over west Africa. *Sustain. Water Resour. Manag.* **6**, 80, <https://doi.org/10.1007/s40899-020-00439-y>.
62. El Adlouni Salaheddine & Taha B.M.J. Ouarda, (2008). Comparison of methods for estimating the parameters of the non-stationary GEV model, *Revue des sciences de l'eau / Journal of Water Science* , Volume 21, numéro 1, p. 35–50, <https://doi.org/10.7202/017929ar>.



63. El Aoula, R., Mahé, G., Mhammdi, N., Ezzahouani, A., Kacimi, I., and Khomsi, K. (2021). Évolution du régime hydrologique dans le bassin versant du Bouregreg, Maroc, Proc. *IAHS*, 384, 163–168, <https://doi.org/10.5194/piahs-384-163-2021>.
64. El-Sharkawy, M., & Cadavid, L. (2002). Response of cassava to prolonged water stress imposed at different stages of growth. *Experimental Agriculture*, 38(3), 333-350. [doi:10.1017/S001447970200306X](https://doi.org/10.1017/S001447970200306X).
65. EPA - <https://www.epa.gov/water-research/hydraulic-modeling>, consulted: 24/04/2023
66. Ernest, A., Toundé Félix, A., Yaovi Aymar, B., Domiho Japhet, K., Sourou Henri, T. V., Constant, H., Valérie, B., Jean-Emmanuel, P., Gil, M., Christophe, C., and Michel, B. (2022). Use of the HEC RAS model for the analysis of exceptional floods in the Ouémé basin , *IAHS-AISH Scientific Assembly*, Montpellier, France, IAHS2022-584, <https://doi.org/10.5194/iahs2022-584>, 2022.
67. Evariste, Adeoti & Ibouiraïma, Yabi A, Mouritala & Ogouwale, E. (2018). *Risques hydro-climatiques et pêcheerie continentale dans le doublet adjohoun-dangbo au sud-est du benin*. UAC/IGATE/FLAHS,50pages.
68. Evy Latifah, Eko Widaryanto, Moch Dawam Maghfoer & Ariffin, (2019). Effect of Water logging Duration on Growth Phases of Tomatoes (*Solanum lycopersicum* L.) Grafted on Eggplant Rootstock. *Journal of Agronomy*, 18: 11-20, [doi : 10.3923/ja.2019.11.20](https://doi.org/10.3923/ja.2019.11.20).
69. FAO-<http://www.fao.org/docrep/010/ai325f/ai325f03.htm>, consulted: 24/04/2023
70. Faye, C., Sadio, C.A.A.S. (2023). Water and Geohazards in Lower Casamance: Risk Perception and Prevention Strategies of the Populations in the Baïla Marigot Basin (Casamance, Senegal). In: D'Amico, S., De Pascale, F. (eds) *Geohazards and Disaster Risk Reduction. Advances in Natural and Technological Hazards Research*, vol 51. https://doi.org/10.1007/978-3-031-24541-1_1





71. Fêmi Cocker, Jean Bosco Kpatindé Vodonou and Jacob A. YABI, (2020). Determinants of the volumes of drinking water used in rural area in the Lower Valley of Oueme in Benin. *Journal of Water Science*, 369-376, ISSN:1718-8598, Vol.32 N°4,2020, pp.369.DOI: <https://doi.org/10.7202/1069571ar>.
72. Fisher, R., & Tippett, L. (1928). Limiting forms of the frequency distribution of the largest or smallest member of a sample. *Mathematical Proceedings of the Cambridge Philosophical Society*, 24(2), 180-190. doi:10.1017/S0305004100015681
73. François-Nicolas Robinne, (2021). Impacts of disasters on forests, in particular forest fires, UNFFS Background paper, 66 pages.
74. Gandin, L.S., (1970). *The planning of meteorological station networks*. Geneva: World Meteorological Organization, WMO Technical Note no. 111.
75. García-Santiago, J. C., Valdez-Aguilar, L. A., Hernández-Pérez, A., Cartmill, A. D., & Valenzuela-García, J. (2017). Depth and Duration of Flooding Affect Growth, Yield, and Mineral Nutrition of Subirrigated Bell Pepper. *HortScience*, 52(2), 295-300. <https://doi.org/10.21273/HORTSCI11389-16>.
76. Giddings L., Soto M., Rutherford B.M. and Maarouf A., (2005). Standardized Precipitation Index Zones for México. *Atmósfera*, vol. 18, n° 1, p. 33-56.
77. Goula B.T.A., G.E. Soro, A. Dao, F.W. Kouassi Et B. Srohourou (2010). Frequency analysis and new cartography of extremes daily rainfall events in Côte d'Ivoire. *J. Appl. Sci.*, 10, 1684-1694, DOI: [10.3923/jas.2010.1684.1694](https://doi.org/10.3923/jas.2010.1684.1694)
78. Gurpreet K., Gurbir S. et al., (2019). Impacts and management strategies for crop production in waterlogged flooded soils: A review. *Agronomy journal*, volume 112, issue 3, 1475-1501p, <https://doi.org/10.1002/agj2.20093>.



79. Habtamu T., & Dinka M.,(2021). Application of ANN and HEC-RAS model for flood inundation mapping in lower Baro Akobo River Basin, Ethiopia, *Journal of Hydrology: Regional Studies*, Volume 36, <https://doi.org/10.1016/j.ejrh.2021.100855>.
80. Hahn, Federico, Salvador Valle, and Carmen Navarro-Gómez. 2022. "Pruning and Water Saving Management Effects on Mango High-Density and Mature Orchards" *Agronomy* 12, no. 11: 2623. <https://doi.org/10.3390/agronomy12112623>.
81. Hallouz, F., Meddi, M., and Mahe, G. 2013. Modification du régime hydroclimatique dans le bassin de l'Oued Mina (nord-ouest d'Algérie), *Journal of Water Science*, 26, 33–38.
82. Hanke J. E. and D. W. Wichern, (2005). Business Forecasting (8th Edition), Pearson, Prentice Hall, New Jersey ISBN 0-13-122856-0 Softcover (software enclosed), 535 pages, *International Journal of Forecasting, Elsevier*, vol. 22(4), pages 823-824.
83. Haque Md Ariful, Sharmin Shishir, Anannya Mazumder & Mehedi Iqbal (2023) Change detection of Jamuna River and its impact on the local settlements, *Physical Geography*, 44:2, 186-206, DOI: 10.1080/02723646.2022.2026075.
84. Hatem Baccour, Mohamed Slimani & Christophe Cudennec, (2012). Structures spatiales de l'évapotranspiration de référence et des variables climatiques corrélées en Tunisie. *Hydrological Sciences Journal*, 57 :4, 818-829, [doi: 10.1080/02626667.2012.672986](https://doi.org/10.1080/02626667.2012.672986).
85. HEC-RAS, (2016). Hydraulic Reference Manual. Version 5.0, 538pages.
86. Hicks F. and Peacock T., (2005). Suitability of HEC-RAS for Flood Forecasting. *Canadian Water Resources Journal*, Vol 30, Issue 2, Pages 159-174, <https://doi.org/10.4296/cwrj3002159>.
87. Houndakinou R, (2005). *Fréquence des évènements pluvieux extrêmes et leurs impacts environnementaux dans la ville de Cotonou*, Mémoire de DEA, UAC, 60 pages.

88. Houndenou C., (2011). *Changements climatiques et inondations au Bénin*. Communication au cours du séminaire sur l'institutionnalisation de la Plate-Forme Nationale de réduction de risques de Catastrophes, Cotonou, 10pages.
89. Hounkpè J., Bernd D., Djigbo B., Abel A., (2015). Non-stationarity flood frequency analysis in the Ouémé river basin, Benin Republic. *Hydrology*, 2(4), 210-229; <https://doi.org/10.3390/hydrology2040210>.
90. Hubbard K.G., (2001). *Station density and areal coverage of networks. Proceedings of an International Workshop Automated Weather Stations for Applications in Agriculture and Water Resources Management: Current Use and Future Perspectives*. Nebraska, USA. Geneva: World Meteorological Organization, WMO/TD no. 1074, 87–91.
91. Hunt J., (2002). Floods in climate change: a review, *Journals: the royal society publishing*, <https://doi.org/10.1098/rsta.2002.1016>.
92. Hunter, T. S., Clites, A. H., Campbell, K. B., & Gronewold, A. D. (2015). Development and application of a North American Great Lakes hydrometeorological database — Part I: Precipitation, evaporation, runoff, and air temperature. *Journal of Great Lakes Research*, 41(1), 65-77. <https://doi.org/10.1016/j.jglr.2014.12.006>.
93. INSAE. 2016. « *Principaux indicateurs sociodémographiques et économiques (RGPH-4, 2013)* ». Rapport d'enquête, Institut National de la Statistique et de l'Analyse Économique, Cotonou.
94. IPCC, (2022). Climate Change 2022: Impacts, Adaptation and Vulnerability Working Group II Contribution to the Sixth Assessment Report of the Intergovernmental Panel on Climate Change, 168p, [DOI: 10.1017/9781009325844](https://doi.org/10.1017/9781009325844).
95. Islam, R., Solaiman, A. H., Kabir, M. H., Arefin, S. M., Azad, M. O., Siddiquee, M. H., Alsanius, B. W., & Naznin, M. T. (2021). Evaluation of Lettuce Growth, Yield, and



Economic Viability Grown Vertically on Unutilized Building Wall in Dhaka City.

Frontiers in Sustainable Cities, 3, 582431. <https://doi.org/10.3389/frsc.2021.582431>

96. Islam, S. M., Gaihre, Y. K., Islam, M. R., Akter, M., Al Mahmud, A., Singh, U., & Sander, B. O. (2020). Effects of water management on greenhouse gas emissions from farmers' rice fields in Bangladesh. *Science of The Total Environment*, 734, 139382. <https://doi.org/10.1016/j.scitotenv.2020.139382>
97. Islam, S.N., Singh, S., Shaheed, H. et al. Settlement relocations in the char-lands of Padma River basin in Ganges delta, Bangladesh. *Front. Earth Sci. China*, 4, 393–402, <https://doi.org/10.1007/s11707-010-0122-5>.
98. J. Barnabé Hounkanrin (2015). *Mise en valeur agricole de la vallee de l'oueme dans la commune de Bonou : diagnostic et trajectoire*. Géographie. Université d'abomey-calavi (bénin),. Français. (NNT :). (tel-03786960), 276p, <https://theses.hal.science/tel-03786960>.
99. Jere S., Banda A, Kasense B, Siluyele I. and Moyo E. (2019). Forecasting Annual International Tourist Arrivals in Zambia Using Holt-Winters Exponential Smoothing. *Open Journal of Statistics*, 9, 258-267. doi: 10.4236/ojs.2019.92019.
100. Jonkman, S. N., and Kelman, I. (2005). An Analysis of the Causes and Circumstances of Flood Disaster Deaths. *Disasters*, 29(1), 75-97. <https://doi.org/10.1111/j.0361-3666.2005.00275.x>
101. Katz, R.W., M.B. Parlange Et P. Naveau (2002). Statistics of extremes in hydrology. *Adv. Water Resour.*, 25, 1287-1304.
102. Kaulgud Sarthak, Vaidya Ripple, Marathe Sanyukta and Tailor Manthan A. (2015). Vulnerability assessment of human settlement on river banks: a case study of vishwamitri river, vadodara, India, *Journal of Environmental Research and Development*, Vol. 9 No. 3A, 1015-1023.



103. Kedowide François-Corneille and Satoguina Honorat, (2016). Evaluation à mi-parcours du « projet de renforcement de l'information climatique et systèmes d'alerte précoce pour un développement résilient en Afrique et adaptation aux changements climatiques au Bénin – SAP-Bénin – pour la période 2014-2015, *Ministère De L'énergie, De L'eau Et Des Mines*, Rapport final, 90p.
104. Kee, Thomas B., Nolan J. Doesken, and J. Kliest, (1993). The relationship of drought frequency and duration of time scales, *Eighth Conference on Applied Climatology*, 17-22 January 1993, Anaheim, California.
105. Kelly, K.S., Krzysztofowicz, R., (1997). A bivariate meta-Gaussian density for use in hydrology. *Stochastic Hydrol Hydraul* 11, 17–31, <https://doi.org/10.1007/BF02428423>.
106. Khadeja Sultana Sathi, Abdul Awal Chowdhury Masud, Maliha Rahman Falguni, Naznin Ahmed, Khussboo Rahman, Mirza Hasanuzzaman, (2022). Screening of Soybean Genotypes for Waterlogging Stress Tolerance and Understanding the Physiological Mechanisms. *Advances in Agriculture*, vol. 2022, Article ID 5544665, 14 pages, 2022. <https://doi.org/10.1155/2022/5544665>.
107. Kim, Y., Seo, C.W., Khan, A.L. et al. Exo-ethylene application mitigates waterlogging stress in soybean (*Glycine max* L.) (2018). *BMC Plant Biol*, 18, 254, <https://doi.org/10.1186/s12870-018-1457-4>.
108. Kizito Sikuka, (2014). Agriculture: a key ingredient for peace and stability in Africa, *Sabinet African Journal*, Vol. 2014, No. 3, <https://hdl.handle.net/10520/EJC159676>.
109. Klimkowska A., Szafrńska, A., & Bieganski, A. (2016). Intelligent selection of plant species for ecological engineering of riverbanks: a step towards successful bank protection. *Ecological Engineering*, 90, 102-109.
110. Kodja D.J., Akognongbe A.J.S., Amoussou E., Mahé Gil, Vissin E.W., Paturel Jean-Emmanuel, Houndenou C. (2020). Influence des estimations d'évapotranspiration



potentielle par les méthodes de Penman-Monteith et de Oudin sur la calibration du modèle hydrologique GR4J dans le bassin versant de l'Ouémé (Afrique de l'Ouest). In : *Bonnardot V. (ed.), Quenol H. (ed.). Changement climatique et territoires. Rennes : LETG, p. 403-408. Changement Climatique et Territoires : Colloque de l'Association Internationale de Climatologie, 33., Rennes (FRA), 2020/07/01-04. ISBN 978-2-907696-26-5.*

111. Kodja J., (2018). Indicators of extreme hydroclimatic events in the Ouémé watershed at Bonou's outlet in West Africa, *hydrosciences Montpellier*, 288p. <https://theses.hal.science/tel-01869842>.
112. Kouassi, A. M., Kouamé, F. K., Koffi, Y. B., Dje B. K., Paturel, E. J., and Oulare, S. (2010). Analyse de la variabilité climatique et de ses influences sur les régimes pluviométriques saisonniers en Afrique de l'Ouest : cas du bassin versant du N'zi (Bandama) en Côte d'Ivoire, *CyberGeo*, DOI:10.4000/cybergeogeo.23388.
113. Kouassi, A. M., Nassa, R. A., Yao, K. B., Kouame, K. F. and Biemi, J. (2018). Modélisation statistique des pluies maximales annuelles dans le district d'Abidjan (sud de la Côte d'Ivoire). *Revue des sciences de l'eau, Journal of Water Science*, 31(2), 147–160. <https://doi.org/10.7202/1051697ar>.
114. Koumassi Herve, (2014). Risques hydroclimatiques et vulnérabilités des écosystèmes dans le bassin versant de la Sota à l'exutoire de Couberi. *Environnement et Société*. Université d'Abomey Calavi. Français. (NNT :). (tel-01572602).
115. Kpoha Josiane Nadèg, Akokponhoue Hounnigbo Bertrand, Orekan Vincent, And N'guessan Bi Vami Hermann (2023). Contribution of remote sensing and GIS to the mapping of land use units and its changes in the face of the flooding problem on the Plateau of Allada in Benin between 1986 and 2020. *International Journal of Innovation*



and *Scientific Research*, ISSN 2351-8014 Vol. 65 No. pp. 164-177,
<http://www.ijisr.issr-journals.org/>.

116. Kundzewicz, Zbigniew W., Jania and Jacek (2007). Extreme hydro-meteorological events and their impacts. From the global down to the regional scale, *Geographia Polonica*, no. 2, s. 9-23, <http://hdl.handle.net/20.500.12128/15640>.
117. Kwiatkowski, D., Phillips, P.C.B., Schmidt, P. and Shin, Y. (1992) Testing the Null Hypothesis of Stationarity against the Alternative of a Unit Root. *Journal of Econometrics*, 54, 159-178.
[http://dx.doi.org/10.1016/0304-4076\(92\)90104-Y](http://dx.doi.org/10.1016/0304-4076(92)90104-Y)
118. Lawin E. A., Biaou, C. A., Komi, K., Hounguè, R., Yao, K. B., & Afouda, A. A. (2018). Mid-Century Daily Discharge Scenarios Based on Climate and Land Use Change in Ouémé River Basin at Bétérou Outlet. *Hydrology*, 5(4), 69.
<https://doi.org/10.3390/hydrology5040069>.
119. Li Z., 2010. Application of HEC-HMS for flood forecasting in Misai and Wan'an catchments in China. *Water Sci. Eng.*, 3 (1), pp. 14-22, [10.3882/j.issn.1674-2370.2010.01.002](https://doi.org/10.3882/j.issn.1674-2370.2010.01.002).
120. Li, Y., Zhang, X., Singh, V. P., and Ren, L. (2015). Spatial-temporal analysis of flood disasters in China during 2001-2010. *Journal of Hydrology*, 528, 143-159.
121. Lins, H. F., & Slack, J. R. (1999). Streamflow trends in the United States. *Geophysical Research Letters*, 26(2), 227-230. <https://doi.org/10.1029/1998GL900291>
122. Liu, Y., Ma, M., Ran, Y., Yi, X., Wu, S., & Huang, P. (2021). Disentangling the effects of edaphic and vegetational properties on soil aggregate stability in riparian zones along a gradient of flooding stress. *Geoderma*, 385, 114883.
<https://doi.org/10.1016/j.geoderma.2020.114883>



123. Loc H. H., Park, E., Chitwatkulsiri, D., Lim, J., Yun, S., Maneechot, L., & Minh Phuong, D. (2020). Local rainfall or river overflow? Re-evaluating the cause of the Great 2011 Thailand flood. *Journal of Hydrology*, 589, 125368. <https://doi.org/10.1016/j.jhydrol.2020.125368>
124. Luliia S. Alessio D., Jeffrey C., Paul B., Attilio C., 2019. Comparing 2D capabilities of HEC RAS and LISFLOOD-FP on complex topography. *Hydrological Sciences Journal*, volume 64, issue 14, pages 1769-1782, <https://doi.org/10.1080/02626667.2019.1671982>.
125. MacKinnon J. G. (1996). Numerical distribution functions for unit root and cointegration tests. *Journal of Applied Econometrics*, vol. 11, issue 6, 601-18
126. Magel, R. C., and Wibowo, S. H. (1997). Comparing the Powers of the Wald-Wolfowitz and Kolmogorov-Smirnov Tests. *Biom. J.* 39, 665–675. doi:10.1002/bimj.4710390605
127. Majumdar S., Das A. & Mandal S., (2023). River bank erosion and livelihood vulnerability of the local population at Manikchak block in West Bengal, India. *Environ Dev Sustain*, 25, 138–175, <https://doi.org/10.1007/s10668-021-02046-z>
128. Malekian, Ashraf & Valizadeh, Einollah & Dastoori, Mona & Samadi, Sohaila & Bayat, Vahid. (2012). Soil water retention and maize (*Zea mays* L.) growth as effected by different amounts of Pumice. *Australian Journal of Crop Science*. 6.450-455pp.ISSN:1835-2707.
129. Mansor Rosnalini, Bahtiar Jamili Zaini, Catherine Chan May May, (2021). Medium-term Electricity Load Demand Forecasting using Holt-Winter Exponential Smoothing and SARIMA in University Campus, *International Journal of Engineering Trends and Technology*, Volume 69 Issue 3, 165-171, doi:10.14445/22315381/IJETT-V69I3P225



130. Mashaël Al Saud, (2009). Assessment of Flood Hazard of Jeddah Area 2009, Saudi Arabia, *Journal of Water Resource and Protection*, Vol.2 No.9, EM-DAT: The OFDA/CRED International Disaster Database, Université catholique de Louvain, Brussels, Bel. Data version: v11.08, //www.emdat.be/.
131. Mbugua Njoki, Kate (2021). Forecasting exotic vegetable wholesale prices using time series analysis methods, *Strathmore University*, <http://hdl.handle.net/11071/12561>.
132. McMichael A. J., Lindgren, E. (2011). Climate change: present and future risks to health, and necessary responses. *Journal of medicine*, vol 270, issue 5, 401-413. <https://doi.org/10.1111/j.1365-2796.2011.02415.x>.
133. Messner F. and Meyer V., (2006). Flood damage, vulnerability and risk perception – challenges for flood damage research. In: Schanze, J., Zeman, E., Marsalek, J. (eds) Flood Risk Management: Hazards, Vulnerability and Mitigation Measures. NATO Science Series, vol 67. *Springer*, Dordrecht. https://doi.org/10.1007/978-1-4020-4598-1_13.
- 134.** Meylan P., Favre A., Musy A., (2010). Predictive Hydrology, A frequency analysis approach, Science Publishers, CRC Press, 39p, <http://www.crcpress.com>.
135. Mirza, MMQ, 2011. Changement climatique, inondations en Asie du Sud et implications. *Reg Environ Change* 11 (Suppl 1), 95–107p, <https://doi.org/10.1007/s10113-010-0184-7>.
136. Mohammad Valipour, 2015. Long-term runoff study using SARIMA and ARIMA models in the United State, Royal Meteorological Society, *Geoscience Data Journal*, Volume 22, Issue 3, 592-598p, <https://doi.org/10.1002/met.1491>.
137. Mohanad S. Al-Musaylha, Ravinesh C. Deoa, Jan F. Adamowskic and Yan Lia, 2018. Short-term electricity demand forecasting with MARS SVR and ARIMA models using aggregated demand data in Queensland Australia, *Advanced Engineering Informatics*, Elsevier, vol. 35, pp. 1-16.



138. Mohanty, A., Hussain, M., Mishra, M., Kattel, D., and Pal, I. (2019). Exploring community resilience and early warning solution for flash floods, debris flow and landslides in conflict prone villages of Badakhshan, Afghanistan. *International Journal of Disaster Risk Reduction*, 33, 5-15.
<https://doi.org/10.1016/j.ijdrr.2018.07.012>
139. Moncoulon D., Labat D., Ardon J., Leblois E., Onfroy, T., Poulard, C., Aji, S., Rémy, A., and Quantin, A. (2014). Analysis of the French insurance market exposure to floods: a stochastic model combining river overflow and surface runoff, *Nat. Hazards Earth Syst. Sci.*, 14, 2469–2485, <https://doi.org/10.5194/nhess-14-2469-2014>.
140. Moreno, J., & Møller, A. P. (2011). Extreme climatic events in relation to global change and their impact on life histories. *Current Zoology*, 57(3), 375-389.
<https://doi.org/10.1093/czoolo/57.3.375>.
141. Mouritala A. 2018. Evaluation de la durabilité agro-écologique des aménagements hydro-agricoles de la plaine inondable dans le tandem dangbo-adjohoun au sud-est du Bénin, *European Scientific Journal*, March 2018 edition Vol.14, No.9, ISSN : 1857 – 7881, [Doi: 10.19044/esj.2018.v14n9p226](https://doi.org/10.19044/esj.2018.v14n9p226).
142. Munim, Z. H., Fiskin, C. S., Nepal, B., & Chowdhury, M. M. H. (2023). Forecasting container throughput of major Asian ports using the Prophet and hybrid time series models. *The Asian Journal of Shipping and Logistics*, 39(2), 67-77.
<https://doi.org/10.1016/j.ajsl.2023.02.004>
143. N'Tcha M'Po, Yèkambèssoun, Emmanuel Agnidé Lawin, Benjamin Kouassi Yao, Ganiyu Titilope Oyerinde, André Attogouinon, and Abel Akambi Afouda. 2017. Decreasing Past and Mid-Century Rainfall Indices over the Ouémé River Basin, Benin (West Africa). *Climate* 5, no. 3: 74. <https://doi.org/10.3390/cli5030074>.



144. Neisingh W.W.J., (2018). Inundation mapping in a dynamic, data-scarce environment using Ka-band passive microwave radiometry. Ouémé Delta, Benin, masters thesis, *TU Delft*, 166p.
145. Nwanne AJ and Ikeh AO (2020). Response of Sweet Potato (*Ipomoea Batatas* (L.) Lam) to Organic Soil Amendment in an Ultisol of Southeastern Nigeria. *Journal of Agronomy & Agricultural Science*, ISSN :2689-8292, <http://dx.doi.org/10.24966/AAS-8292/100019>.
146. Oerke E.-C., (2006). Crop losses to pests, *The Journal of Agricultural Science* , Volume 144 , Issue 1 , pp. 31 – 43, DOI: <https://doi.org/10.1017/S0021859605005708>
147. Ogouwalé E., Yabi I., Boko M., 2003. Mise en evidence d'un changement climatique dans la variabilité pluviométrique au Bénin. In *Publication de l'AIC*, 15, 205-208p.
148. Olanrewaju R., Ekiotuasighan B., Akpan G., (2017). Analysis of rainfall pattern and flood incidences in warri metropolis, nigeria. *Geography, Environment, Sustainability*;10(4):83-97. <https://doi.org/10.24057/2071-9388-2017-10-4-83-97>
149. Olorunwa, O. J., Adhikari, B., Brazel, S., Bheemanahalli, R., Barickman, T. C., & Reddy, K. R. (2023). Waterlogging stress reduces cowpea (*Vigna unguiculata* L.) genotypes growth, seed yield, and quality at different growth stages: Implications for developing tolerant cultivars under field conditions. *Agricultural Water Management*, 284, 108336. <https://doi.org/10.1016/j.agwat.2023.108336>.
150. Parolin, P., & Wittmann, F. (2010). Struggle in the flood: Tree responses to flooding stress in four tropical floodplain systems. *AoB PLANTS*, 2010. <https://doi.org/10.1093/aobpla/plq003>.
151. PCM, (2015). *Projet commune du millénaire* - Bonou, 2 pages.



152. Perron P., (1988). Trends and random walks in macroeconomic time series: Further evidence for a new approach. *Journal of economic dynamics and control*, 12 2, 297-332.
153. Peter Akpodiogaga-a & Ovuyovwiroye Odjugo, (2010). General Overview of Climate Change Impacts in Nigeria, *Journal of Human Ecology*, 29:1, 47 55, DOI: [10.1080/09709274.2010.11906248](https://doi.org/10.1080/09709274.2010.11906248).
154. Petrow, T., Merz, B. (2009). Trends in flood magnitude, frequency and seasonality in Germany in the period 1951–2002. *Journal of Hydrology*, 371, 129-141.
155. Phillips P. C. B. and Perron P., (1988). Testing for a unit root in time series regression. *Biometrika*, 75 2, 335-346.
156. PNUD, (2012). Bureau de la prévention des crues et du relèvement, *inforapide*, octobre 2012, 2 pages.
157. Posthumus H., J. Morris, Hess T, Neville D., Philips E., and Baylis A., (2009). Impacts of summer 2007 floods on agriculture in England, *Journal of flood risk management*, volume 2, issue 3, P.182-189, <https://doi.org/10.1111/j.1753-318X.2009.01031.x>.
158. Prafulkumar V. Timbadiya, Prem Lal Patel and Prakash D. Porey (2011). Calibration of HEC-RAS Model on Prediction of Flood for Lower Tapi River, India, *Journal of Water Resource and Protection*, Vol. 3 No. 11, Article ID: 8680, 7 pages, [doi:10.4236/jwarp.2011.311090](https://doi.org/10.4236/jwarp.2011.311090).
159. Pramantha R. Q., E Agustian L., and Refnitasari L., (2012). The characteristics of riverbank slum settlement in Indonesia. Case study: Depok, Palembang, Surabaya, and Surakarta, *IOP Conf. Ser.: Earth Environ. Sci.* 916 012012, doi 10.1088/1755-1315/916/1/012012.



160. Promkhambut A., Younger A., Polthanee A. and Akkasaeng C., (2010). Morphological and physiological responses of sorghum (*Sorghum bicolor* L. Moench) to waterlogging, *Asian Journal of Plant Sciences*, 9 (4): 183-193, doi: 10.3923/ajps.2010.183.193.
161. Renard, B., & Lang, M. (2007). Use of a Gaussian copula for multivariate extreme value analysis: Some case studies in hydrology. *Advances in Water Resources*, 30(4), 897-912. <https://doi.org/10.1016/j.advwatres.2006.08.001>
162. Riad, S., Mania, J., Bouchaou, L., and Najjar, Y. (2004). Rainfall-runoff model using an artificial neural network approach. *Mathematical and Computer Modelling*, 40(7-8), 839-846. <https://doi.org/10.1016/j.mcm.2004.10.012>
163. Romaric OGOUWALE, Blaise DONOU and Maman Sani ISSA (2022). Analyse des extrêmes hydro climatiques dans le bassin inferieur du fleuve Oueme à l'exutoire de Bonou (Bénin). Variabilité climatique et production de riz pluvial en zone humide : cas de la sous-préfecture de Gagnoa (Côte d'Ivoire), *Regardsuds*, numero2.
164. Sadio P. M., Mbaye M. M., Samo Diatta and Mouhamadou Bamba Sylla, (2020). Hydro-climate variability and change in the Casamance river basin (Senegal), *La Houille Blanche*, 106:6, 89-96, DOI: 10.1051/lhb/2021002.
165. Salama, M.I., Sayed, R.A., El-Shereif Ali and Mankolah M.A. (2017). Response of Washington Navel Orange Trees to Some Soil Amendments and Foliar application of GA3 under Clay Soil Conditions. *J. Sus. Agric. Sci.*, 43. 39-54. 10.21608/JSAS.2017.3490.
166. Sandra Hardy, Pat Barkley, Andrew Creek, and Nerida Donovan (2012). Impacts and management of flooding and waterlogging in citrus orchards. *Department of Primary Industries, factsheet*, 9 pages, www.dpi.nsw.gov.au/publications for updates Primefact 1189, First edition.



167. Sarker, M. N. I., Wu, M., Alam, G. M., & Shouse, R. C. (2020). RETRACTED: Life in riverine islands in Bangladesh: Local adaptation strategies of climate vulnerable riverine island dwellers for livelihood resilience. *Land Use Policy*, 94, 104574. <https://doi.org/10.1016/j.landusepol.2020.104574>
168. ScienceDirect-<https://www.sciencedirect.com/topics/agricultural-and-biological-sciences/flood-tolerant-plants> , consulted: 24/04/2023
169. Shang K., Chen Z., Liu Z., Song L., Zheng W. and Yang B. (2021). Haze Prediction Model Using Deep Recurrent Neural Network. *Atmosphere* , 12, 1625. <https://doi.org/10.3390/atmos12121625>.
170. Shelton, M. L. (2009). *Hydroclimatology: perspectives and applications*. Cambridge University Press, 425 pages.
171. Sher, A., Barbanti, L., Ansar, M., and Malik, M. A. (2013). Growth response and plant water status in forage sorghum ['Sorghum bicolor'(L.) Moench] cultivars subjected to decreasing levels of soil moisture. *Australian Journal of Crop Science*, 7(6), 801-808. <https://search.informit.org/doi/10.3316/informit.365320590503145>.
172. Shiwachi, Hironobu & KIKUNO, Hidehiko & OHATA, Junya & KIKUCHI, Yu & Irie, Kenji. (2016). Growth of Water Yam (*Dioscorea alata* L.) under Alkaline Soil Conditions. *Tropical Agriculture and Development*. 76-82. 10.11248/jsta.59.76.
173. Shrestha, U.S., Amatya, S.S. (2022). River Ecology Services and People of Riparian Settlements in the Tamakoshi River Basin, Central Nepal. In: Pradhan, P.K., Leimgruber, W. (eds) *Nature, Society, and Marginality. Perspectives on Geographical Marginality*, vol 8. Springer, Cham. https://doi.org/10.1007/978-3-031-21325-0_7
174. Singh, J., Schädler, M., Demetrio, W., Brown, G. G., and Eisenhauer, N. (2019). Climate change effects on earthworms - a review. *Soil organisms*, 91(3), 114. <https://doi.org/10.25674/so91iss3pp114>



175. Sinsin B., Azontondé H.A., Houéhanou T.D., Yabi J.A., and Assogba-Komlan F. (2019). Agricultural practices in flood-prone areas in Benin: Insights from farmers' perceptions. *International Journal of Disaster Risk Reduction*, 37, 101112. <https://doi.org/10.1016/j.ijdrr.2019.101112>.
176. Sjöberg J., Viklander M., Nilsson K., and Galle B. (2014). Climate change adaptation of urban drainage systems—a review. *Water Science and Technology*, 69(4), 705-713.
177. SNU, 2010. *Rapport de la gestion des inondations de 2010 au Bénin*, 86 pages.
178. Sönmez S.K.L., Yucesoy M., Yucel B. and Yilmaz B., (2005). The effect of bee propolis on oral pathogens and human gingival fibroblasts. *Journal of Ethnopharmacology*, vol. 102, p. 371-376. doi : [10.1016/j.jep.2005.06.035](https://doi.org/10.1016/j.jep.2005.06.035).
179. SORO G. (2011). *Modélisation statistique des pluies extrêmes en Côte d'Ivoire*. Thèse de doctorat, Univ. Nangui-Abrogoua, Côte d'Ivoire, 172 p. Doi : [10.7202/705145ar](https://doi.org/10.7202/705145ar).
180. Sri Wahyuningsih, Febria Cahya Indrani, Joko Restuono , Kartika Noerwijati , Abdullah Taufiq , Yuliantoro Baliadi, Rohmad Budiono, Nguyen Van Minh and Peeyush Soni,(2021). Growth and Productivity of Four Cassava Cultivars on Several Levels of Mixed Fertilizers. *Jordan Journal of Biological Sciences*, Volume 14, Number 5, ISSN 1995-6673, Pages 939 – 944, <https://doi.org/10.54319/jjbs/140509>.
181. Stedinger J.R., R.M. Vogel and E. Foufoula, (1993). Frequency analysis of extreme events. in: *Handbook of Hydrology*, D.R. Maidment (éditeur), McGraw Hill Inc., Chapitre 18, pp. 1-66.
182. Suh H.D., Cho K.Y., Park S.K., Lee K.H., (1987). Effect of flooding on the growth and yield of hot pepper (*Capsicum annuum* L.). *World Vegetables Center*, 29(1):1-9, <https://worldveg.tind.io/record/6339?ln=en>.



183. Sullivan, M., VanToai, T., Fausey, N., Beuerlein, J., Parkinson, R., & Soboyejo, A. (2001). Evaluating on-farm flooding impacts on soybean. *Crop Science*, 41, 93-100. <https://doi.org/10.2135/cropsci2001.41193x>.
184. Tania Gascon. Impact de la résolution spatiale et temporelle des entrées pluviométriques pour la modélisation hydrologique en Afrique de l'Ouest et implication dans l'utilisation des produits satellitaires : Etude de cas sur le Bassin de l'Ouémé au Benin. Hydrologie. *Université Grenoble Alpes*, 2016. Français. (NNT : 2016GREAU046). (tel-01633466)
186. Tchegnon, P., and Guidibi, E. (2006). Monographie De La Commune D'adjohoun. Cotonou: *Cabinet Afrique Conseil*, 1-60.
187. Teg Alam, Ali AlArjani, (2021). A Comparative Study of CO2 Emission Forecasting in the Gulf Countries Using Autoregressive Integrated Moving Average, Artificial Neural Network, and Holt-Winters Exponential Smoothing Models. *Advances in Meteorology*, vol. 2021, Article ID 8322590, 9 pages, <https://doi.org/10.1155/2021/8322590>.
188. Tiina Huvio, Jukka Kola and Tulor Lundström (2004). Small scale farmers in liberalized trade environment, university of Helsinki, 238 pages.
189. Totin V. S., Amoussou E., Odoulami L., Boko M., and Blivi B., (2016). Seuils pluviométriques des niveaux de risques d'inondation dans le bassin de l'Ouémé au Bénin, *XXIXème colloque de l'Association de Climatologie*, Lausanne – Besançon, pp 369-374.
190. Trambly Y, Gabriele V., and Wei Z., (2020). Observed changes in flood hazard in Africa, *Environmental Research Letters*, volume 15, number 10, [doi 10.1088/1748-9326/abb90b](https://doi.org/10.1088/1748-9326/abb90b).



191. Tujuba, Milkinesh & Ayana, Negash. (2020). Evaluation of Released Tomato (*Lycopersicon Esculentum* Mill.) Varieties for Fruit Yield and Quality Parameters in Western Ethiopia. *Agricultural and Biological Sciences Journal*, Vol. 6, No. 2, 2020, pp. 100-113, <http://www.aiscience.org/journal/absj>.
192. U.S. Geological Survey [USGS]-<https://www.usgs.gov/special-topic/water-science-school/science/inland-flooding-floodplains-and-wetlands>, consulted: 24/04/2023
193. Veintimilla-Reyes, J., Cisneros, F., and Vanegas, P. (2016). Artificial Neural Networks Applied to Flow Prediction: A Use Case for the Tomebamba River. *Procedia Engineering*, 162, 153-161. <https://doi.org/10.1016/j.proeng.2016.11.031>
194. Voesenek, L., & Sasidharan, R. (2013). Ethylene–and oxygen signalling–drive plant survival during flooding. *Plant Biology*, 15, 426– 435. <https://doi.org/10.1111/plb.12014>.
195. Vwioko E. D., A. M. Imoni, A. A. Ali, and M. Abdeldaym (2019). Sodium Azide Priming Enhances Waterlogging Stress Tolerance in Okra (*Abelmoschus esculentus* L.). *Agronomy*, 9(11), 679. <https://doi.org/10.3390/agronomy9110679>.
196. Waïdi Seydou (2020). Vulnerabilite du paysannat aux changements climatiques dans la depression mediane au sud-benin. *Sciences de l'environnement*. Université d'abomey-calavi (Bénin), 265p. <https://theses.hal.science/tel-03788541>.
197. Waloddi Weibull, (1951). A statistical distribution function of wide applicability, *J. Appl. Mech.-Trans. ASME*, 18(3).
198. Wasonga Daniel O., Jouko Kleemola, Laura Alakukku, and Pirjo S.A. Mäkelä. (2020). "Growth Response of Cassava to Deficit Irrigation and Potassium Fertigation during the Early Growth Phase". *Agronomy*, 10, no. 3: 321. <https://doi.org/10.3390/agronomy10030321>.



199. WC Boughton, (1989). A review of the USDA SCS curve number method, *Australian Journal of Soil Research* 27(3) 511 – 523, <https://doi.org/10.1071/SR9890511>.
200. Wu J., Sheng Y. P., and Zhou, J. (2016). Hydraulic modeling of urban drainage system using SWMM: a review of developments and applications. *Journal of Hydrology*, 543, 1-24.
201. Wu H., Hayes M.J., Weiss A. and Hu Q, (2001). An evaluation of the Standardized Precipitation Index, the China Z-index and the statistical Z-score. *International Journal of Climatology*, vol. 21, n° 6, p. 745-758. DOI : [10.1002/joc.658](https://doi.org/10.1002/joc.658).
202. YABI. Ibouaïma, (2019). Changements climatiques et inondations dans la commune de Ouinhi au Sud-Est du Bénin : pour la transformation de la catastrophe en opportunités, *Revue espace géographique et Société Marocaine*, (27).
203. Yang Jingping & Chen Jie, (1998). The effects of soil waterlogging at different growth stages on the growth and development of spring corn. *Acta Agriculturae Zhejiangensis*;10(4):188-192. <https://europepmc.org/article/cba/319884>.
204. Zaman M., (1989). The Social and Political Context of Adjustment to Riverbank Erosion Hazard and Population Resettlement in Bangladesh, *Human Organization*, 48 (3): 196–205. <https://doi.org/10.17730/humo.48.3.v55465j651259835>
205. Zanaga D., Van De Kerchove, R., Daems, D., De Keersmaecker, W., BJanrockmann, C., Kirches, G., ... & Arino, O. (2022). *ESA WorldCover 10 m 2021 v200*.
206. Zhang K., Han L., Qin C., & Wu, W. (2019). Urban expansion and its impact on land use/land cover changes in the middle reaches of the Yangtze River, China. *Applied Geography*, 105, 65-76.



APENDICES



Some Pictures for crops damage from flooded



Picture: Examples of flood damage in the commune of Ouinhi a: Flooded school; b: Affected crops; c: Damaged roads; d = Flooded and destroyed houses Shot: Donou October, 2010 and

Ouinhi town hall August 2010 (source: Yabi, 2019)

Table 1: Land Use and Land Cover classification summary (source: ESA, 2016)

Class (ESA classification)	Description	Area (km ²)	Rang
80	Water	0.021	1
50	Built up areas	6.636	2
90	Herbaceous wetlands	8.397	3
20	Shrubs cover areas	45.188	4
30	Grassland	56.029	5
40	Cropland	66.426	6
10	Tree cover areas	133.230	7



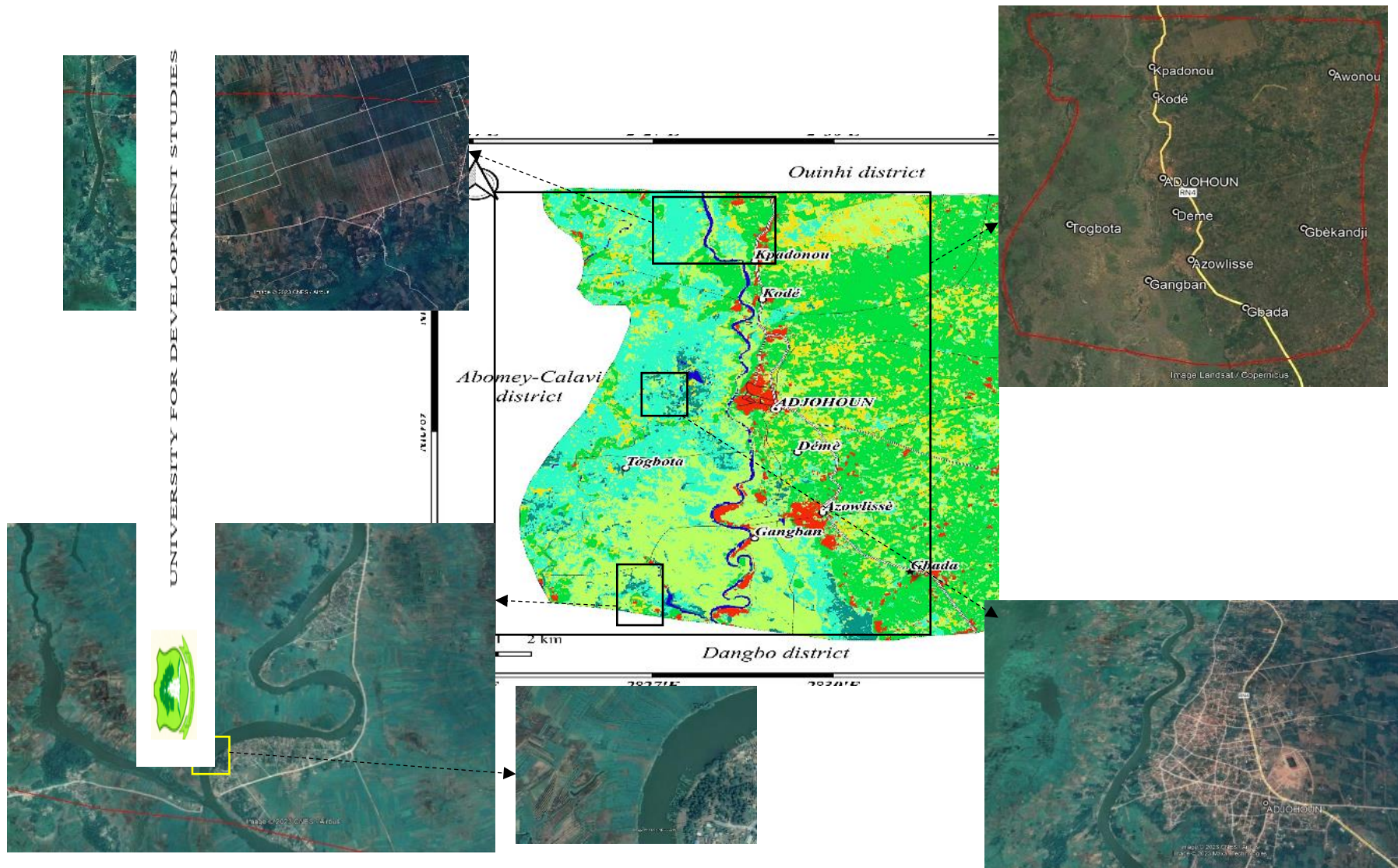


Table 2: Manning coefficient

Class of land use (ID)	Parameter
	Manning coefficient
Tree covers areas	0.10
shrubs cover areas, grassland,	0.08
Cropland	0.3
Herbaceous wetlands	0.035
built up areas	0.012
Water	0.05

Source: UC Louvain, HEC RAS/Modeling User's Manual

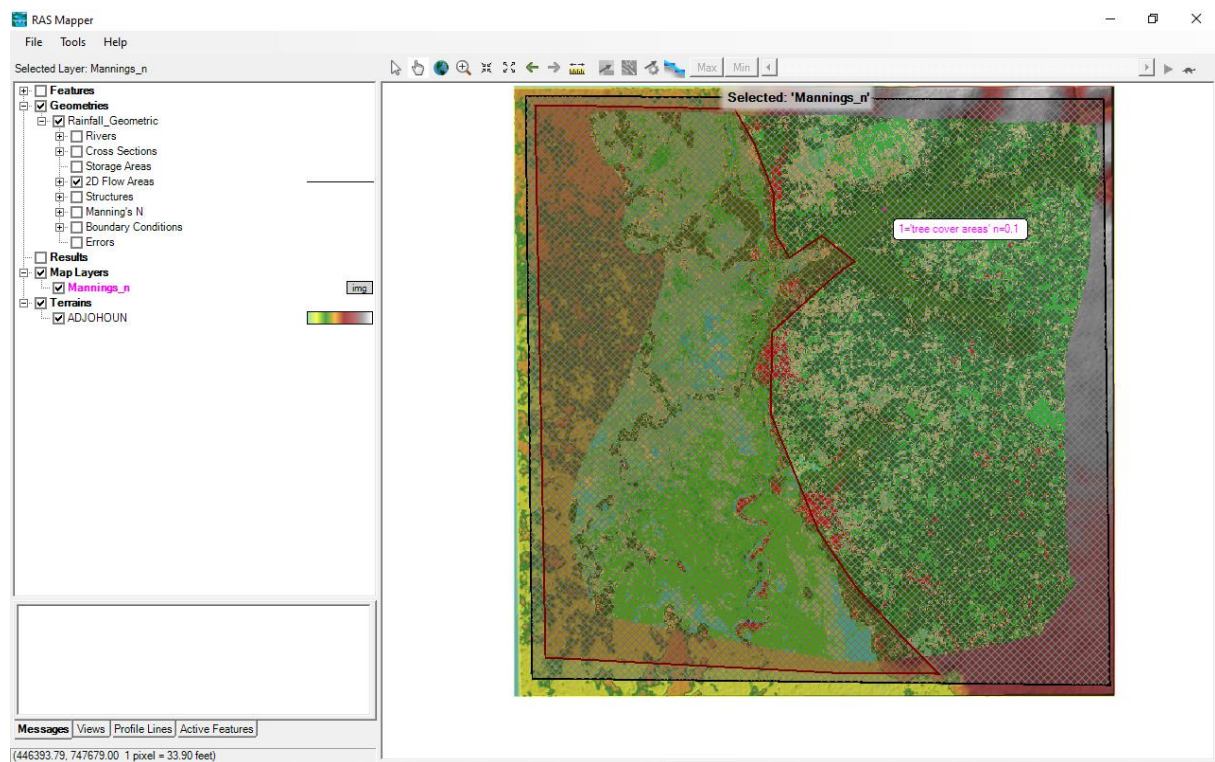


Figure 1: Ras mapper, application of manning coefficient for simulation

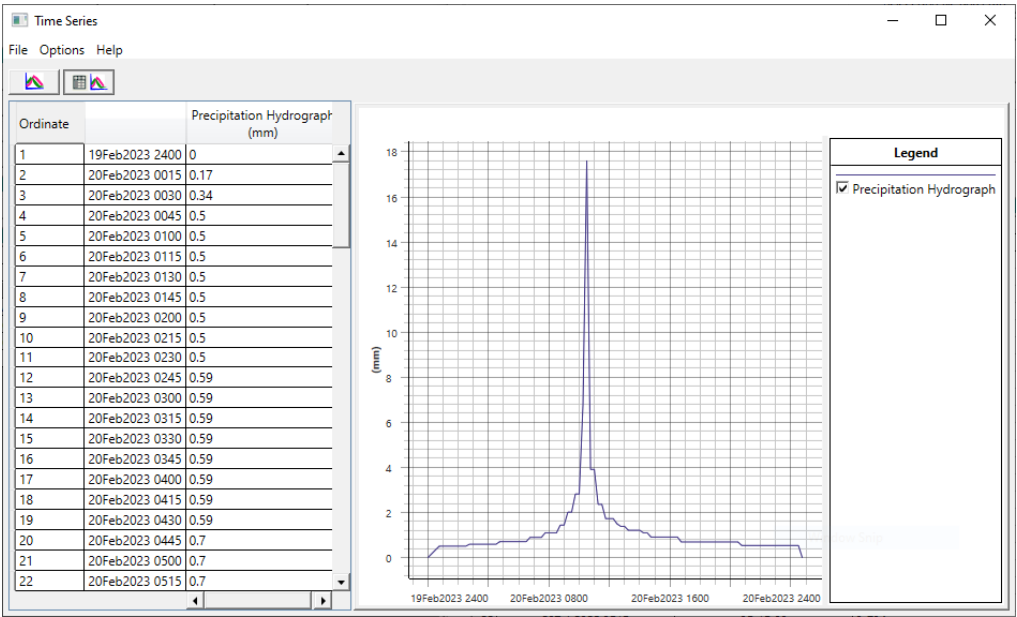


Figure 2: Hyetograph curve for 115mm/24h under HEC RAS

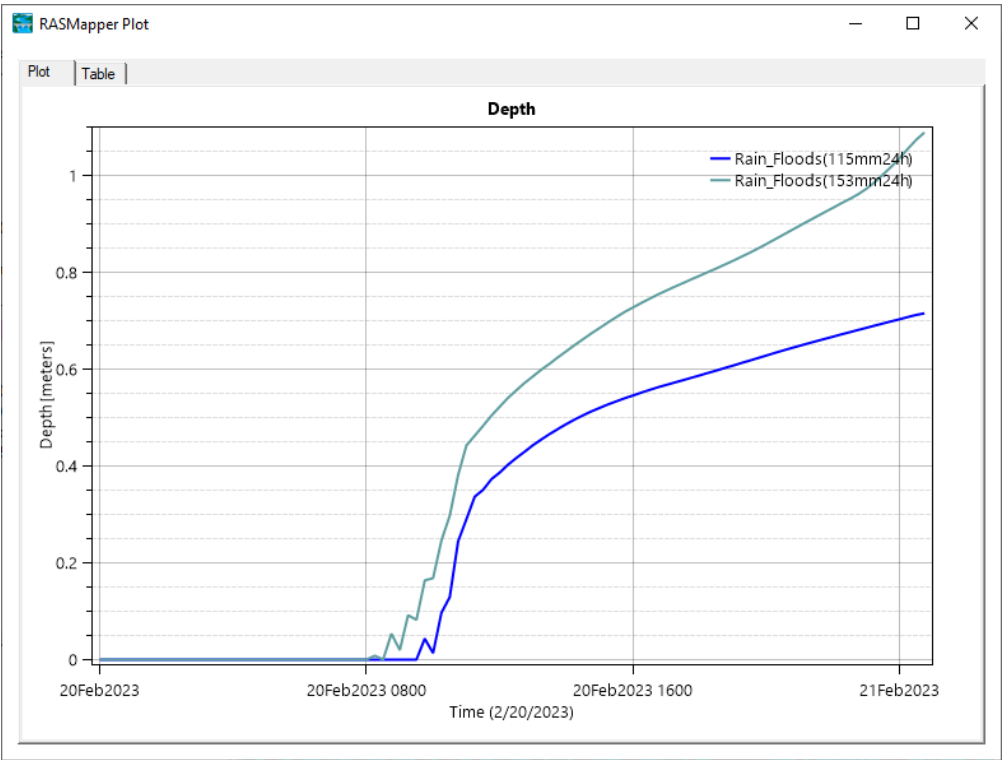


Figure 3: Water level profile during 115mm & 153mm/24h at (Xcoord=440474.21, Ycoord=736906.10)